EPRI

2022 TECHNICAL REPORT

BWRVIP-346: BWR Vessel and Internals Project

Testing and Evaluation of the Duane Arnold 288°-R ISP(E) Reinserted Surveillance Capsule

PREPARED UNDER THE NUCLEAR QA PROGRAM

BWRVIP-346: BWR Vessel and Internals Project

Testing and Evaluation of the Duane Arnold 288°-R ISP(E) Reinserted Surveillance Capsule

3002023520

Final Report, May 2022

EPRI Project Manager
S. Williams

All or a portion of the requirements of the EPRI Nuclear Quality Assurance Program apply to this product.

YES NO

EPRI
3420 Hillview Avenue, Palo Alto, California 94304-1338 ▪ PO Box 10412, Palo Alto, California 94303-0813 ▪ USA
800.313.3774 ▪ 650.855.2121 ▪ askepri@epri.com ▪ www.epri.com

DISCLAIMER OF WARRANTIES AND LIMITATION OF LIABILITIES

THIS DOCUMENT WAS PREPARED BY THE ORGANIZATION(S) NAMED BELOW AS AN ACCOUNT OF WORK SPONSORED OR COSPONSORED BY THE ELECTRIC POWER RESEARCH INSTITUTE, INC. (EPRI). NEITHER EPRI, ANY MEMBER OF EPRI, ANY COSPONSOR, THE ORGANIZATION(S) BELOW, NOR ANY PERSON ACTING ON BEHALF OF ANY OF THEM:

(A) MAKES ANY WARRANTY OR REPRESENTATION WHATSOEVER, EXPRESS OR IMPLIED, (I) WITH RESPECT TO THE USE OF ANY INFORMATION, APPARATUS, METHOD, PROCESS, OR SIMILAR ITEM DISCLOSED IN THIS DOCUMENT, INCLUDING MERCHANTABILITY AND FITNESS FOR A PARTICULAR PURPOSE, OR (II) THAT SUCH USE DOES NOT INFRINGE ON OR INTERFERE WITH PRIVATELY OWNED RIGHTS, INCLUDING ANY PARTY'S INTELLECTUAL PROPERTY, OR (III) THAT THIS DOCUMENT IS SUITABLE TO ANY PARTICULAR USER'S CIRCUMSTANCE; OR

(B) ASSUMES RESPONSIBILITY FOR ANY DAMAGES OR OTHER LIABILITY WHATSOEVER (INCLUDING ANY CONSEQUENTIAL DAMAGES, EVEN IF EPRI OR ANY EPRI REPRESENTATIVE HAS BEEN ADVISED OF THE POSSIBILITY OF SUCH DAMAGES) RESULTING FROM YOUR SELECTION OR USE OF THIS DOCUMENT OR ANY INFORMATION, APPARATUS, METHOD, PROCESS, OR SIMILAR ITEM DISCLOSED IN THIS DOCUMENT.

REFERENCE HEREIN TO ANY SPECIFIC COMMERCIAL PRODUCT, PROCESS, OR SERVICE BY ITS TRADE NAME, TRADEMARK, MANUFACTURER, OR OTHERWISE, DOES NOT NECESSARILY CONSTITUTE OR IMPLY ITS ENDORSEMENT, RECOMMENDATION, OR FAVORING BY EPRI.

THE FOLLOWING ORGANIZATIONS PREPARED THIS REPORT:

Electric Power Research Institute (EPRI)

MP Machinery & Testing, LLC

TransWare Enterprises Inc.

THE TECHNICAL CONTENTS OF THIS PRODUCT WERE PREPARED IN ACCORDANCE WITH THE EPRI QUALITY PROGRAM MANUAL THAT FULFILLS THE REQUIREMENTS OF 10 CFR 50 APPENDIX B. THIS PRODUCT IS SUBJECT TO THE REQUIREMENTS OF 10 CFR PART 21. CERTIFICATION OF CONFORMANCE CAN BE OBTAINED FROM EPRI.

CONTRACTUAL ARRANGEMENTS BETWEEN THE CUSTOMER AND EPRI MUST BE ESTABLISHED BEFORE QUALITY APPLICATION TO ASSURE FULFILLMENT OF QUALITY PROGRAM REQUIREMENTS.

NOTE

For further information about EPRI, call the EPRI Customer Assistance Center at 800.313.3774 or e-mail askepri@epri.com.

Together…Shaping the Future of Energy®

ACKNOWLEDGMENTS

The following organizations prepared this report:

Electric Power Research Institute (EPRI)

Principal Investigators
S. Williams
E. Long
R. Carter

MP Machinery & Testing, LLC
2161 Sandy Drive
State College, PA 16803

Principal Investigator
Dr. M. P. Manahan, Sr.

TransWare Enterprises Inc.
1565 Mediterranean Drive
Sycamore, IL 60178

Principal Investigators
D. Jones
K. Watkins
K. Jones

This report describes research sponsored by EPRI and its BWRVIP participating members.

This publication is a corporate document that should be cited in the literature in the following manner:

BWRVIP-346: BWR Vessel and Internals Project: Testing and Evaluation of the Duane Arnold 288°-R ISP(E) Reinserted Surveillance Capsule. EPRI, Palo Alto, CA: 2022. 3002023520.

PRODUCT DESCRIPTION

In the late 1990s, a Boiling Water Reactor Vessel and Internals Project (BWRVIP) Integrated Surveillance Program (ISP) was developed to improve surveillance of the U.S. BWR fleet. This report describes testing and evaluation of the Duane Arnold Energy Center's (DAEC) 288° surveillance capsule that was reinserted into the reactor at the beginning of Cycle 9 (hereinafter the DAEC 288°-R capsule). The DAEC 288°-R capsule contained reconstituted Charpy specimens that were initially irradiated in the DAEC reactor during Cycles 1 through 7. These results will be used to monitor reactor pressure vessel (RPV) neutron embrittlement as part of the BWRVIP ISP (E) representing materials for the first license renewal (LR) of up to 60 years of extended operation, as described in BWRVIP-86, Rev. 1-A.

Background

The BWRVIP ISP represents a major enhancement to the process of monitoring embrittlement for the U.S. fleet of BWRs. The ISP optimizes surveillance capsule tests while at the same time maximizing the quantity and quality of data, resulting in a more cost-effective program. The BWRVIP ISP provides more representative data that can be used to assess embrittlement in RPV beltline materials and improved trend curves in the BWR range of irradiation conditions.

Challenges and Objectives

Neutron irradiation exposure reduces the toughness of reactor vessel steel plates, welds, and forgings. The objectives of this project were twofold:

- To document the results of neutron dosimetry and Charpy V-notch (CVN) toughness tests for the surveillance materials (plate heat [B0673-1] and an unknown weld heat of shielded metal arc weld [DA1 SMAW]) in the DAEC 288°-R surveillance capsule that was reinserted with select reconstituted CVN specimens and irradiated from Cycle 9 to Cycle 27.
- To compare the results with the embrittlement trend prediction of the U.S. Nuclear Regulatory Commission (U.S. NRC) Regulatory Guide 1.99, Revision 2.

Approach

The DAEC 288°-R surveillance capsule was reinserted with reconstituted CVN specimens and irradiated starting from Cycle 9 until the plant permanently ceased operations after Cycle 27 in August 2020. The surveillance capsule contained flux wires for neutron flux monitoring, Charpy V-notch impact test specimens, and tensile specimens. The project team removed the capsule from the reactor in October 2020 and transported it to facilities for testing and evaluation. The team used dosimetry to gather information about the neutron fluence accrual of specimens from the capsule. They then performed a neutron transport calculation in accordance with Regulatory

Guide 1.190 and compared it to the dosimetry results. Testing of Charpy V-notch specimens was performed according to the American Society for Testing and Materials (ASTM) standards.

Results and Findings

The report includes capsule neutron exposure and CVN test results for DAEC surveillance plate heat B0673-1 and surveillance weld heat DA1 SMAW. The project compared irradiated Charpy data to unirradiated data in order to determine the shifts in Charpy index temperatures for the surveillance plate and weld materials due to irradiation. The measured shift for the surveillance plate is less than the predicted shift + margin using Regulatory Guide 1.99, Revision 2 (RG 1.99R2). The measured shift for the surveillance weld heat is also less than the predicted shift + margin using RG 1.99R2. Researchers also measured flux wires and determined the fluence of the 288°-R reinserted surveillance capsule.

Applications, Value, and Use

Results of this work will be used in the BWRVIP ISP that integrates individual BWR surveillance programs into a single program. The ISP provides high quality data for monitoring BWR vessel embrittlement. The ISP results in significant cost savings to the BWR fleet and provides more accurate monitoring of embrittlement in BWR vessels.

Keywords

BWR
Charpy V-notch testing
Mechanical properties
Radiation embrittlement
Reactor pressure vessel integrity
Reactor vessel surveillance program

Deliverable Number: 3002023520

Product Type: Technical Report

Product Title: BWRVIP-346: BWR Vessel and Internals Project: Testing and Evaluation of the Duane Arnold 288°-R ISP(E) Reinserted Surveillance Capsule

PRIMARY AUDIENCE: Plant engineers responsible for reactor vessel integrity

SECONDARY AUDIENCE: Boiling Water Reactor Vessel and Internals Project (BWRVIP) Program Owners

KEY RESEARCH QUESTION

The objectives of this project were:

- To withdraw and test the Duane Arnold Energy Center (DAEC) 288° reconstituted and reinserted surveillance capsule, designated as the DAEC 288°-R ISP(E) capsule, in accordance with the approved test matrix of the BWRVIP Integrated Surveillance Program (ISP) and ISP "extended" or ISP(E) as described in BWRVIP-86, Revision 1-A and BWRVIP-321-A.
- To document the results of neutron dosimetry and Charpy V-notch toughness tests for the DAEC 288°-R ISP(E) capsule surveillance materials (plate heat B0673-1 and weld heat DA1 SMAW shield metal arc weld [SMAW]) per American Society for Testing and Materials (ASTM) E 85-82 and to determine capsule fluence per U.S. Nuclear Regulatory Commission (U.S. NRC) Regulatory Guide 1.190.
- To compare the results with embrittlement trend predictions of the U.S. NRC Regulatory Guide 1.99, Revision 2.

RESEARCH OVERVIEW

The BWRVIP ISP combines individual BWR surveillance programs into a single program that monitors the reduction in toughness of RPV steel plates, welds, and forgings as a result of neutron irradiation exposure. The DAEC 288°-R ISP(E) surveillance capsule was withdrawn and tested per the schedule in BWRVIP-86, Revision 1-A as amended by an NRC-approved early withdrawal schedule. The capsule contained reconstituted Charpy specimens from the original DAEC 288° capsule which was irradiated in the DAEC reactor from Cycle 1 through Cycle 7. The reconstituted capsule had been irradiated in the reactor since it was reinserted prior to Cycle 9 and contained flux wires for neutron flux monitoring, Charpy V-notch (CVN) impact test specimens, and tensile specimens. The project team removed the capsule from the reactor in October of 2020 and subsequently transported it to facilities for testing and evaluation. The team used dosimetry to gather information about the neutron fluence accrual of the capsule specimens. They also performed a neutron transport calculation in accordance with Regulatory Guide 1.190, comparing the results to dosimetry results. Testing of the base metal and weld metal CVN specimens was performed according to ASTM standards.

KEY FINDINGS

- The report includes capsule neutron exposure and Charpy V-notch test results for the DAEC surveillance plate heat B0673-1 and the DAEC surveillance weld heat DA1 SMAW.
- The project compared irradiated Charpy data to unirradiated data in order to determine shifts in Charpy index temperatures for the surveillance plate and surveillance weld materials due to irradiation.
- For the surveillance plate, the measured shift is less than the predicted shift plus margin using Regulatory Guide 1.99, Revision 2. For the surveillance weld, the measured shift is less than the predicted shift plus margin using Regulatory Guide 1.99, Revision 2.

- Researchers measured flux wires and performed a fluence calculation to determine the fluence for the 288°-R ISP(E) reinserted surveillance capsule.

WHY THIS MATTERS

Results of this work will be used in the BWRVIP ISP, which is utilized by U.S. BWR fleet owners to satisfy the requirements of 10 CFR 50, Appendix G and Appendix H. The ISP provides high quality data to monitor BWR RPV embrittlement. The ISP results in significant cost savings for the BWR fleet and provides more accurate monitoring of embrittlement in BWR vessel materials. Plants for which the DAEC surveillance materials are assigned as the representative surveillance materials under the ISP must consider these test results in development of RPV integrity evaluations and plant operating pressure-temperature limit curves.

HOW TO APPLY RESULTS

Instructions for using the data, results, and conclusions are provided in the following technical report:

BWRVIP-135, Revision 4: BWR Vessel and Internals Project, Integrated Surveillance Program (ISP) Data Source Book and Plant Evaluations. EPRI, Palo Alto, CA: 2021. 3002020996.

LEARNING AND ENGAGEMENT OPPORTUNITIES

- The program plan for the BWRVIP ISP is described in the following technical report: BWRVIP-86, Revision 1-A: BWR Vessel and Internals Project, Updated BWR Integrated Surveillance Program (ISP) Implementation Plan. EPRI, Palo Alto, CA: 2012.1025144.
- Data collected under the ISP and instructions for use of the data are contained in the following technical report: BWRVIP-135, Revision 4: BWR Vessel and Internals Project, Integrated Surveillance Program (ISP) Data Source Book and Plant Evaluations, EPRI, Palo Alto, CA: 2021. 3002020996.
- The program plan for the Subsequent License Renewal Applicants (SLRA) is described in the following technical report: BWRVIP-321-A: Boiling Water Reactor Vessel and Internals Project: Plan for Extension of the BWR Integrated Surveillance Program (ISP) Through the Second License Renewal (SLR). EPRI, Palo Alto, CA: 2021. 3002020504.

EPRI CONTACT: Steven K. Williams, Principal Technical Leader, swilliams@epri.com

PROGRAM: Boiling Water Reactor Vessel and Internals Program (BWRVIP), P41.01.03

IMPLEMENTATION CATEGORY: Category 1 - Regulatory

EPRI
3420 Hillview Avenue, Palo Alto, California 94304-1338 • PO Box 10412, Palo Alto, California 94303-0813 USA
800.313.3774 • 650.855.2121 • askepri@epri.com • www.epri.com

CONTENTS

LIST OF FIGURES

LIST OF TABLES

1
INTRODUCTION

Test coupons of reactor vessel ferritic beltline materials are irradiated in reactor surveillance capsules to facilitate evaluation of vessel fracture toughness in vessel integrity evaluations. The key values that characterize fracture toughness are the reference temperature of nil-ductility transition (RT_{NDT}) and the upper shelf energy (USE). These are defined in 10CFR50, Appendix G [1] and in Appendix G of the ASME Boiler and Pressure Vessel Code, Section XI [2]. Appendix H of 10CFR50 [1] and ASTM E185-82 [3] establish the methods to be used for testing of surveillance capsule materials.

In the late 1990s, the BWR Vessel and Internals Project (BWRVIP) initiated the BWRVIP Integrated Surveillance Program (ISP) as documented in BWRVIP-86, Rev. 1-A [4], and the BWRVIP assumed responsibility for testing and evaluation of ISP capsules. The surveillance plate and weld from the Duane Arnold Energy Center (DAEC) reactor pressure vessel were designated as "ISP representative surveillance materials" to be tested by the ISP according to an approved capsule withdrawal and test schedule.

This report addresses the withdrawal and testing of the DAEC 288°-R surveillance capsule. The capsule contained flux wires for neutron flux monitoring, Charpy V-notch impact test specimens, and tensile specimens. The 288°-R capsule contained Charpy specimens that were initially irradiated in the DAEC reactor during Cycles 1 through 7, inclusive. Selected Charpy specimens were reconstituted and then reinserted into the Duane Arnold reactor at the beginning of Cycle 9. The reinserted capsule was subsequently irradiated for 19 cycles of operation before it was removed in October 2020 and shipped to MP Machinery & Testing, LLC for opening and testing of the Charpy V-notch surveillance specimens. Evaluation of the fluence environment was conducted by TransWare Enterprises, Inc. Final evaluation of the Charpy test data and irradiated material properties and compilation of this report were performed by EPRI. The Charpy V-notch surveillance materials were tested per ASTM E185-82, and the information and the associated evaluations provided in this report have been performed in accordance with the requirements of 10CFR50, Appendix B [5].

This report compares the irradiated material properties of surveillance plate heat B0673-1 and surveillance weld heat DA1 SMAW to their unirradiated (e.g., baseline) properties. The observed embrittlement (as characterized by the shift in the Charpy energy curve 30 ft-lb (41J) index temperature or ΔT_{30}) is compared to that predicted by U.S. Nuclear Regulatory Commission (U.S. NRC) Regulatory Guide 1.99, Revision 2 [6]. Other BWRVIP ISP reports will integrate the results from the 288°-R surveillance capsule with the results from the prior capsules withdrawn from DAEC (288°, 36° and 108°), as well as the Supplemental Surveillance Program Capsule SSP F (for both the DAEC surveillance plate and weld materials), for a broader characterization of embrittlement behavior.

1.1 Implementation Requirements

The results documented in this report will be utilized by the BWRVIP ISP and by individual utilities to demonstrate compliance with 10CFR50, Appendix H, Reactor Vessel Material Surveillance Program Requirements. Therefore, the implementation requirements of 10CFR50, Appendix H govern and the implementation requirements of Nuclear Energy Institute (NEI) 03-08, Guideline for the Management of Materials Issues [7], are not applicable.

2
MATERIALS AND TEST SPECIMEN DESCRIPTION

The General Electric (GE) designed DAEC 288°-R surveillance capsule was removed from the plant on October 22, 2020, and subsequently shipped to MP Machinery and Testing, LLC (MPM) for analysis. The capsule was a GE standard single basket design containing a total of three Charpy packets and four tensile tubes. Two of the tensile tubes were empty and the other two contained miniature tensile specimens. Within each Charpy packet were a total of 12 Charpy V-notch specimens and three high purity dosimetry wires. The DAEC 288°-R capsule is not an original plant capsule. The capsule was constructed by GE using weld reconstituted Charpy specimens and miniature tensile specimens to provide material embrittlement data for operation in the extended license period. This is the fourth surveillance capsule to be removed from DAEC and tested. The original 288° capsule was tested by GE and the data are given in Reference [8]. The 36° capsule was also tested by GE and the results are reported in Reference [9]. The 108° capsule was tested by MPM and the data are given in Reference [10].

2.1 Dosimeters

The dosimetry wires for packets G41 and G43 were located along the ends of the Charpy specimens at various radial distances from the core. The dosimetry wires for the G42 packet were found both along the Charpy specimen ends, and, also under the Charpy specimens. So, for the purpose of dosimetry analysis, the uncertainty must consider the shielding provided by a Charpy bar thickness and the fact that the wire locations vary both radially and axially.

It was observed during capsule unloading that the G42 packet leaked, and the Ni and Cu wires were damaged. Further, the Ni wire had partially disintegrated and moved from its initial position and was found lying across the surface of the Charpy specimens. The Cu wire was also partially disintegrated, but the testing facility was able to clean and extract enough material for dosimetry analysis.

Each of the three Charpy packets contained one high purity iron wire, one high purity copper wire, and one high purity nickel wire for fluence evaluation. Further details on the exact wire locations during the irradiation are provided in the capsule opening discussion given in Section 2.3. A detailed discussion of the radiometric analysis of the capsule dosimetry wires is provided in Appendix A.

2.2 Test Materials

The DAEC 288°-R surveillance capsule Charpy V-notch specimen inventory, material descriptions, unirradiated (baseline) Charpy impact data, and previously measured data are summarized in this section of the report.

2.2.1 Capsule Loading Inventory

The DAEC 288°-R surveillance capsule inventory is provided in Table 2-1. All of the capsule specimens, which include Charpy specimens, tensile specimens, and dosimeters, were recovered from the capsule basket. Testing was performed on all 12 of the weld specimens and all 15 of the base metal specimens. The heat affected zone (HAZ) specimens were cleaned and put into the repository storage without being impact tested. The dosimetry wires were counted and weighed to determine specific activities. All six of the tensile specimens (three base and three weld), remain untested and are being held in reserve for future surveillance program use. The technical advantage of storing the tensile specimens untested is that there will be options in the future for how these specimens will be used to obtain useful data. For example, the tensile specimen geometry is conducive to fabrication of sub-size Charpy specimens. Further, research is underway which will enable the determination of plane-strain fracture toughness data from Charpy and miniaturized Charpy-sized specimens. With these new technologies in view, the stored materials may be used to measure fracture toughness if needed in the future. Therefore, all tensile and HAZ specimens have been placed into the archive storage. The broken Charpy specimen halves have also been added to long-term archive storage for future use in mechanical behavior specimen testing, chemistry analysis, and microstructural studies.

A drawing of the Charpy test specimen is shown in Figure 2-1 for reference. Photographs of the capsule are given in Figures 2-2 through 2-4. The markings on the outside of the capsule, including the reactor code and the capsule code, were recorded and verified.

Table 2-1
DAEC 288°-R Surveillance Capsule Specimen Inventory

Charpy[1] Packet No.[2]	Number of Charpy Specimens			Number of Flux Wires			Relative Vertical Position
	Base	Weld	HAZ	Fe	Cu	Ni	
G41	11	0	1	1	1	1	Lowest Charpy Packet in Basket
G42	4	0	8	1	1	1	Middle Charpy Packet in Basket
G43	0	12	0	1	1	1	Highest Charpy Packet in Basket

1. The surveillance program also includes tensile specimens, but the tensile specimens were not tested. The six tensile specimens for this capsule were located at axial positions below Charpy packet G42 and above Charpy Packet G41 as shown in Figure 2-9.
2. The packet numbers in this table are organized by axial position in the capsule with packet G41 at the lowest elevation in the reactor and packet G43 at the highest elevation in the reactor.

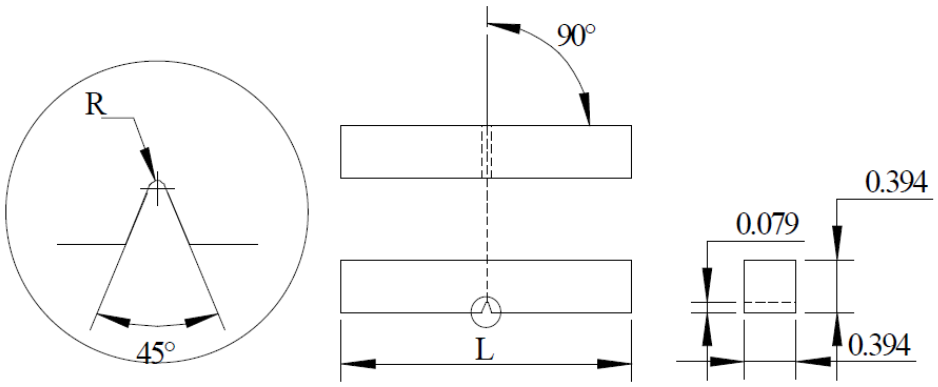

ASTM E 23 permissible variations shall be as follows:

Notch length to edge:	90 ± 2 degrees
Adjacent sides shall be at:	90 degrees ± 10 minutes
Cross-sectional dimensions:	± 0.003 inches
Length of specimen (L):	2.165 (+0.0, -0.100) inches
Centering of notch (L/2):	± 0.039 inches
Angle of notch:	± 1 degree
Radius of notch:	0.010 ± 0.001 inches
Notch depth:	± 0.001 inches
Finish requirements:	63 µ-inch on notched surface and opposite face; 4 µ-inch elsewhere

Figure 2-1
Drawing Showing the Charpy Test Specimen Geometry and ASTM E 23 Permissible Variations

Figure 2-2
Photograph of the DAEC 288°-R Capsule (top) and a Magnified View of the External Identification Markings (bottom)

Figure 2-2 shows the side of the surveillance capsule which faced the reactor vessel. The identification code, "117C4936 G025", was engraved near the hook.

Figure 2-3
Photograph of the DAEC 288°-R Capsule (top) and a Magnified View (bottom)

Figure 2-3 shows the side of the surveillance capsule which faced the reactor core. The reactor and capsule codes are seen near the hook.

Note that the reactor and basket codes (small holes in the corners of the capsule basket) as shown in Figure 2-3 and the identification code, "117C4936 G025" as shown in Figure 2-2, are on opposite sides of the capsule.

Figure 2-4
Photograph of the Inside of the DAEC 288°-R Capsule

2.2.2 Material Description

The DAEC plant is a GE BWR/4 design and the construction was performed by Chicago Bridge & Iron (CB&I). The pressure vessel shell and plate materials are ASME SA533B, class 1 low alloy steel. The surveillance base metal specimens were machined from plate heat number B0673-1 in the longitudinal orientation (LT). Unirradiated baseline data are available for this material, and for the weld and HAZ materials as well. All of the base metal specimens were stamped on the ends with the FAB code markings assigned by GE.

The weld and HAZ Charpy surveillance specimens were made by welding together two pieces of the surveillance test plate heat B0673-1. Reference [9] reports that the weld procedure used for the surveillance specimens was the same as that used for the welds in the beltline region. The welded surveillance plates were given a stress relief heat treatment at 1150°F to simulate the pressure vessel fabrication conditions.

2.2.3 Chemical Composition

Table 2-2 details the best estimate average chemistry values for plate heat B0673-1 surveillance material. Table 2-3 details the best estimate average chemistry values for weld heat DA1 SMAW surveillance material. Chemical compositions are presented in weight percent. If there are multiple measurements on a single specimen, those are first averaged to yield a single value for that specimen, and then the different specimens are averaged to determine the heat best estimate.

Table 2-2
Best Estimate Chemistry of Available Data Sets for Plate Heat B0673-1

Cu (wt%)	Ni (wt%)	P (wt%)	S (wt%)	Si (wt%)	Specimen ID	Source
0.15	0.7	0.006	—	0.07	ETJ	Reference [11], Appendix A-3
0.15	0.69	0.006	—	0.06	ETK	
0.14	0.62	0.010	—	0.01	EB4	
0.141	0.62	0.014	—	0.02	EBA	
0.145	0.65	0.010	—	0.09	EBE	
0.15	0.61	0.011	—	0.18	Baseline CMTR	
0.15	**0.65**	**0.010**	**—**	**0.07**	**←Best Estimate Average**	

Table 2-3
Best Estimate Chemistry of Available Data Sets for Weld Heat DA1 SMAW

Cu (wt%)	Ni (wt%)	P (wt%)	S (wt%)	Si (wt%)	Specimen ID	Source
0.02	1.00	0.011	—	0.32	EU3 irrad	Reference [11], Appendix B-5
0.02	0.90	0.010	—	0.33	EU6 irrad	
0.025	0.96	0.011	—	0.02	EJM	
0.025	0.94	0.008	—	0.02	EJJ	
0.024	0.88	0.010	—	0.02	EJA	
0.02	**0.94**	**0.010**	—	**0.14**	**← Best Estimate Average**	

2.2.4 CVN Baseline Properties

Table 2-4 contains the unirradiated Charpy data for the B0673-1 surveillance plate material. Table 2-5 contains the unirradiated Charpy data for the DA1 SMAW surveillance weld material.

Table 2-4
Unirradiated Longitudinal Charpy V-Notch Impact Test Results for Surveillance Base Metal (Heat B0673-1) Specimens from the DAEC Surveillance Program [11]

Base Unirradiated: Heat B0673-1, Longitudinal							
Specimen ID	Test Temperature		Impact Energy		Lateral Expansion		Percent Shear
	°F	(°C)	ft-lb	(J)	mils	(mm)	%
ED4	-100.0	(-73.3)	6.50	(8.81)	7.0	(0.18)	0.0
ED1	-80.0	(-62.2)	4.20	(5.69)	5.0	(0.13)	0.0
ECT	-40.0	(-40.0)	9.00	(12.20)	14.0	(0.36)	10.0
EDK	-40.0	(-40.0)	24.00	(32.54)	30.0	(0.76)	5.0
ED7	-30.0	(-34.4)	38.00	(51.52)	35.0	(0.89)	5.0
EDT	-30.0	(-34.4)	49.00	(66.43)	30.0	(0.76)	5.0
ED6	-20.0	(-28.9)	47.00	(63.72)	43.0	(1.09)	10.0
ED5	-10.0	(-23.3)	43.00	(58.30)	43.0	(1.09)	20.0
ECP	0.0	(-17.8)	56.50	(76.60)	49.0	(1.24)	25.0
ECM	40.0	(4.4)	98.50	(133.55)	73.0	(1.85)	40.0
ECL	120.0	(48.9)	134.50	(182.36)	73.0	(1.85)	80.0
ECK	200.0	(93.3)	158.50	(214.89)	93.0	(2.36)	85.0
EDY	300.0	(148.9)	163.50	(221.67)	81.0	(2.06)	90.0
EDA	400.0	(204.4)	No Break		No Break		No Break

Table 2-5
Unirradiated Charpy V-Notch Impact Test Results for Surveillance Weld Metal (Heat DA1 SMAW) Specimens from the DAEC Surveillance Program [11]

Weld Unirradiated: Heat DA1 SMAW							
Specimen ID	Test Temperature		Impact Energy		Lateral Expansion		Percent Shear
	°F	(°C)	ft-lb	(J)	mils	(mm)	%
EET	-100.0	(-73.3)	6.50	(8.81)	11.0	(0.28)	10.0
EEK	-80.0	(-62.2)	5.50	(7.46)	10.0	(0.25)	15.0
EK3	-60.0	(-51.1)	16.80	(22.78)	19.0	(0.48)	40.0
EK4	-50.0	(-45.6)	21.50	(29.15)	22.0	(0.56)	20.0
EEE	-40.0	(-40.0)	49.00	(66.43)	45.0	(1.14)	20.0
EK2	-20.0	(-28.9)	58.00	(78.64)	57.0	(1.45)	50.0
EEL	0.0	(-17.8)	52.5	(71.18)	50.0	(1.27)	30.0
EEY	40.0	(4.4)	65.00	(88.13)	61.0	(1.55)	50.0
EED	120.0	(48.9)	102.00	(138.29)	88.0	(2.24)	80.0
EEM	200.0	(93.3)	94.00	(127.45)	65.0	(1.65)	70.0
EK5	300.0	(148.9)	88.20	(119.58)	93.0	(2.36)	60.0
EK6	400.0	(204.4)	113.70	(154.15)	96.0	(2.44)	70.0

The baseline test data were fit to a hyperbolic tangent curve using the computer program CVGRAPH, Version 6.02 [12]. Figures 2-5 and 2-6 show the fitted Charpy energy data curve for the unirradiated plate and weld, respectively. Figures 2-7 and 2-8 show the fitted lateral expansion curve for the unirradiated plate and weld, respectively. Table 2-6 summarizes the unirradiated (baseline) Charpy V-notch properties (index temperatures) of plate heat B0673-1 and weld heat DA1 SMAW. In this table and throughout this report, T_{30} is the 30 ft-lb (41 J) transition temperature; T_{50} is the 50 ft-lb (68 J) transition temperature; T_{35mil} is the 35 mil (0.89 mm) lateral expansion temperature; and USE is the average energy absorption at full shear fracture appearance.

Table 2-6
Baseline CVN Properties

Material Identity	Material	T_{30} °F (°C)	T_{50} °F (°C)	T_{35mil} °F (°C)	Upper Shelf Energy (USE) ft-lb (J)
B0673-1 (LT Orientation)	Duane Arnold Surveillance Plate	-35.5 (-37.5)	-7.3 (-21.8)	-23.6 (-30.9)	158.1 (214.4)
DA1 SMAW	Duane Arnold Surveillance Weld	-45.4 (-43.0)	-10.2 (-23.4)	-37.3 (-38.5)	99.0 (134.2)

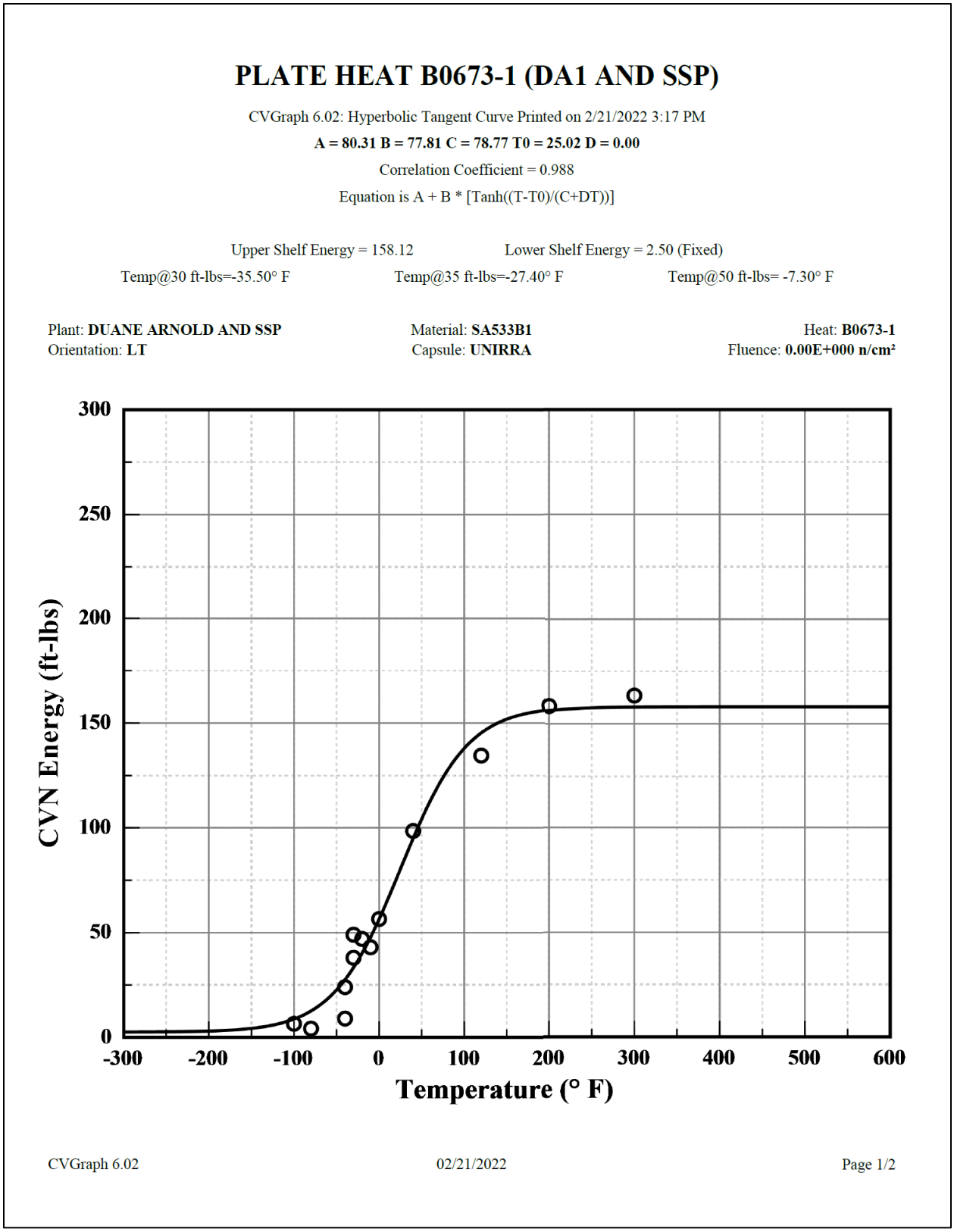

Figure 2-5
Charpy Energy Plot for Plate Heat B0673-1 (LT) Unirradiated

Plant: **DUANE ARNOLD AND SSP** Material: **SA533B1** Heat: **B0673-1**
Orientation: **LT** Capsule: **UNIRRA** Fluence: **0.00E+000 n/cm²**

PLATE HEAT B0673-1 (DA1 AND SSP)

Charpy V-Notch Data

Temperature (° F)	Input CVN	Computed CVN	Differential
-100	6.5	8.7	-2.25
-80	4.2	12.6	-8.41
-40	9.0	27.6	-18.56
-40	24.0	27.6	-3.56
-30	38.0	33.4	4.64
-30	49.0	33.4	15.64
-20	47.0	40.1	6.88
-10	43.0	47.8	-4.83
0	56.5	56.4	0.10
40	98.5	94.9	3.57
120	134.5	145.3	-10.81
200	158.5	156.3	2.19
300	163.5	158.0	5.53

CVGraph 6.02 02/21/2022 Page 2/2

Figure 2-5 (Continued)
Charpy Energy Plot for Plate Heat B0673-1 (LT) Unirradiated

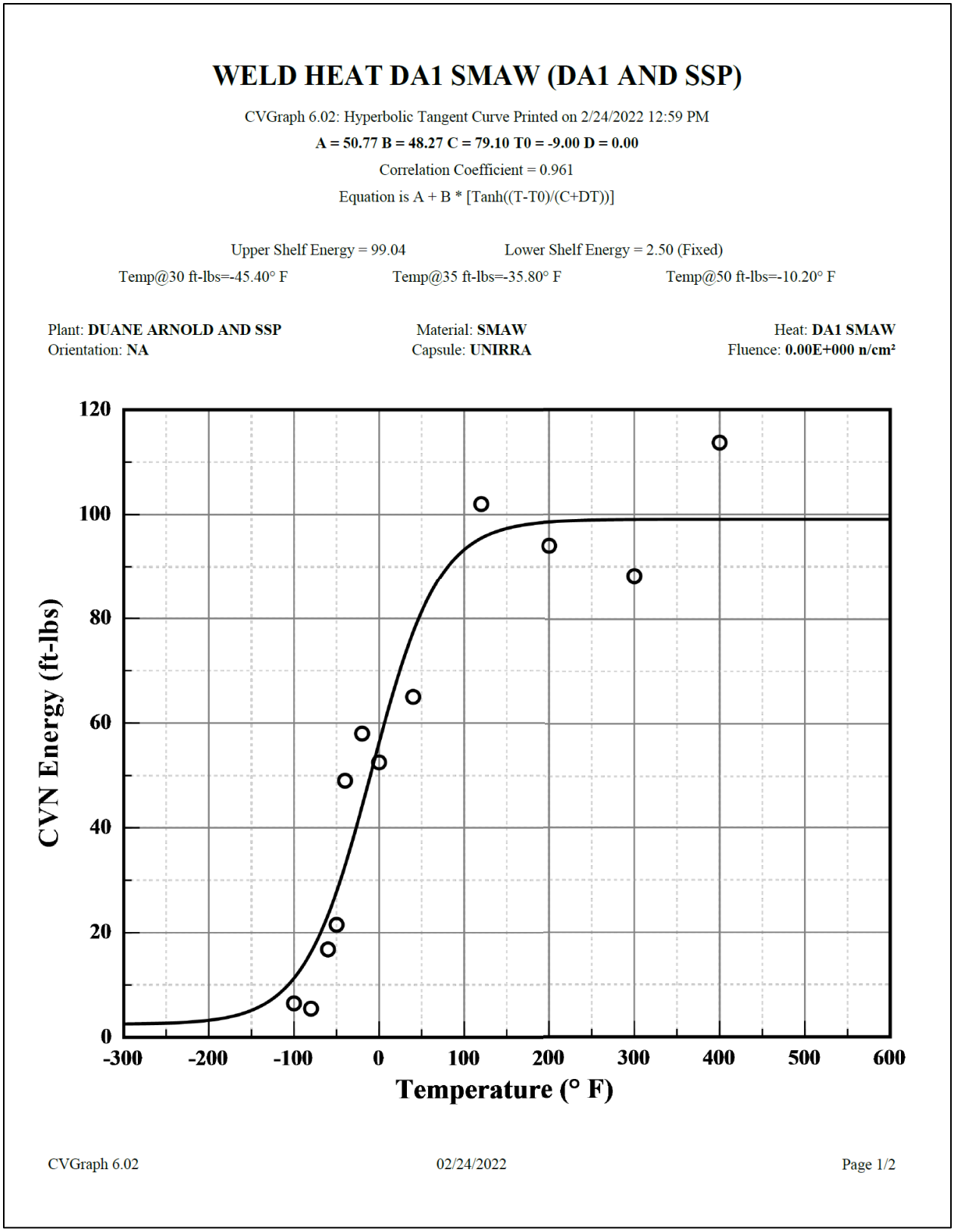

Figure 2-6
Charpy Energy Plot for Weld Heat DA1 SMAW Unirradiated

Plant: **DUANE ARNOLD AND SSP** Material: **SMAW** Heat: **DA1 SMAW**
Orientation: **NA** Capsule: **UNIRRA** Fluence: **0.00E+000 n/cm²**

WELD HEAT DA1 SMAW (DA1 AND SSP)

Charpy V-Notch Data

Temperature (° F)	Input CVN	Computed CVN	Differential
-100	6.5	11.3	-4.79
-80	5.5	16.3	-10.75
-60	16.8	23.3	-6.55
-50	21.5	27.8	-6.28
-40	49.0	32.8	16.23
-20	58.0	44.1	13.90
0	52.5	56.2	-3.74
40	65.0	77.4	-12.36
120	102.0	95.5	6.52
200	94.0	98.6	-4.56
300	88.2	99.0	-10.80
400	113.7	99.0	14.66

CVGraph 6.02 02/24/2022 Page 2/2

Figure 2-6 (Continued)
Charpy Energy Plot for Weld Heat DA1 SMAW Unirradiated

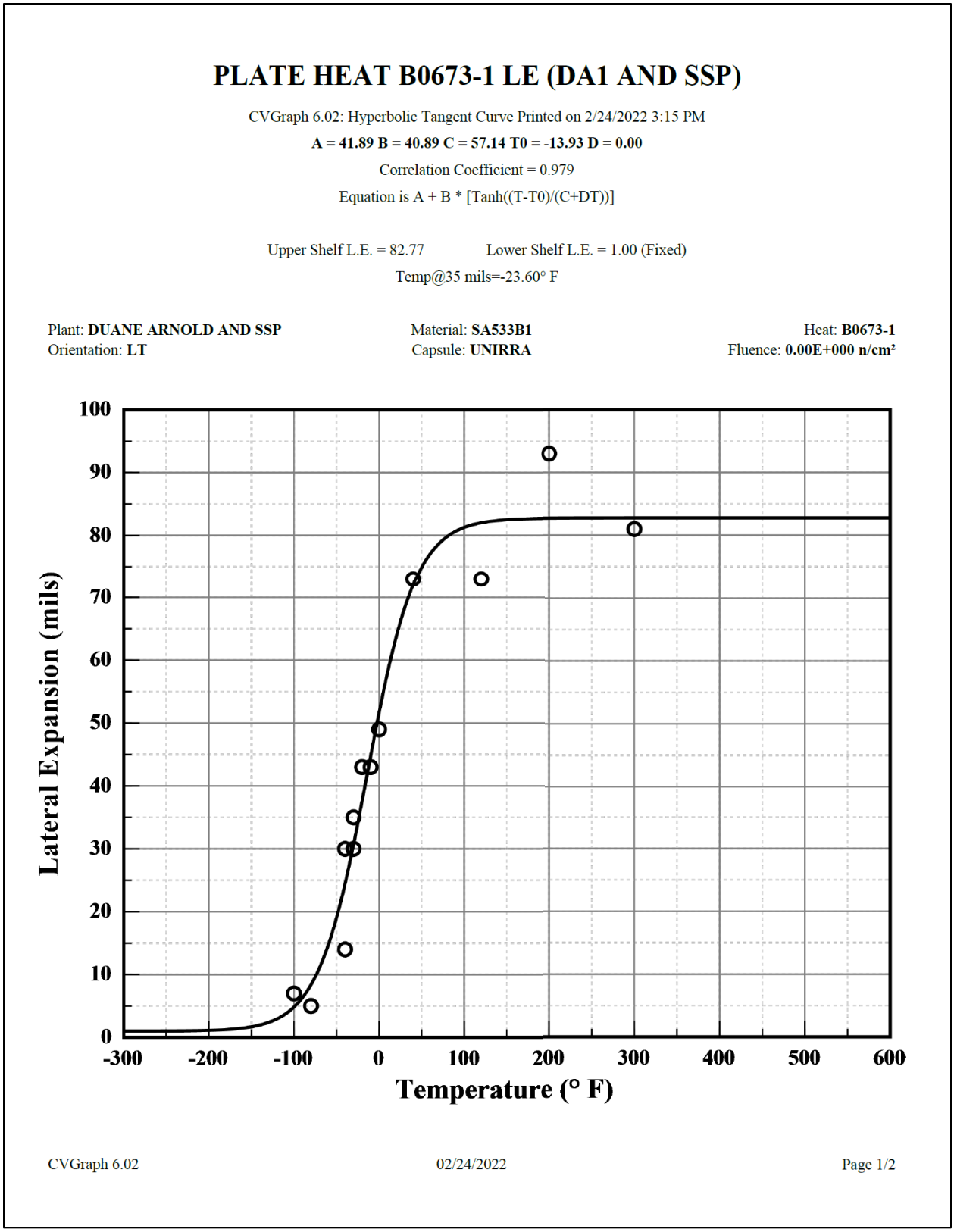

Figure 2-7
Lateral Expansion Plot for Plate Heat B0673-1 (LT) Unirradiated

Plant: **DUANE ARNOLD AND SSP** Material: **SA533B1** Heat: **B0673-1**
Orientation: **LT** Capsule: **UNIRRA** Fluence: **0.00E+000 n/cm²**

PLATE HEAT B0673-1 LE (DA1 AND SSP)

Charpy V-Notch Data

Temperature (° F)	Input L. E.	Computed L. E.	Differential
-100	7.0	4.8	2.17
-80	5.0	8.4	-3.37
-40	14.0	24.4	-10.43
-40	30.0	24.4	5.57
-30	35.0	30.7	4.32
-30	30.0	30.7	-0.68
-20	43.0	37.6	5.44
-10	43.0	44.7	-1.70
0	49.0	51.7	-2.66
40	73.0	72.0	0.98
120	73.0	82.0	-9.03
200	93.0	82.7	10.27
300	81.0	82.8	-1.77

CVGraph 6.02 02/24/2022 Page 2/2

Figure 2-7 (Continued)
Lateral Expansion Plot for Plate Heat B0673-1 (LT) Unirradiated

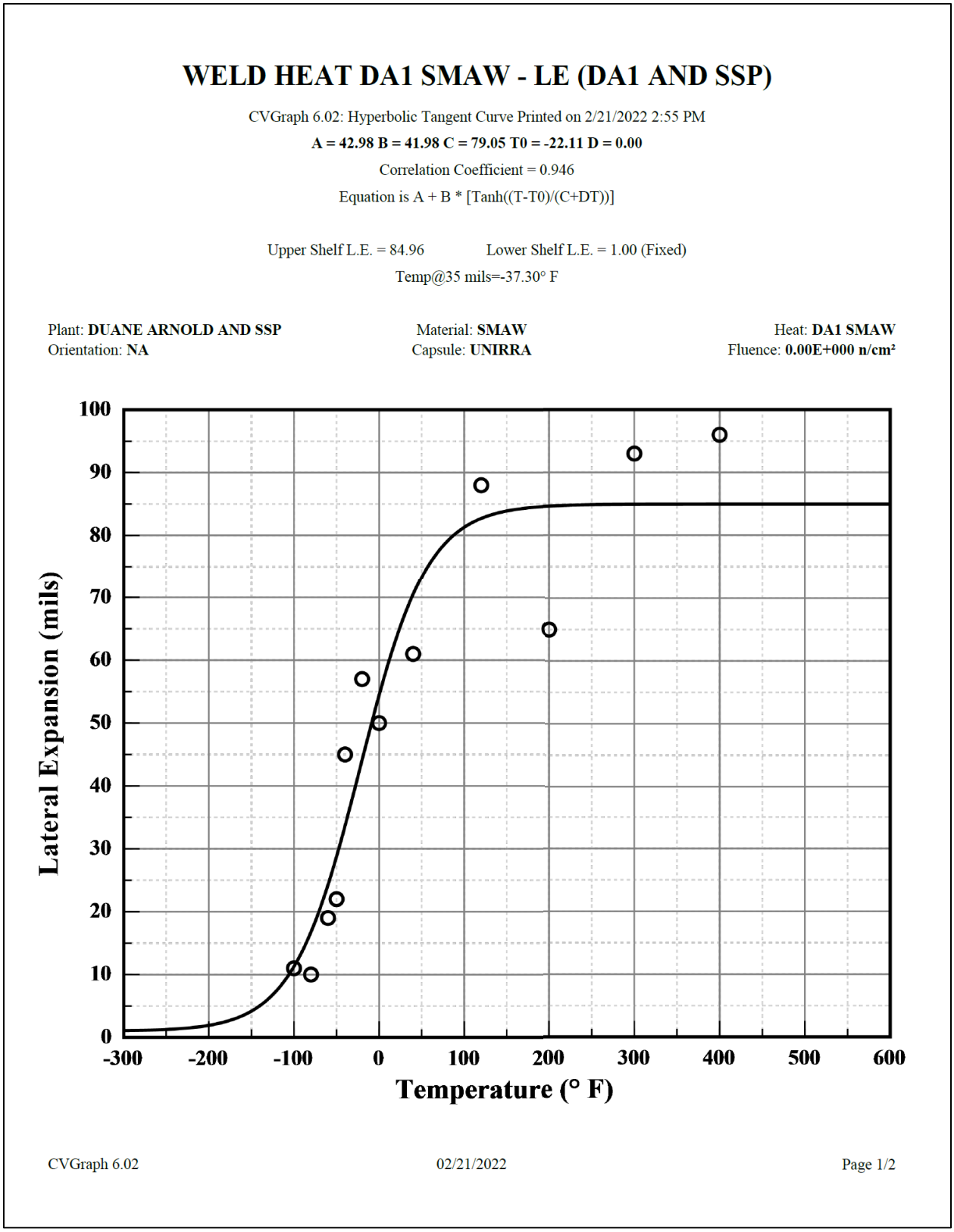

Figure 2-8
Lateral Expansion Plot for Weld Heat DA1 SMAW Unirradiated

Plant: **DUANE ARNOLD AND SSP** Material: **SMAW** Heat: **DA1 SMAW**
Orientation: **NA** Capsule: **UNIRRA** Fluence: **0.00E+000 n/cm²**

WELD HEAT DA1 SMAW - LE (DA1 AND SSP)

Charpy V-Notch Data

Temperature (° F)	Input L. E.	Computed L. E.	Differential
-100	11.0	11.3	-0.27
-80	10.0	16.8	-6.77
-60	19.0	24.3	-5.27
-50	22.0	28.8	-6.76
-40	45.0	33.6	11.36
-20	57.0	44.1	12.90
0	50.0	54.4	-4.42
40	61.0	70.5	-9.52
120	88.0	82.7	5.28
200	65.0	84.7	-19.66
300	93.0	84.9	8.06
400	96.0	85.0	11.04

CVGraph 6.02 02/21/2022 Page 2/2

Figure 2-8 (Continued)
Lateral Expansion Plot for Weld Heat DA1 SMAW Unirradiated

2.3 Capsule Opening

The DAEC 288°-R reinsertion surveillance capsule was opened on February 15, 2021. As shown in Figures 2-2 through 2-4, this surveillance capsule consisted of a container holding three Charpy packets and four tensile tubes. Each Charpy packet contained 12 Charpy specimens. The outside of the capsule had identification markings which could be clearly read. On one side, the capsule container was marked with the reactor and basket codes. The reactor code matches the reactor code in Reference [9]. The capsule container was also engraved with the marking "117C4936 G025" on the other side facing the reactor core.

Attention was paid to the location of the Charpy packets, specimens, and dosimetry wires during disassembly of the capsule. The dosimetry wire locations along the ends of the Charpy specimens are shown in Figure 2-9 along with the specimen IDs. The inside of the G41 packet is shown in Figures 2-10 through 2-15. Lack of fusion defects from the weld reconstitution are apparent in most of the specimens. While some small lack of fusion defects are expected, the size of these defects in the GE specimens is a concern that was addressed. As discussed in Section 2.4 of this report, further characterization of the base and weld specimens was needed since many notches were found to be near the reconstitution weld interface. The dosimetry wires and Charpy specimens were placed in individually marked containers for positive identification throughout the work.

During the G42 packet opening, water was observed leaking from the packet (Figure 2-16). As shown in Figures 2-17 through 2-20, the specimens were found to be heavily oxidized, and the Ni and Cu wires are partially disintegrated. Most of the G42 specimens were HAZ, so a decision was made to place these specimens into the repository without any further cleaning or testing. The basis for the decision to set aside the compromised HAZ specimens is that the ISP does not test HAZ specimens, which was approved by the NRC in BWRVIP-86, Rev. 1-A. In addition, testing of HAZ specimens is no longer required by 10 CFR 50, Appendix H. However, the four base metal specimens from the G42 packet were carefully lapped to remove the oxide and prepare them for testing.

The contents of the G43 packet are shown in Figures 2-21 through 2-24. Visual examination of the G43 weld specimens revealed that several specimens were prepared by GE with the notch too close to the reconstituted weld interface. As mentioned, additional characterization work was needed, and this is reported in Section 2.4.

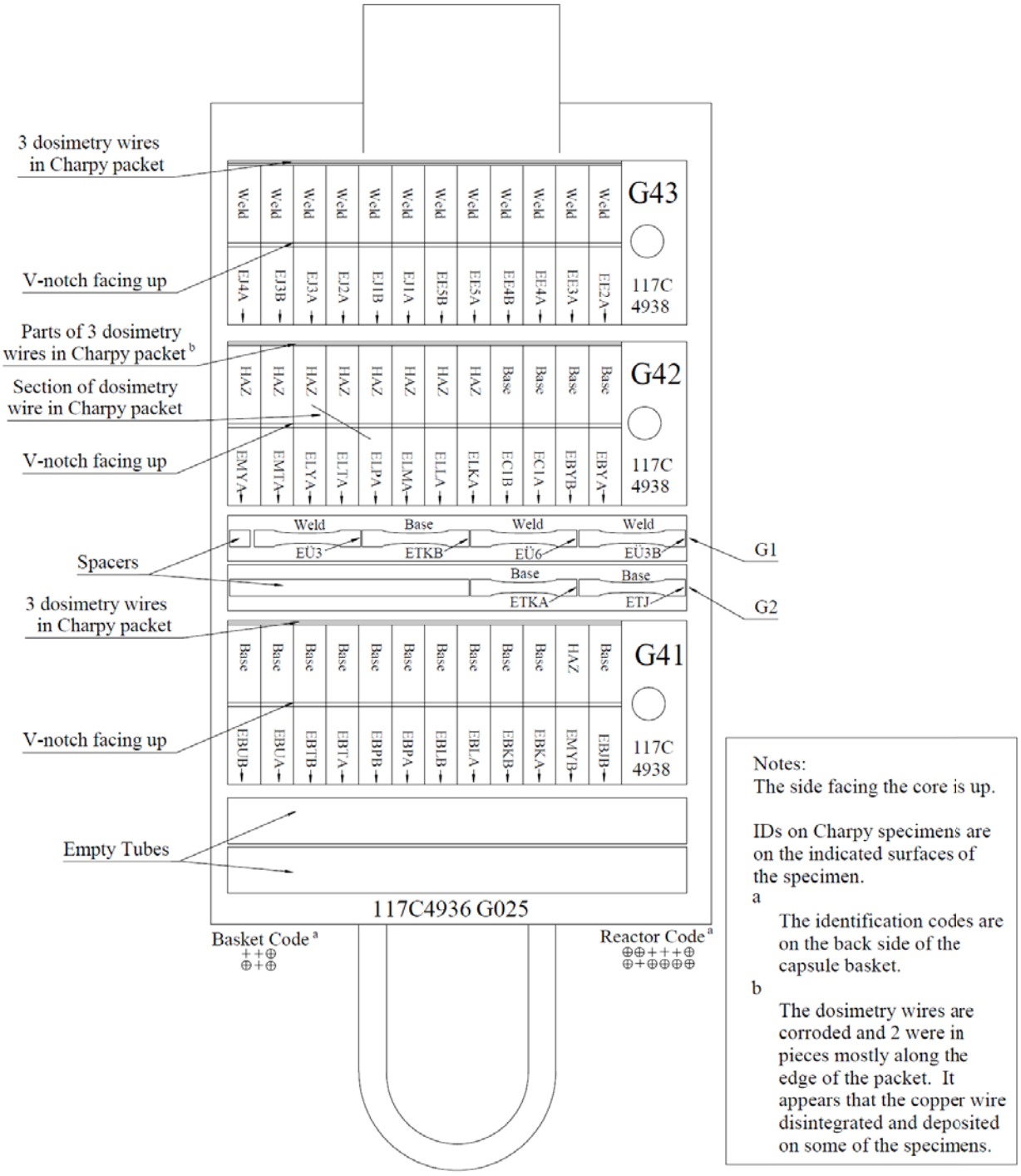

Figure 2-9
Drawing of the Identification Markings Found Inside the DAEC 288°-R Capsule

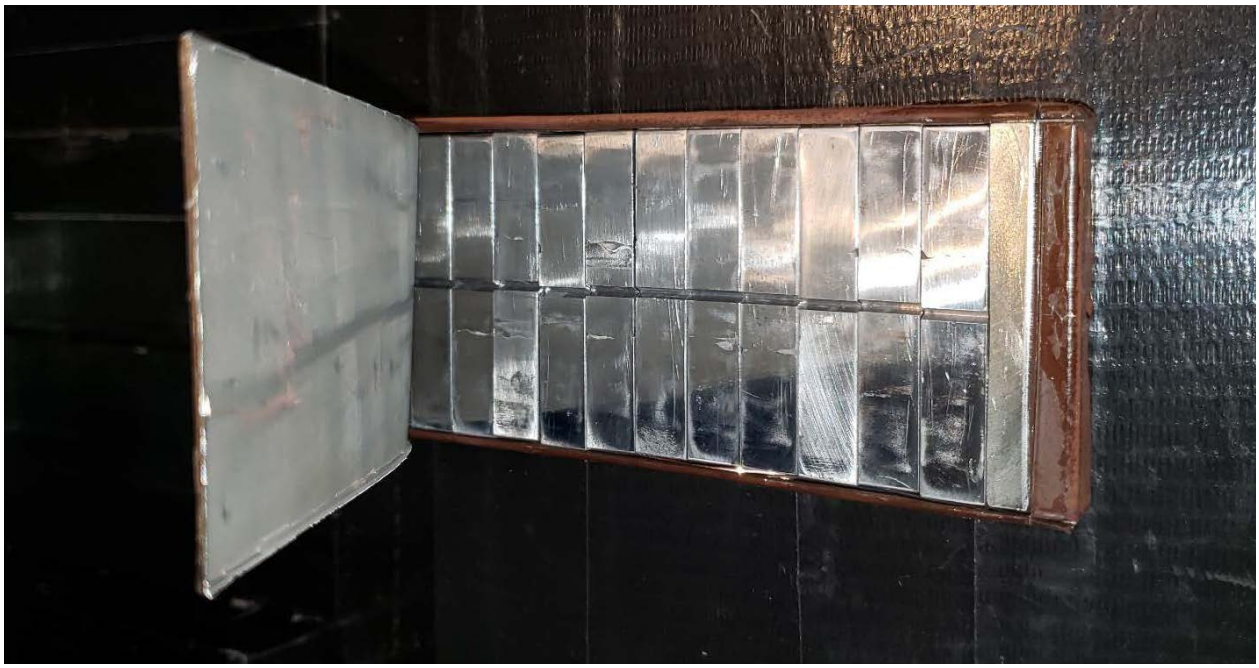

Figure 2-10
Photograph of the Inside of the G41 Charpy Packet within the DAEC 288°-R Capsule

Figure 2-11
Photograph of the Inside of the G41 Charpy Packet within the DAEC 288°-R Capsule Showing Dosimetry Wires Locations

Figure 2-12
Photograph of the Specimens (Notch Side Up) from the G41 Charpy Packet within the DAEC 288°-R Capsule Showing Voids

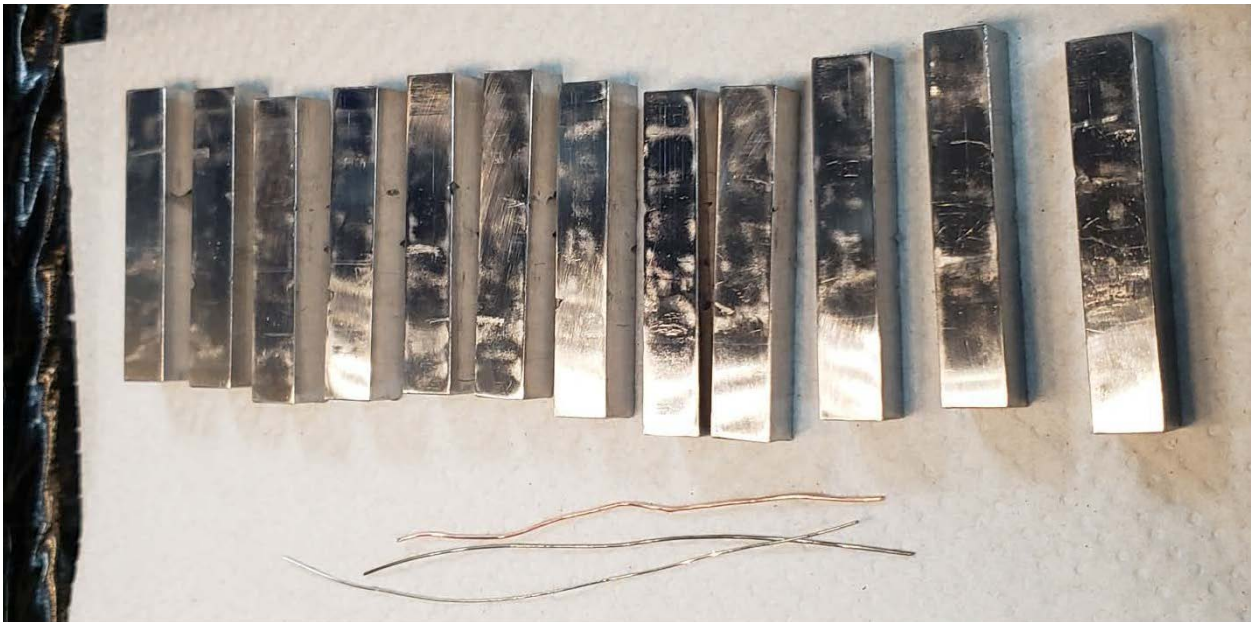

Figure 2-13
Photograph of the Specimens (Notch Side Down) from the G41 Charpy Packet within the DAEC 288°-R Capsule Showing Voids

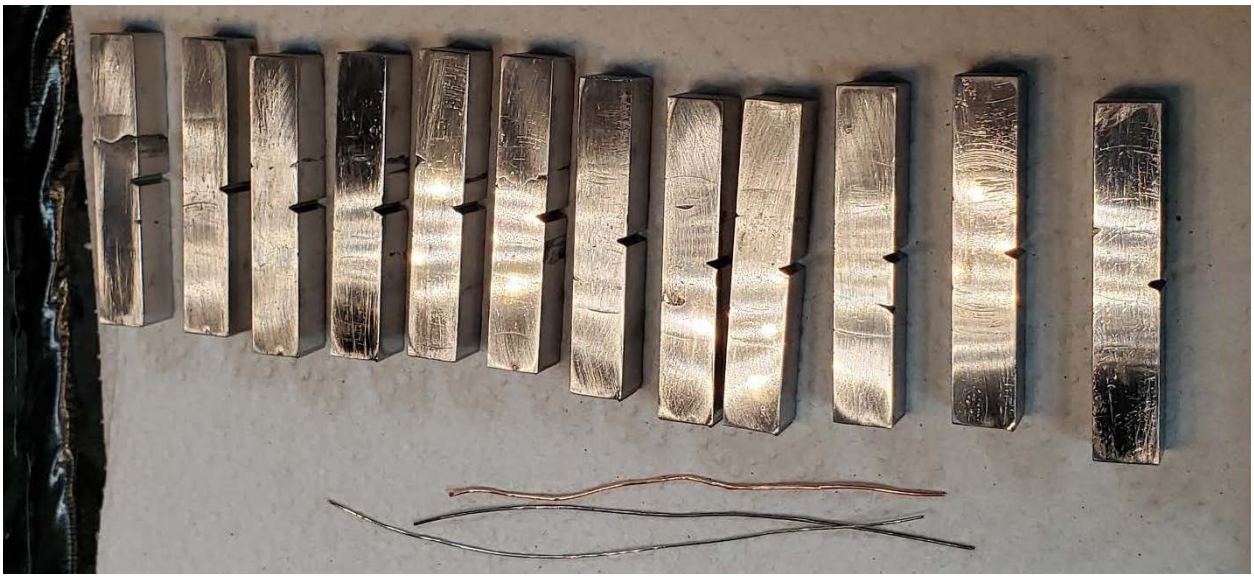

Figure 2-14
Photograph of the Specimens (Notch Side Right) from the G41 Charpy Packet within the DAEC 288°-R Capsule Showing Voids

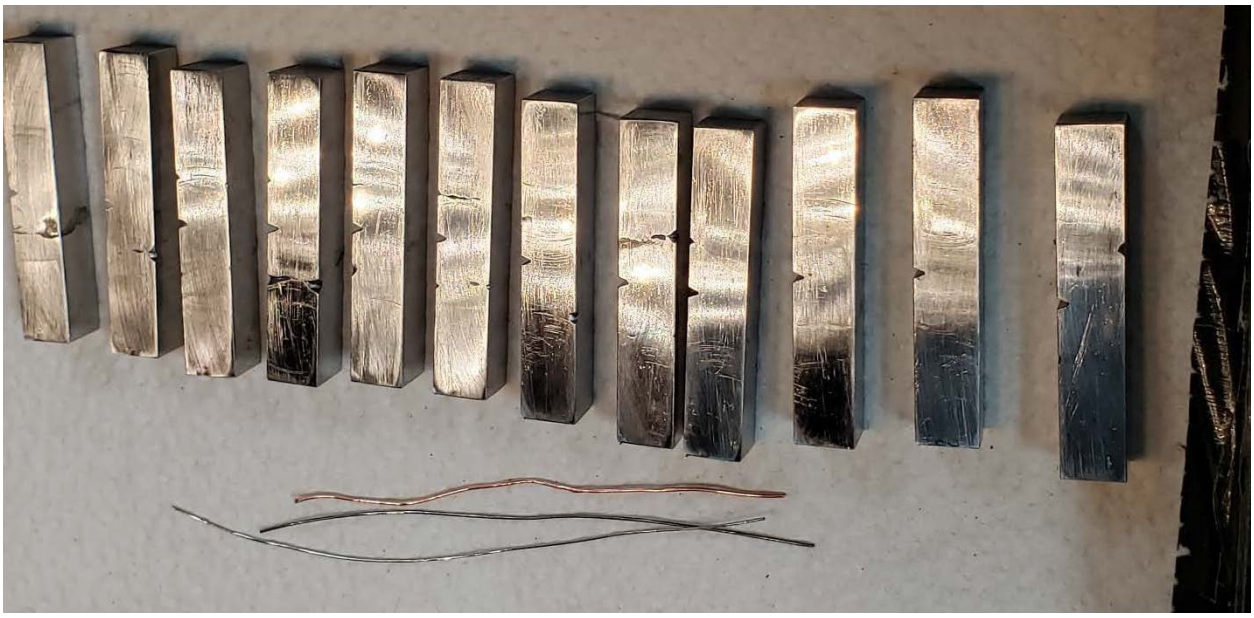

Figure 2-15
Photograph of the Specimens (Notch Side Left) from the G41 Charpy Packet within the DAEC 288°-R Capsule Showing Voids

Figure 2-16
Photograph of the G42 Charpy Packet within the DAEC 288°-R Capsule During Cutting Showing Water Leakage from Inside The Packet

Figure 2-17
Photograph of the Inside of the G42 Charpy Packet within the DAEC 288°-R Capsule

Figure 2-18
Photograph of the Inside of the G42 Charpy Packet within the DAEC 288°-R Capsule Showing Dosimetry Wires Locations

Figure 2-19
Photograph of the Inside of the G42 Charpy Packet within the DAEC 288°-R Capsule with the Specimens Removed Showing Dosimetry Wire Corrosion

Figure 2-20
Photograph of the Specimens from Inside of the G42 Charpy Packet within the DAEC 288°-R Capsule

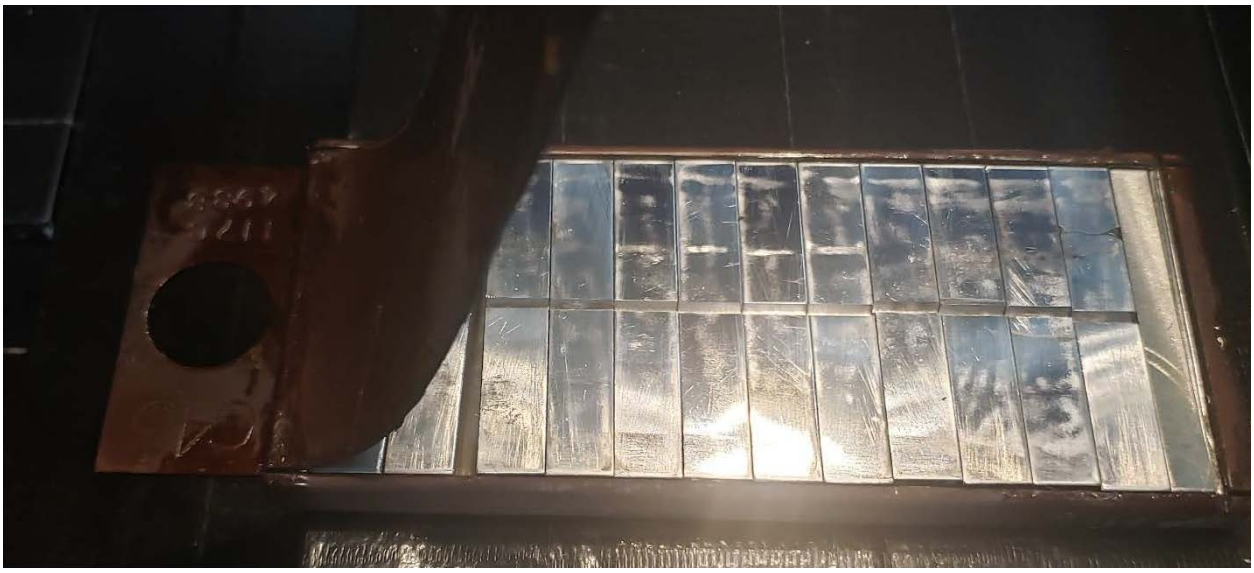

Figure 2-21
Photograph of the Inside of the G43 Charpy Packet within the DAEC 288°-R Capsule

Figure 2-22
Photograph of the Inside of the G43 Charpy Packet within the DAEC 288°-R Capsule

Figure 2-23
Photograph of the Inside of the G43 Charpy Packet within the DAEC 288°-R Capsule Showing Dosimetry Wires Locations

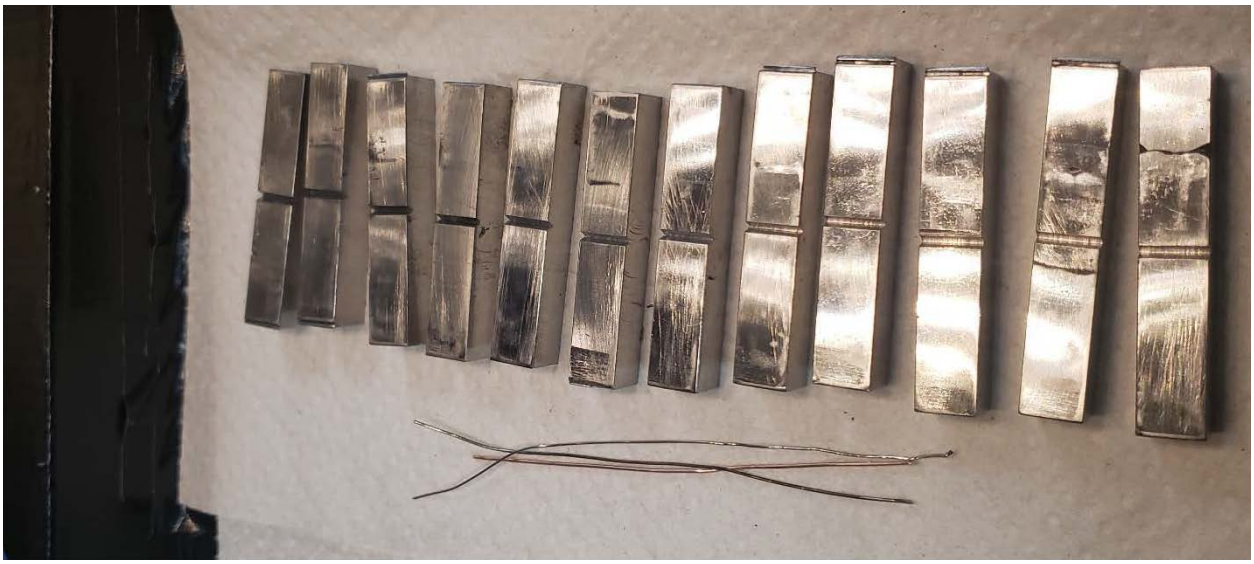

Figure 2-24
Photograph of the Specimens and Dosimetry Wires within the G43 Charpy Packet

2.4 Characterization of DAEC 288°-R Reinserted Capsule Base Metal and Weld Metal Reconstituted Surveillance Specimens

The base and weld Charpy specimens were measured in the as-received condition to determine whether they meet the requirements of ASTM E 23. A summary of the results of these measurements is given in Table 2-7. The key finding is that the specimens do not meet the specimen thickness and width requirements. It is apparent that GE machined the specimens after reconstitution welding to remove the weld splash and to ensure the specimens are flat and square. The GE post-reconstitution machining procedure does not fully meet ASTM E 23 specification because it has resulted in undersized specimen width and thickness. Based on review of fabrication records for reconstituted CVN specimens for Hatch 2 (another ISP host plant) circa 1991, it is possible that the CVN specimen thickness and/or width can fall below the minimum requirement of 0.391 inches by approximately 1% after final machining, etching and/or polishing of the reconstituted specimens. There are no industry or regulatory guidance regarding use of CVN specimens that deviate from ASTM standards. However, the slightly smaller cross section of the DAEC 288°-R capsule CVN specimens would likely reduce the absorbed energy, which is conservative. Since the measured CVN specimen cross section dimensions were approximately 1% or less of this lower tolerance for the CVN specimens tested, all other ASTM E23 requirements are met, and are consistent with prior experience fabricating reconstituted specimens, the CVN results are valid.

Of greater concern is the location of the weld specimen notches relative to the reconstitution weld HAZ interface. All of the base and weld specimens were etched on the top and bottom surfaces (as viewed with the specimen on the test machine supports). The surfaces that come in contact with the anvils and striker were not etched so as to not compromise the ASTM E 23 surface finish requirements. An example of an etched base metal specimen is shown in Figure 2-25. The reconstitution welds are shown to the right and left of the notch in this figure. The width of the reconstitution welds was measured and found to average about 5 mm in length, and these weld bands are surrounded by 0.5 mm HAZ bands. The width of the reconstitution welds is consistent with data reported in Reference [13] and related literature references.

As shown in Figures 2-26 and 2-27, there are reconstituted weld specimens that cannot be tested because they were notched in the reconstituted weld, or HAZ, and not near the center of the reactor pressure vessel weld. Measurements were made for all of the capsule base and weld specimens to characterize the distance from the root of the notch (i.e., the crack plane) to the closest reconstitution weld HAZ interface. These data are reported in Table 2-8. The key data are in the column labelled “Undisturbed Material Available for Testing”. Reference [13] refers to these data as the length between the reconstitution HAZ interfaces that is available for the plastic zone normal to the crack plane (PZN). In other words, the PZN must not interact with the reconstitution weld material to ensure the impact test results are valid. Reference [13] used a simple analytical fracture model to calculate the required PZN as a function of test temperature for both irradiated and unirradiated A533B steel. These data were used to define the following conservative, but reasonable, PZN screening criteria so that target test temperatures could be estimated for the capsule specimens:

PZN	Target Temperature Range	PZN	Target Temperature Range
2 mm	Lower Shelf	8 mm	Upper Transition Region
4 mm	Lower Transition Region	13 mm	Upper Shelf

Figure 2-25
Base Metal Specimen EBTB Showing Etched Surface.

The etch reveals the reconstitution welds to the left and right of the notch. The welds are nominally 5 mm wide and 0.5 mm HAZ bands.

Figure 2-26
Weld Specimen EE5B Showing the Top Surface which was Etched to Reveal the Location of the Reconstitution Weld Interfaces.

GE incorrectly machined the notch at the weld HAZ. This specimen cannot be tested in this condition.

Figure 2-27
Weld Specimen EJ3A Showing Notch Placement in the Reconstitution Weld and not in the Reactor Pressure Vessel Weld.

Consistent with specimen EE5B (Figure 2-26), specimen EJ3A also cannot be tested in this condition.

As shown in Table 2-8, there are not enough weld specimens available to characterize the transition region shift nor the upper shelf energy. A study was performed to determine the best way to re-notch the specimens so that the PZN falls within the irradiated material. Based on the results of the study, the majority of the reconstituted weld specimens were re-notched on a surface adjacent to the previous notched surface at a 0.2-inch offset distance. This was done to place the notch more centrally located within the irradiated weld material insert. The re-notched specimens were then cut to length so that the new notch was centered on the specimen. Specimens EJ3B and EE4B could be tested at the lower shelf and lower transition region in the as received condition. Re-notching would decrease the amount of undisturbed irradiated material available for testing, therefore these two specimens were not re-notched. Table 2-9 shows that once the remaining specimens were re-notched, all specimens could be tested at a designated target temperature range specified in the table. Specimens with the most undisturbed irradiated material available (at least 9.2 mm) for the PZN were tested on the upper shelf as no specimens had the recommended 13 mm available.

Table 2-7
Base and Weld Charpy Specimen Measurements in the As-received Condition

Charpy Packet	Sample ID	Material	Specimen Thickness (inches)	Specimen Width (inches)	Meets ASTM E23 Cross Section Requirement[1]	Meets ASTM E23 Radius Requirement[2]	Meets ASTM E23 Angle Requirement[3]	Meets ASTM E23 Remaining Ligament Requirement[5]	Meets ASTM E23 Adjacent Side Requirement[6]
G41	**EBJB**	Base	0.3895	0.3900	No	Yes[7]	Yes	Yes	Yes
G41	**EBKA**	Base	0.3905	0.3890	No	Yes	Yes	Yes	Yes
G41	**EBKB**	Base	0.3890	0.3890	No	Yes	Yes	Yes	Yes
G41	**EBLA**	Base	0.3890	0.3890	No	Yes	Yes	Yes	Yes
G41	**EBLB**	Base	0.3875	0.3880	No	Yes	Yes	Yes	Yes
G41	**EBPA**	Base	0.3910	0.3880	No	Yes	Yes	Yes	Yes
G41	**EBPB**	Base	0.3900	0.3895	No	Yes	Yes	Yes	Yes
G41	**EBTA**	Base	0.3890	0.3890	No	Yes[7]	Yes	Yes	Yes
G41	**EBTB**	Base	0.3890	0.3880	No	Yes	Yes	Yes	Yes
G41	**EBUA**	Base	0.3890	0.3900	No	Yes	Yes	Yes	Yes
G41	**EBUB**	Base	0.3870	0.3885	No	Yes	Yes	Yes	Yes
G42	**EBYA[8]**	Base	0.3920	0.3865	No	Yes	Yes	Yes	Yes
G42	**EBYB[8]**	Base	0.3900	0.3900	No	Yes	Yes	Yes	Yes
G42	**EC1A[8]**	Base	0.3910	0.3885	No	Yes	Yes	Yes	Yes
G42	**EC1B[8]**	Base	0.3880	0.3880	No	Yes[7]	Yes	Yes	Yes
G42	**EBYA**	Base	0.3905	0.3875	No	Yes	Yes	Yes	Yes
G42	**EBYB**	Base	0.3870	0.3890	No	Yes	Yes	No[4]	Yes
G42	**EC1A**	Base	0.3900	0.3885	No	Yes	Yes	Yes	Yes
G42	**EC1B**	Base	0.3880	0.3880	No	Yes	Yes	Yes	Yes
G43	**EE2A**	Weld	0.3895	0.3885	No	Yes[7]	Yes	Yes	Yes
G43	**EE3A**	Weld	0.3895	0.3885	No	Yes	Yes	Yes	Yes
G43	**EE4A**	Weld	0.3905	0.3895	No	Yes	Yes	No[4]	Yes
G43	**EE4B**	Weld	0.3920	0.3890	No	Yes	Yes	Yes	Yes
G43	**EE5A**	Weld	0.3890	0.3890	No	Yes	Yes	Yes	Yes
G43	**EE5B**	Weld	0.3890	0.3880	No	Yes[7]	Yes	Yes	Yes
G43	**EJ1A**	Weld	0.3905	0.3895	No	Yes	Yes	Yes	Yes
G43	**EJ1B**	Weld	0.3905	0.3915	No	Yes	Yes	Yes	Yes
G43	**EJ2A**	Weld	0.3895	0.3885	No	Yes	Yes	Yes	Yes
G43	**EJ3A**	Weld	0.3890	0.3890	No	Yes	Yes	Yes	Yes
G43	**EJ3B**	Weld	0.3895	0.3900	No	Yes[7]	Yes	Yes	Yes
G43	**EJ4A**	Weld	0.3900	0.3895	No	Yes	Yes	Yes	Yes

1. ASTM E 23 requires the cross section dimensions to be 0.394 ± 0.003 inches.
2. ASTM E 23 requires the notch radius to be 0.0100 ± 0.001 inches
3. ASTM E 23 requires the included angle to be 45° ± 1
4. Meets ligament requirement in center of notch, but not on at least one side of the specimen
5. ASTM E 23 requires the ligament length to be 0.315 ± 0.001 inches
6. ASTM E 23 requires the adjacent sides to be 90° ± 10 minutes
7. One side of the notch could not be measured due to burr. Acceptance is based on the side that could be measured
8. Measurements are made as-received prior to oxide removal.

Table 2-8
Measurement of the Undisturbed Materials between Reconstitution Weld Interfaces

Charpy Packet	Sample ID	Material	Crack Plane to Left Weld [FAB ID Left, Top Surface] (inches)[1]	Crack Plane to Right Weld [FAB ID Left, Top Surface] (inches)[1]	Crack Plane to Left Weld [FAB ID Left, Bottom Surface] (inches)[1]	Crack Plane to Right Weld [FAB ID Left, Bottom Surface] (inches)[1]	Minimum Distance Crack Plane to Weld (mm)	Undisturbed Material Available for Testing (mm)	Specimen can be Tested? Y/N	Highest Target Test Temperature Region
G41	**EBJB**	Base	0.1845	0.1435	0.2655	0.1945	3.6	7.3	YES	Mid-Transition
G41	**EBKA**	Base	0.1880	0.2380	0.2120	0.1815	4.6	9.2	YES	Upper Transition
G41	**EBKB**	Base	0.1690	0.2865	0.2935	0.1880	4.3	8.6	YES	Upper Transition
G41	**EBLA**	Base	0.1755	0.2435	0.2460	0.1600	4.1	8.1	YES	Upper Transition
G41	**EBLB**	Base	0.1540	0.2010	0.2460	0.2160	3.9	7.8	YES	Mid-Transition
G41	**EBPA**	Base	0.1980	0.2475	0.2195	0.2055	5.0	10.1	YES	Upper Transition
G41	**EBPB**	Base	0.1780	0.2335	0.2145	0.2070	4.5	9.0	YES	Upper Transition
G41	**EBTA**	Base	0.2665	0.2870	0.1915	0.2150	4.9	9.7	YES	Upper Transition
G41	**EBTB**	Base	0.2295	0.2285	0.2890	0.2240	5.7	11.4	YES	Upper Shelf
G41	**EBUA**	Base	0.1885	0.2635	0.2515	0.2310	4.8	9.6	YES	Upper Transition
G41	**EBUB**	Base	0.2145	0.2465	0.2730	0.2245	5.4	10.9	YES	Upper Shelf
G42	**EBYA**	Base	0.1690	0.2175	0.2120	0.2010	4.3	8.6	YES	Upper Transition
G42	**EBYB**	Base	0.1585	0.2185	0.2400	0.1860	4.0	8.1	YES	Upper Transition
G42	**EC1A**	Base	0.2035	0.2640	0.2575	0.1530	3.9	7.8	YES	Upper Transition
G42	**EC1B**	Base	0.1900	0.2760	0.2710	0.1705	4.3	8.7	YES	Upper Transition
G43	**EE2A**	Weld	0.0685	0.3860	0.0990	0.3890	1.7	3.5	YES	Lower Shelf
G43	**EE3A**	Weld	0.1335	0.3875	0.0875	0.2710	2.2	4.4	YES	Lower Transition
G43	**EE4A**	Weld	0.4250	-0.0210	0.3920	0.0000	-0.5	0.0	NO	-
G43	**EE4B**	Weld	0.1405	0.1790	0.2090	0.1825	3.6	7.1	YES	Mid-Transition
G43	**EE5A**	Weld	0.3410	0.0815	0.4345	0.0795	2.0	4.0	YES	Lower Transition
G43	**EE5B**	Weld	0.0000	0.4980	0.0415	0.4305	0.0	0.0	NO	-
G43	**EJ1A**	Weld	0.3205	0.0950	0.4630	0.0445	1.1	2.3	YES	Lower Shelf
G43	**EJ1B**	Weld	0.4060	0.0745	0.5230	0.0380	1.0	1.9	YES	Lower Shelf
G43	**EJ2A**	Weld	-0.0235	0.5200	0.0395	0.4090	-0.6	0.0	NO	-
G43	**EJ3A**	Weld	0.3905	-0.0335	0.4935	-0.0615	-1.6	0.0	NO	-
G43	**EJ3B**	Weld	0.2370	0.1610	0.3075	0.1055	2.7	5.4	YES	Lower Transition
G43	**EJ4A**	Weld	0.4720	0.0695	0.4515	0.0550	1.4	2.8	YES	Lower Shelf

1. In all of the measurements, the end of the specimen with the FAB code was on the left. Top surface is defined as the surface observed with the notch facing down. Bottom surface is defined as the surface shown when the notch is facing up.

Table 2-9
Measurement of the Undisturbed Material Between the Reconstitution Weld Interfaces After Re-notching

Charpy Packet	Sample ID	Material	Crack Plane to Left Weld [FAB ID Left, Notch Front] (inches)[1]	Crack Plane to Right Weld [FAB ID Left, Notch Front] (inches)[1]	Crack Plane to Left Weld [FAB ID Left, Notch Rear] (inches)[1]	Crack Plane to Right Weld [FAB ID Left, Notch Rear] (inches)[1]	FAB ID Left Minimum Center to Weld (mm)	Minimum Distance Crack Plane to Weld (mm)	Undisturbed Material Available for Testing (mm)	Specimen can be Tested? Y/N	Highest Target Test Temperature Region
G41	**EBJB**	Base	0.1845	0.1435	0.2655	0.1945	0.1435	3.6	7.3	YES	Lower Shelf
G41	**EBKA**	Base	0.1880	0.2380	0.2120	0.1815	0.1815	4.6	9.2	YES	Upper Transition
G41	**EBKB**	Base	0.1690	0.2865	0.2935	0.1880	0.1690	4.3	8.6	YES	Lower Transition
G41	**EBLA**	Base	0.1755	0.2435	0.2460	0.1600	0.1600	4.1	8.1	YES	Lower Transition
G41	**EBLB**	Base	0.1540	0.2010	0.2460	0.2160	0.1540	3.9	7.8	YES	Lower Transition
G41	**EBPA**	Base	0.1980	0.2475	0.2195	0.2055	0.1980	5.0	10.1	YES	Upper Transition
G41	**EBPB**	Base	0.1780	0.2335	0.2145	0.2070	0.1780	4.5	9.0	YES	Upper Transition
G41	**EBTA**	Base	0.2665	0.2870	0.1915	0.2150	0.1915	4.9	9.7	YES	Upper Transition
G41	**EBTB**	Base	0.2295	0.2285	0.2890	0.2240	0.2240	5.7	11.4	YES	Upper Shelf
G41	**EBUA**	Base	0.1885	0.2635	0.2515	0.2310	0.1885	4.8	9.6	YES	Upper Transition
G41	**EBUB**	Base	0.2145	0.2465	0.2730	0.2245	0.2145	5.4	10.9	YES	Upper Shelf
G42	**EBYA**	Base	0.1690	0.2175	0.2120	0.2010	0.1690	4.3	8.6	YES	Lower Transition
G42	**EBYB**	Base	0.1585	0.2185	0.2400	0.1860	0.1585	4.0	8.1	YES	Lower Transition
G42	**EC1A**	Base	0.2035	0.2640	0.2575	0.1530	0.1530	3.9	7.8	YES	Lower Shelf
G42	**EC1B**	Base	0.1900	0.2760	0.2710	0.1705	0.1705	4.3	8.7	YES	Mid Upper Transition
G43	**EE2A**	Weld	0.2685	0.1860	0.2990	0.1890	0.1860	4.7	9.4	YES	Upper Transition
G43	**EE3A**	Weld	0.3335	0.1875	0.2875	0.0710	0.0710	1.8	3.6	YES	Lower Shelf
G43	**EE4A**	Weld	0.2250	0.1790	0.1920	0.2000	0.1790	4.5	9.1	YES	Mid Upper Transition
G43	**EE4B**	Weld	0.1405	0.1790	0.2090	0.1825	0.1405	3.6	7.1	YES	Mid Lower Transition
G43	**EE5A**	Weld	0.1410	0.2815	0.2345	0.2795	0.1410	3.6	7.2	YES	Mid Lower Transition
G43	**EE5B**	Weld	0.2000	0.2980	0.2415	0.2305	0.2000	5.1	10.2	YES	Upper Transition
G43	**EJ1A**	Weld	0.1205	0.2950	0.2630	0.2445	0.1205	3.1	6.1	YES	Lower Transition
G43	**EJ1B**	Weld	0.2060	0.2745	0.3230	0.2380	0.2060	5.2	10.5	YES	Upper Shelf
G43	**EJ2A**	Weld	0.1765	0.3200	0.2395	0.2090	0.1765	4.5	9.0	YES	Mid Upper Transition
G43	**EJ3A**	Weld	0.1905	0.1665	0.2935	0.1385	0.1385	3.5	7.0	YES	Lower Transition
G43	**EJ3B**	Weld	0.2370	0.1610	0.3075	0.1055	0.1055	2.7	5.4	YES	Lower Shelf
G43	**EJ4A**	Weld	0.2720	0.2695	0.2515	0.2550	0.2515	6.4	12.8	YES	Upper Shelf

1. In all of the measurements, the end of the specimen with the FAB code was on the left. Top surface is defined as the surface observed with the notch facing down. Bottom surface is defined as the surface shown when the notch is facing up.

3
NEUTRON FLUENCE CALCULATION

This section presents the results of an analysis to determine the dosimetry activity and fast neutron fluence for the DAEC 288°-R capsule that was removed from the reactor at the end of Cycle 27. The 288°-R capsule contained Charpy specimens that were initially irradiated in the DAEC reactor during Cycles 1 through 7, inclusive. Selected Charpy specimens were reconstituted and then reinserted into the DAEC reactor at the beginning of Cycle 9. The 288°-R capsule was removed from the reactor at the end of Cycle 27 and the contents of the reconstituted capsule were evaluated.

Prior dosimetry analyses for DAEC were reported in Reference [10]. For completeness, each of the dosimetry evaluations performed for the DAEC reactor are listed in Table 3-1.

Table 3-1
Summary of the Duane Arnold Surveillance Capsules Flux Wires

Capsule Location	Time of Removal	EFPY at Removal	Reference
30° Flux Wire Holder	EOC 2	1.6	[10]
288° Capsule	EOC 7	5.9	[10]
36° Capsule	EOC 14	14.4	[10]
108° Capsule	EOC 23	28.3	[10]
288°-R Capsule[1]	EOC 27	28.4	---

1. The EFPY reported for the 288°-R capsule is the irradiation time determined for the flux wires that were loaded in the reconstituted capsule.

It is noted that different values for Effective Full Power Years (EFPY) are reported for the reconstituted 288°-R capsule in this document. The 28.4 EFPY value that is listed in Table 3-1 is the irradiation time that the fresh dosimeter flux wires were irradiated during Cycles 9 through 27, inclusive. In contrast, the reconstituted Charpy specimens in the same capsule are reported to have a higher irradiation time of 34.3 EFPY, as these specimens had been previously irradiated in Cycles 1 through 7, inclusive. This is also in contrast to the total accumulated irradiation time of 35.5 EFPY for the reactor at the end of Cycle 27. These distinctions are made throughout this report.

The determination of activation, fluence and combined uncertainty for the surveillance capsules and flux wires listed in Table 3-1 is based upon the RAMA Fluence Methodology [14], the RAMA Fluence Methodology Procedures Manual [15], and the RAMA Fluence Methodology Theory Manual [16].

The RAMA Fluence Methodology (hereinafter referred to as "RAMA") was developed by TransWare Enterprises Inc. under sponsorship of EPRI and the BWRVIP. In accordance with the requirements of U.S. Nuclear Regulatory Commission (NRC) Regulatory Guide 1.190, "Calculational and Dosimetry Methods for Determining Pressure Vessel Neutron Fluence" [17], RAMA is qualified against industry standard benchmarks for both boiling water reactor (BWR) and pressurized water reactor (PWR) designs. The RAMA methodology and TransWare's application of the methodology have been reviewed by the NRC and given generic approval for determining fast neutron fluence in both BWR and PWR pressure vessels [18] with no discernable bias in the computed results.

3.1 Description of the Reactor System

This section provides an overview of the reactor design and operating data inputs that were used to develop the computational fluence model for the DAEC reactor. All reactor design and operating data inputs used to develop the model are plant-specific and were provided by DAEC - NextEra Energy personnel. The inputs for the fluence geometry model were developed from nominal and as-built drawings for the reactor pressure vessel, vessel internals, fuel assemblies, and containment structures. No modifications were made to the DAEC RAMA geometry model since the previous fluence assessment in 2017. The reactor operating history was also updated to provide a historical accounting of how the reactor operated for Cycles 1 through 27.

3.1.1 Overview of the Reactor System Design

The DAEC is a General Electric BWR/4 class reactor with a core loading of 368 assemblies. The unit began commercial operation in 1974 with a design rated power of 1,593 MWt. Power uprates were achieved in Operating Cycles 8 and 18 raising the thermal power output to 1,658 and 1,912 MWt, as shown in Section 3.4.2.

Figure 3-1 illustrates the basic planar configuration of the DAEC reactor at an axial elevation near the reactor core mid-plane. All the radial regions of the reactor that are required for fluence evaluations are shown. Beginning at the center of the reactor and projecting outward, the regions include: the core region; core reflector region (bypass water); central shroud wall; downcomer water region including the jet pumps; RPV wall; cavity region between the RPV wall and insulation; insulation; cavity region between the insulation and biological shield; and the biological shield wall. Cladding is included on the inner RPV surface as well as the inner and outer surfaces of the biological shield wall. Also represented in Figure 3-1 are notations indicating the control rod and fuel assembly locations within the core. Note that the fuel locations are shown only for the northeast quadrant of the core region.

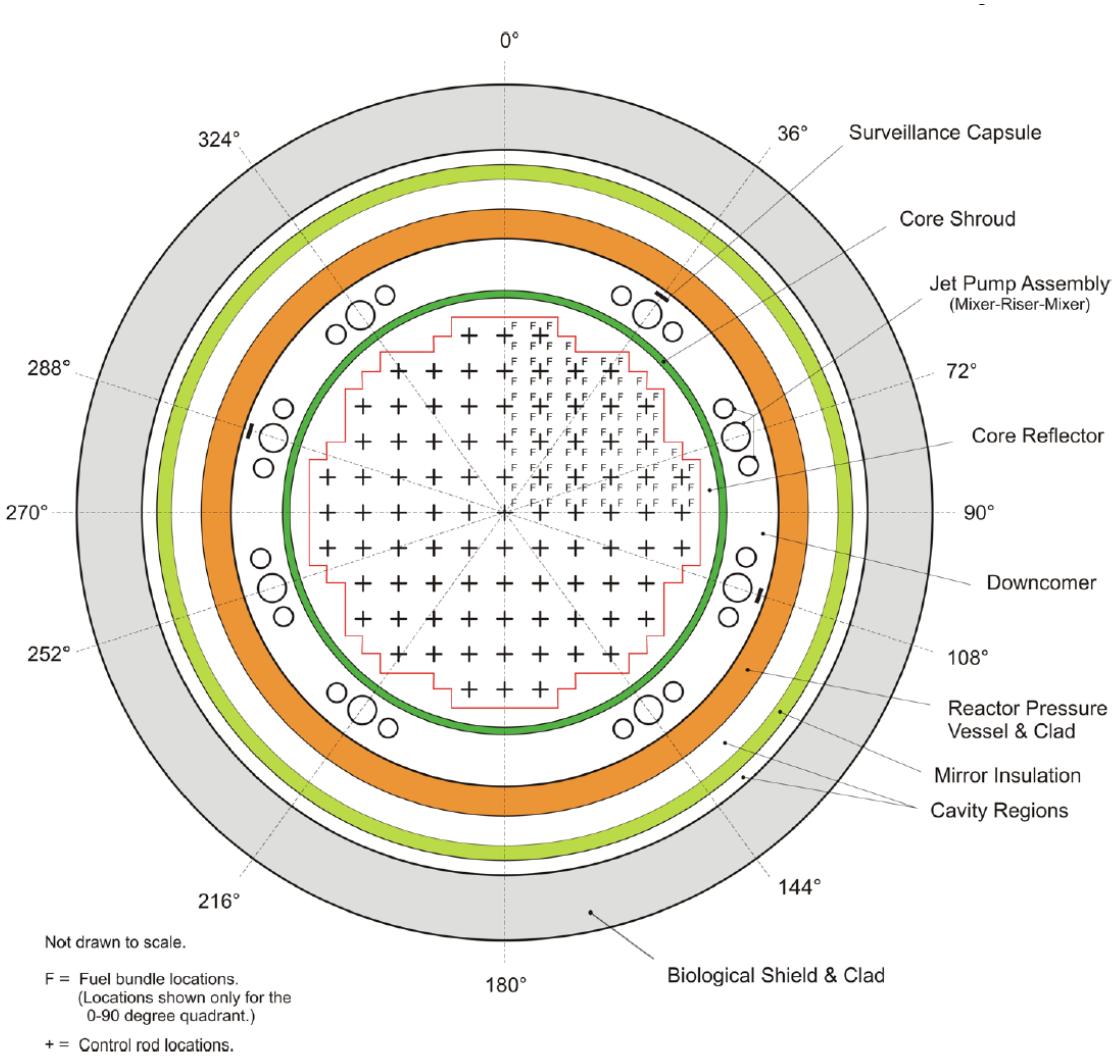

Figure 3-1
Planar View of the DAEC Reactor Fluence Model

3.1.2 Reactor System Mechanical Design Inputs

The mechanical design inputs used to construct the DAEC fluence geometry model are based upon nominal design and as-built dimensional information. As-built data is preferred when constructing plant-specific reactor fluence models; however, as-built data is not always available and nominal dimensions are used.

For the DAEC fluence model, the predominant dimensional information used to construct the fluence model is nominal design data. As-built dimensional data was used for the following reactor components:

- RPV clad wall inner radius
- Upper, central, and lower shroud outer radii
- Upper and lower shroud flange radii

- Upper and lower shroud head flange radii
- Inner radius of spargers from center of shroud
- Top guide small support pad proximal width
- Top guide small support pad inner portion radial length
- Top guide plate thickness
- Radial distance from RPV center to jet pump mixer pipes at upper elevation
- Distance from RPV clad inner radius to capsule outer radius

An important component of a computational reactor pressure vessel fluence model is the accurate description of the surveillance capsules installed in the pressure vessel. Figure 3-1 shows that the DAEC reactor was initially equipped with three surveillance capsules. The surveillance capsules are distributed around the circumference of the pressure vessel at the 36°, 108° and 288° azimuths relative to the reactor north 0° angular direction. The capsules were installed at an elevation around the reactor core mid-plane. Each capsule was mounted radially near the inside surface (0T) of the RPV wall. The importance of surveillance capsules in fluence analyses is that they contain flux wires that are irradiated during reactor operation. When a capsule is removed from the reactor, the irradiated flux wires are evaluated to obtain activity measurements. The measurements are used to validate the fluence model. At this time, it is noted that all three OEM capsules have been removed from the DAEC reactor, and an additional capsule was reinstalled at the 288° location at beginning of Cycle 9 and removed at the end of Cycle 27.

3.1.3 Reactor System Material Compositions

Each region of the reactor is comprised of materials that can include reactor fuel, metal, water, insulation, concrete, and air. Accurate material information is essential for the fluence evaluation as the material compositions determine the scattering and absorption of neutrons throughout the reactor system and, thus, affect the determination of neutron fluence in the RPV, surveillance capsules, vessel internal components, and ex-vessel structures.

Table 3-2 provides a summary of the materials for the principal components and regions of the DAEC reactor. The material attributes for the metal, insulation, concrete, and air compositions (i.e., material densities and isotopic concentrations) are assumed to remain constant for the operating life of the reactor. The bulk water coolant properties throughout the reactor system, except for the core region, are determined assuming rated power and flow conditions. The coolant properties remain constant unless there is a reported change in system heat balance conditions that affect the water properties in the reactor. The nuclear fuel compositions and coolant properties in the reactor core region change continuously during reactor operation. The fuel and coolant properties in the core region are updated for each reactor statepoint condition based on the actual or predicted operating states of the reactor. Water properties immediately above and below the core region are updated on a cycle-by-cycle basis based on average cycle operating conditions.

Table 3-2
Summary of Material Compositions by Component Region for DAEC

Region	Material Composition
Control Rods and Guide Tubes	Stainless Steel
Core Support Plate	Stainless Steel
Fuel Support Pieces	Stainless Steel
Fuel Assembly Lower Tie Plate	Stainless Steel, Zircaloy, Inconel
Reactor Core	^{235}U, ^{238}U, ^{239}Pu, ^{240}Pu, ^{241}Pu, ^{242}Pu, O_{fuel}, Zircaloy
Reactor Coolant/Moderator	Water
Core Reflector	Water
Fuel Assembly Upper Tie Plate	Stainless Steel, Zircaloy, Inconel
Top Guide	Stainless Steel
Core Spray Sparger Pipes	Stainless Steel
Core Spray Sparger Flow Areas	Water
Shroud	Stainless Steel
Downcomer Region	Water
Jet Pump Riser and Mixer Flow Area	Water
Jet Pump Riser and Mixer Metal	Stainless Steel
Jet Pump Riser Brace and Pads	Stainless Steel, Inconel
Surveillance Capsule Specimens	Carbon Steel
Reactor Pressure Vessel Clad	Stainless Steel
Reactor Pressure Vessel Wall	Carbon Steel
Cavity Regions	Air (Nitrogen)
Insulation	Aluminum, Stainless Steel, Air
Biological Shield Clad	Carbon Steel
Biological Shield Wall	Reinforced Concrete

3.1.4 Reactor Operating Data Inputs

An accurate evaluation of reactor vessel and component fluence requires an accurate accounting of the reactor's operating history. The principal operating parameters that affect the determination of neutron fluence in light water reactors include the following: core configurations, fuel assembly designs, power history, exposure and isotopic distributions, and water density distributions. The following subsections provide additional information on the characterization of reactor operating data for fluence evaluations.

3.1.4.1 Core Configuration and Fuel Designs

The reactor core configuration and the fuel assembly designs loaded in the reactor determine the neutron source and spatial source distribution contributing to the irradiation of the pressure vessel, vessel internals and ex-vessel supporting structures. The DAEC core is comprised of 368 fuel assemblies in a fixed configuration. Several designs of fuel assemblies may be loaded in the reactor core in any given operating cycle. To determine accurate spatial fluence profiles throughout the reactor system, it is important to account for the different fuel designs loaded in the reactor over the operating lifetime of the reactor, especially those designs that reside in the peripheral locations of the core region.

Table 3-3 provides a summary of the many fuel assembly designs that have been loaded in the DAEC reactor core for each operating cycle evaluated in this report. It is noted that fuel loadings for Cycles 1, 4, and 18 were divided into two individual periods, identified as 1A, 1B, 4A, 4B, 18A, and 18B. Table 3-3 also identifies the dominant fuel design loaded on the core periphery for each cycle with shading and indicates the dominant (most numerous) assembly present in **bold** font.

3.1.4.2 Reactor Power History

Reactor power history is the measure of reactor power levels, reactor power spatial distributions, fuel exposure distributions, and fuel isotopic distributions that a reactor experiences over its operating life. The power history data used in the DAEC fluence evaluation includes daily power levels for Cycles 1 through 27. The power history for DAEC also accounts for periods of reactor shutdown due to refueling outages and other events that affect the activation and decay of dosimetry data.

Table 3-4 provides a summary of the rated power history and EFPY per cycle for the DAEC reactor. The accumulated EFPY is computed from the operating data and is verified against power production and exposure data obtained separately from plant records.

3.1.4.3 Reactor Statepoint Data

Statepoints break up operating history into ranges of operation based on similar power, exposure, and isotopic distributions. Typically, several statepoints are chosen for each cycle to represent the different operating conditions experienced by the reactor over the course of that cycle.

Core simulator data was provided to characterize the operating conditions of DAEC for the historical Cycles 1 through 27. The data calculated with core simulator codes represents the best-available information about the reactor core's operating history over the reactor's operating life. In this analysis, the core simulator data was processed by TransWare to generate statepoint data files for input to the fluence model.

Because core simulator codes are used for a variety of core analysis functions, 10’s to 100’s of core calculations may be performed to track and monitor the operation of a reactor over the course of an operating cycle. Not all core calculations are suitable for use in fluence evaluations. Therefore, each cycle of operating data is investigated to select the statepoints that are suitable for use in fluence evaluations. When all reactor conditions are considered, the number of core simulator statepoints selected for a fluence evaluation can vary appreciably from cycle to cycle.

A separate neutronics transport calculation is performed for each selected statepoint. The neutron fluxes calculated for each statepoint are then combined with the appropriate daily power history data described in Section 3.4.2 to provide an accurate accounting of the neutron fluence for the reactor pressure vessel, reactor vessel internals, and surveillance capsules. The periods of reactor shutdown are also accounted for in this process, particularly to allow for an accurate calculation of irradiated surveillance capsule activities

Table 3-3
Summary of Duane Arnold Core Loading Inventory

Cycle	Fuel Designs							
	7x7	8x8				10x10		
	GE3	GE4	GE6	GE8	GE10	GE12	GE14	GNF2
1A	368							
1B	368							
2	284	84						
3	184	184						
4A	96	272						
4B	96	272						
5	8	272	88					
6		196	172					
7		68	300					
8			368					
9			240	128				
10			120	248				
11			16	248	104			
12				160	208			
13				32	336			
14					368			
15					368			
16					368			
17					240	128		
18A					104	128	136	
18B					104	128	136	
19						80	288	
20							368	
21							368	
22							368	
23							368	
24							216	152
25							64	304
26								368
27								368

Table 3-4
Cycle Data for Duane Arnold

Cycle Number	Rated Thermal Power (MWt)	Accumulated Effective Full Power Years (EFPY)
1A	1593	0.6
1B	1593	1.0
2	1593	1.6
3	1593	2.3
4A	1593	2.4
4B	1593	3.1
5	1593	3.9
6	1593	4.8
7	1593	5.9
8	1658	7.1
9	1658	8.2
10	1658	9.3
11	1658	10.6
12	1658	11.7
13	1658	13.0
14	1658	14.4
15	1658	15.6
16	1658	16.9
17	1658	18.2
18A	1658	18.7
18B	1912	19.8
19	1912	21.5
20	1912	23.2
21	1912	25.0
22	1912	26.5
23	1912	28.3
24	1912	30.1
25	1912	31.9
26	1912	33.7
27	1912	35.5

3.1.4.4 Reactor Coolant Properties

The reactor coolant water densities used in the fluence model are determined using combinations of core simulator codes and reactor heat balance data.

The water densities used for the core inlet and the reactor core region are derived directly from the thermal-hydraulic calculations performed by core simulator codes. In general, core simulator codes provide active and bypass flow water density data for each fuel assembly in the core and incrementally along the axial height of the assembly as the coolant flows from core inlet to core exit. The water densities in the reflector region around the core, and inside the core shroud, are determined using the average pressure of the core region, assuming the water is a saturated liquid.

The water densities above the core, and specifically in the shroud upper plenum region, assume the steam quality exiting the core. There is no mixing of the exit steam with the unvoided or slightly voided bypass flow also exiting the core. This treatment of core exit water densities provides conservative conditions for determining fluence in the upper vessel components and for determining the upper elevation of the RPV beltline. The core exit steam is also used to fill the steam separator standpipes that extend above the shroud head.

The core spray sparger piping, which is present in the upper shroud plenum region, is filled with saturated water on the inside of the piping and is surrounded by the plenum core exit steam on the outside of the pipes.

The bulk water densities in the other regions of the reactor vessel are determined from plant specific heat balance data. The water densities that are calculated in this manner include the jet pump flow, and feedwater. Heat balance data provides water properties in terms of temperature, pressure, and enthalpy assuming 100% power and flow operating conditions. The water densities determined at full power conditions remain constant throughout the cycle, and for all power states of the reactor throughout a cycle, which should be bounding for best-estimate fluence predictions.

3.2 Methodology

This section provides an overview of the methodology and modeling approach used to determine fast neutron fluence and activation for the DAEC surveillance capsules. The fluence model for DAEC is a plant-specific model that is constructed from the design inputs described in Section 3.1, *Description of the Reactor System.* The computational tools used in the fluence and activation analyses are based on the RAMA software. The RAMA Fluence Methodology is described in the RAMA Theory Manual [16]. A general approach for using the toolset is presented in the RAMA Procedures Manual [15].

3.2.1 Computational Method

The RAMA Fluence Methodology is a system of computer codes, a data library, and an uncertainty methodology that determines best-estimate fluence and activations in light water reactor pressure vessels and vessel internal components. The primary software that comprises the methodology includes model builder codes, a particle transport code, and a fluence calculator code.

The primary inputs for the fluence methodology are mechanical design parameters and reactor operating history data. The mechanical design inputs are obtained from plant-specific design drawings, which include as-built measurements when available. The reactor operating history data is obtained from multiple sources, such as core simulator software, system heat balance calculations, daily operating logs, and cycle summary reports. A variety of outputs are available from the fluence methodology that include neutron flux, fast neutron fluence, dosimetry activation, and an uncertainty analysis.

The model builder codes consist of geometry and material processor codes that generate input for the RAMA transport code. The geometry model builder code uses mechanical design inputs and meshing specifications to generate three-dimensional geometry models of the reactor. The material processor code uses reactor operating data and material property inputs to process fuel materials, structural materials, and water densities that are consistent with the geometry meshing generated by the geometry model builder code.

The RAMA transport code performs three-dimensional neutron flux calculations using a deterministic, multigroup, particle transport theory method with anisotropic scattering that is based upon the Method of Characteristics [19]. The transport solver is coupled with a general geometry modeling capability based on combinatorial geometry techniques. The coupling of general (arbitrary) geometry with a deterministic transport solver provides a flexible, efficient, and stable method for calculating neutron flux in light water reactor pressure vessels, vessel components, and structures. The primary inputs for the transport code include the geometry and material data generated by the model builder codes and numerical integration and convergence parameters for the iterative transport calculation. The primary output from the transport code is the neutron flux in multigroup form for every material region mesh in the fluence model.

The fluence calculator code determines fluence and activation in the reactor pressure vessel, surveillance specimens, and vessel components over specified periods of reactor operation. The fluence calculator also includes treatments for isotopic production and decay that are required to calculate specific activities for irradiated materials, such as the dosimetry specimens in the surveillance capsules. The primary inputs to the fluence calculator include the multigroup neutron flux from the transport code, response functions for the various materials in the reactor, reactor power levels for the operating periods of interest, specification of which components to evaluate, and the energy ranges of interest for evaluating neutron fluence. The reactor operating history is generally represented with several reactor statepoints that represent the core power and core power distributions of the reactor over the operating life of the reactor. These statepoints are integrated with the daily variations in reactor power levels to predict the fluence and activations accumulated throughout the reactor system.

The RAMA nuclear data library contains atomic mass data, nuclear cross-section data, response functions, and other nuclear constants that are needed for each of the code tools. The structure and contents of the data contained within the nuclear data file are based on the BUGLE-96 nuclear data library [20], with extended data representations derived from the VITAMIN-B6 data library [21].

The uncertainty methodology provides an assessment of the overall accuracy of the fluence and activation calculations. Variations in the dimensional data, reactor operating data, dosimetry measurement data, and nuclear data are evaluated to determine if there is a statistically significant bias in the calculated results that might affect the determination of the best-estimate

fluence for the reactor. The plant-specific results are also weighted with comparative results from experimental benchmarks and other plant analyses and analytical uncertainties pertaining to the methodology to determine if the plant-specific model under evaluation is statistically acceptable as defined in Regulatory Guide 1.190 [17].

3.2.2 Fluence Model

Section 3.1, *Description of the Reactor System*, describes the design inputs that were provided for constructing the DAEC reactor fluence model. These design inputs are used to develop a plant-specific, three-dimensional computer model of the DAEC reactor for determining fast neutron fluence and activation in the reactor dosimetry specimens.

Figure 3-2 and Figure 3-3 provide general illustrations of the primary components, structures, and regions developed for the DAEC fluence model. Figure 3-2 shows the planar configuration of the reactor model at an elevation corresponding to the reactor core mid-plane elevation. Figure 3-3 shows an axial configuration of the reactor model. Note that the figures are not drawn to scale and do not include representations of the meshing developed for this evaluation. The figures are intended only to provide a perspective for the layout of the model, and specifically how the various components, structures, and regions lie relative to the reactor ore region (i.e., the neutron source). Additional detail is beyond the scope of this document.

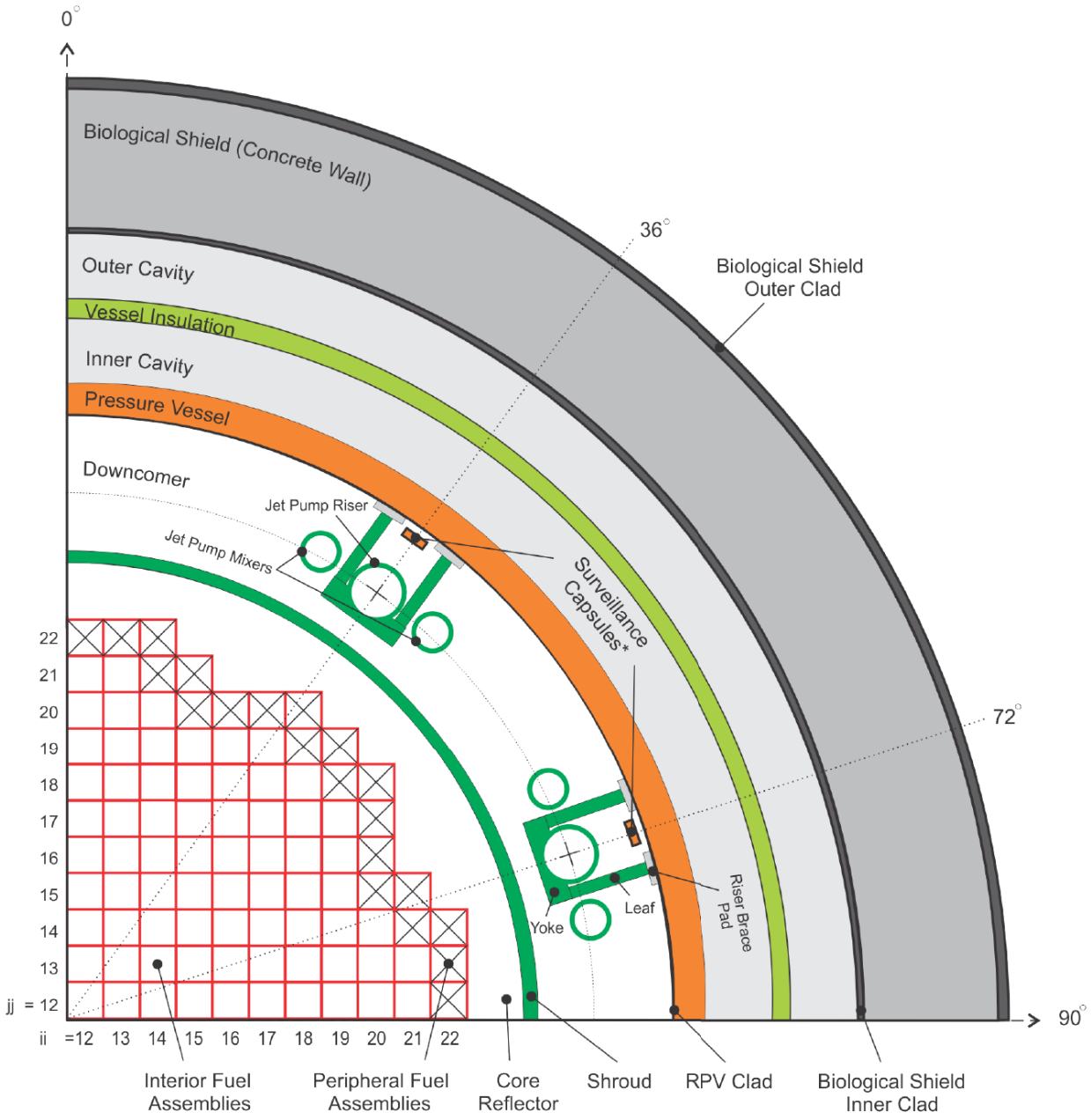

Notes:

- This drawing is not to scale
- The reactor model represented in the analysis assumes quadrant symmetry in the azimuthal dimension.
- The capsule modeled at 36° represents the 36° capsule and the 72° capsule represents the 108° and 288° capsules in the reactor.

Figure 3-2
Planar View of the DAEC Fluence Model at the Core Mid-Plane Elevation in Quadrant Symmetry

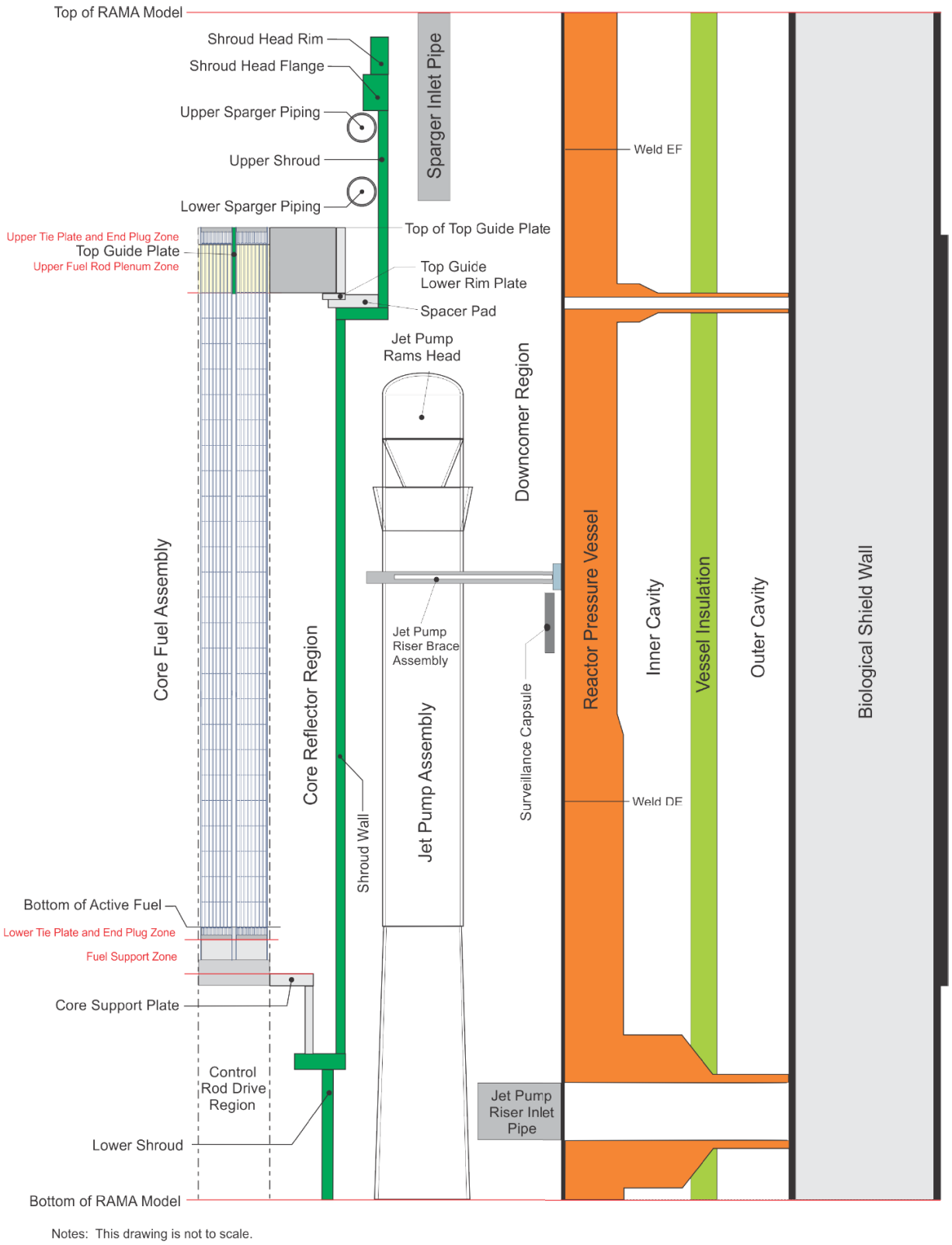

Figure 3-3
Axial View of the DAEC Fluence Model

3.2.2.1 Geometry Model

The DAEC fluence model is constructed on a Cartesian coordinate system using a generalized three-dimensional geometry modeling technique based on combinatorial geometry. The axial plane of the reactor model is defined by the (x,y) coordinates of the modeling system and the axial elevation at which a plane exists is defined along a perpendicular z-axis of the modeling system. This allows any point in the reactor model to be referenced by specifying the (x,y,z) coordinates for that point.

The geometry modeling system allows for solid body elements to be constructed to describe the various components, regions, and structures of the reactor. The primary elements ("primitives") used to construct the fluence model include rotatable boxes, cylinders, parallelepipeds, truncated cones, spheres, approximated toroids, and wedges. This modeling approach permits a model to be developed in any level of high-definition detail, such as is necessary for fluence and activation evaluations.

Figure 3-1 illustrates a planar cross-section view of the Duane Arnold reactor design at an axial elevation corresponding to the reactor core mid-plane. It is shown for this one elevation that the reactor design is a complex geometry composed of various combinations of rectangular, cylindrical, and wedge-shaped bodies. When the reactor is viewed in three dimensions, the varying heights of the different components, structures, and regions create additional geometry modeling complexities. An accurate representation of these geometrical complexities in a predictive computer model is essential for calculating accurate, best-estimate fluence in the reactor pressure vessel, surveillance capsules, vessel internals, and the supporting structures inside and outside of the reactor vessel.

Figure 3-2 and Figure 3-3 provide general illustrations of the planar and axial geometry complexities that are represented in the fluence model. For comparison purposes, the planar view illustrated in Figure 3-2 corresponds to the core elevation illustrated in Figure 3-1. The fluence model assumes reflective azimuthal quadrant symmetry in the planar dimension.

Figure 3-2 illustrates the quadrant geometry that is modeled in this analysis. In terms of the modeling coordinate system, this quadrant is designated the "northeast" quadrant of the reactor system. The 0-degree azimuth, which has a "north" designation, corresponds to the 0-degree azimuth referenced in the plant drawings for the reactor pressure vessel. Azimuthal position is incremented clockwise, resulting in the 90-degree azimuth being designated as the "east" direction.

Figure 3-3 illustrates the axial configuration of the primary components, structures, and regions in the fluence model. The figure shows that the axial height of the fluence model spans from a lower elevation below the recirculation inlet and outlet nozzles to above the core shroud head rim.

As previously noted, Figure 3-2 and Figure 3-3 are not drawn precisely to scale and are intended only to provide a perspective of how the various components, structures, and regions of the reactor are positioned relative to the reactor core region. The following subsections provide additional information on the constituent models developed for the individual components, structures, and regions of the fluence model.

3.2.2.2 Reactor Core and Core Reflector

The reactor core contains the nuclear fuel that is the source of the neutrons that irradiate all components and structures of the reactor. The core is surrounded by a shroud structure that serves to channel the reactor coolant through the core region during reactor operation. The coolant-containing region between the core and the core shroud is the core reflector. The reactor core geometry is rectangular in design and is modeled with rectangular elements to preserve its shape in the analysis. The core reflector region interfaces with the rectangular shape of the core region and the curved shape of the core shroud. It is, therefore, modeled using a combination of rectangular and cylindrical elements.

The core region is centered in the reactor pressure vessel and is radially-characterized in the analysis with two fundamental fuel zones: interior fuel assemblies and peripheral fuel assemblies. The peripheral fuel assemblies are the primary contributors to the neutron source in the fluence calculation. Because these assemblies are loaded at the core edge where neutron leakage from the core is greatest, there is a sharp power gradient across these assemblies that requires consideration. To account for the power gradient, the peripheral fuel assemblies are sub-meshed with additional elements that approximate the pin-wise details of the fuel assembly geometry and power distribution within the pins. The interior fuel assemblies make a lesser contribution to the reactor fluence and are, therefore, modeled in various homogenized forms in accordance with their contributions to the reactor fluence. For computational efficiency, homogenization treatments are used in the interior core region primarily to reduce the number of mesh regions that must be solved in the transport calculation. The meshing configuration for each fuel assembly location in the core region is determined by parametric studies to ensure an accurate estimate of neutron flux and fluence throughout all regions of the reactor system.

Each fuel assembly design, whether loaded in the interior or peripheral locations in the core, is represented with five axial material zones: the fuel nose piece zone, the fuel lower tie plate/end plug zone, the fuel zone, the fuel upper plenum zone, and the fuel upper tie plate/end plug zone. The structural materials in the top and bottom regions for each unique assembly design are represented in the model to address the shielding effects that these materials have on the components above and below the core region. The fuel zone contains the nuclear fuel and structural materials for the fuel assemblies. Because the composition of the fuel materials varies with core exposure (i.e., burnup) and by cycle (e.g., core loading), each fuel location in the reactor core is represented uniquely in the fluence model.

3.2.2.3 Reactor Core Shroud

The core shroud is a canister-like structure that surrounds the reactor core. It channels the reactor coolant and steam produced by the core into the steam separators. Axially the shroud extends almost the entire height of the model and is divided into three sections: lower, central, and upper. The lower shroud extends from the bottom of the model to the core support plate flange, the central shroud extends from the core support plate flange to the top guide flange, and the upper shroud extends from top guide flange to the top of the shroud head rim.

The shroud structure is illustrated in Figure 3-3. It is shown that the shroud wall and flanges are cylindrical in design and are accurately modeled with cylindrical elements.

3.2.2.4 Downcomer Region

The downcomer region lies between the core shroud and the reactor pressure vessel. The downcomer is effectively cylindrical in design, but with geometrical complexities created by the presence of jet pumps and surveillance capsules in the region. The majority of the downcomer region is modeled with cylindrical elements. The areas of the downcomer containing the jet pumps and surveillance capsules are modeled with the appropriate geometry elements to represent their design features and to preserve their radial, azimuthal, and axial placement in the downcomer region. These structures are described further in the following subsections.

3.2.2.4.1 Jet Pumps

DAEC has eight jet pump assemblies in the downcomer region, which provide the main recirculation flow for the core. In the fluence model, jet pump assemblies are positioned azimuthally at 36° and 72°, which when symmetry is applied to the model, represents all eight jet pumps in the reactor. The 36° jet pump represents the 36°, 144°, 216° and 324° jet pumps; and the 72° jet pump represents the 72°, 108°, 252°, and 288° jet pumps.

The jet pump assembly model includes representations for the riser, mixer, and diffuser pipes, nozzles, rams head, riser inlet pipe, and riser brace yoke, leaves and pads. The jet pump assembly is modeled using cylindrical elements for the jet pump riser and mixer pipes. The mixer nozzles, adapters, and diffusers are modeled as stepped shells to represent the axially-varying radii. The riser pipe is correctly situated between the mixer pipes. Holding the riser pipe in place are riser brace elements, which are approximated as rectangular regions by radially segmented cylindrical arc elements. The jet pump assembly includes hold down beams and brackets, built with rectangular elements that are attached to the rams head. Toroidal elements are used to model the rams head piping

3.2.2.4.2 Surveillance Capsules

Section 3.1 describes the surveillance capsules installed in the DAEC reactor. The three (3) OEM surveillance capsules installed in the DAEC reactor are positioned in close proximity to the RPV inner wall surface at the 36°, 108° and 288° azimuthal angles around the pressure vessel. For this analysis, which assumes quadrant symmetry in the azimuthal dimension, the capsule modeled at 36° represents the 36° capsule and the 72° capsule represents the 108° and 288° capsules in the reactor. A separate flux wire holder is attached externally to the 36° surveillance capsule container. Although the flux wire holder is not shown in the figures of this report, it is included in the model and is represented at the 36° capsule location. Additionally, the reconstituted 288°-R capsule is represented at the 72° location.

The vessel surveillance capsules are rectangular in design but are approximated in the model with cylindrical elements to facilitate their inclusion in the cylindrical geometry that defines the downcomer region model. This modeling approximation is acceptable due to the small view factor of the capsule relative to its radial distance from the reactor core. The coolant water that surrounds the capsule containers on all sides is explicitly modeled for its scattering and attenuation effects in the neutronics calculation.

3.2.2.5 Reactor Pressure Vessel

The reactor pressure vessel and vessel cladding lie outside the downcomer region, with both modeled using cylindrical elements. The cladding-pressure vessel interface is a key location for RPV fluence calculations and is preserved in the model. This interface defines the inside surface (0T) for the pressure vessel base metal where the RPV fluence is calculated. DAEC has cladding only on the inside surface of the pressure vessel wall.

Representations of the forgings for the recirculation inlet (N2) and instrumentation (N16) nozzles are included in the RPV wall. The nozzle forgings and safe-ends extend radially outward into the cavity region to the biological shield wall. These nozzle representations are modeled in their true cylindrical forms using cylindrical and conical elements to preserve their basic design features.

3.2.2.6 Thermal Insulation

The reactor vessel thermal insulation lies in the cavity region outside the pressure vessel wall. The insulation is cylindrical in design and follows the contour of the pressure vessel wall. It is modeled with cylindrical elements.

3.2.2.7 Inner and Outer Cavity

There are effectively two cavity regions represented in the model. The inner cavity region lies between the outer surface of the pressure vessel wall and the inner surface of the vessel insulation. The outer cavity region lies between the outer surface of the vessel insulation and inner surface of the biological shield wall cladding. The cavity regions follow the cylindrical contours of the pressure vessel wall, vessel insulation, and biological shield, and are therefore modeled with cylindrical elements.

3.2.2.8 Biological Shield Model

The biological shield (concrete) defines the outermost region of the fluence model. The biological shield for the modeled elevations is effectively cylindrical in design and is modeled with cylindrical elements. Cladding is modeled on the inside and outside surfaces of the concrete wall.

3.2.2.9 Above-Core Components

Figure 3-3 includes illustrations of other components and regions that lie above the reactor core region. The predominant above-core components represented in the model include the top guide, core spray spargers, and upper core shroud wall, shroud head, and steam separator standpipes. The upper shroud is mentioned in further detail in Section 3.2.2.3.

3.2.2.9.1 Top Guide

The top guide component lies above the core region and is appropriately modeled to include discrete representations of the top guide plates and accounting for the fuel assembly parts, top guide pads, and coolant between the plates. The fuel assembly parts are modeled in two axial segments: the fuel rod plenum and the fuel assembly upper tie plate, which includes the fuel rod upper end plugs. The top guide is modeled with combinations of rectangular and cylindrical

elements. The top guide pads are approximated as cylindrical elements. The fuel assembly parts are modeled with the elements of the reactor core region.

3.2.2.9.2 Core Spray Spargers and Piping

The core spray spargers include upper and lower sparger annulus pipes and a vertical inlet pipe. The core spray spargers are appropriately represented as torus structures in the model. The sparger pipes reside inside the upper shroud wall above the top guide. The spargers are modeled as pipe-like structures and include a representation of reactor coolant inside the pipes. The sparger spray nozzles are not represented individually. Instead, the region in which they reside is represented as a homogeneous cylinder comprised of steam and stainless steel.

3.2.2.10 Below-Core Component Models

Figure 3-3 includes illustrations of other components and regions that lie below the reactor core region. The predominant below core (i.e., below active fuel) components represented in the fluence model include the lower fuel assembly parts, fuel support pieces, core support plate, core support plate rim bolts, cruciform control rods, control rod guide tubes, and lower shroud wall. The lower shroud wall and fuel assembly components are described in previous sections, with the remaining components described in the following subsections.

3.2.2.10.1 Core Support Plate and Rim Bolts

The core support plate includes appropriate penetrations for the fuel support pieces, control rod guide tubes, cruciform control rods, and the core support plate rim bolts. Core support plate rim bolts protrude from the top of the core support plate and traverse through the plate, rim, and core shroud lower flange. The core support plate and rim are modeled using cylindrical and rectangular elements, while the rim bolts are modeled by cylindrical elements.

3.2.2.10.2 Fuel Support Pieces

The nuclear fuel assemblies loaded in the reactor are seated on fuel support pieces, which then rest in the core support plate and control blade guide tubes. Two types of fuel support pieces are included in the fluence model: a four-assembly fuel support piece, and a single-assembly fuel support piece for peripheral assembly locations. The four-assembly fuel support piece allows for the presence of a cruciform control rod and the associated coolant flow. Combinations of cylindrical, rectangular, and wedge elements are used to construct the fuel support piece models.

3.2.2.10.3 Control Blades and Guide Tubes

The fluence model allows for the representation of cruciform-shaped control blades and tubular control blade guide tubes in the below-core regions of the reactor. Coolant flow paths are included in the model to account for the scattering of neutrons in the subcooled water regions outside the guide tube and around the control blade inside the guide tube. The control blade and guide tube components are modeled using combinations of rectangular and cylindrical elements.

3.2.2.11 Summary of the Geometry Modeling Approach

To summarize the reactor modeling process, there are several key features that allow the reactor design to be accurately represented for capsule fluence evaluations. Following is a summary of some of the key features of the model:

- Combinations of rectangular, cylindrical, conical, spherical, toroidal, and wedge elements are used in the model to provide an accurate geometrical representation of the components, structures, and regions in the reactor.
- The reactor core is modeled with rectangular and wedge elements to represent the true geometrical shape of the core. The fuel assemblies in the core region are also sub-meshed with additional rectangular and wedge elements to represent the power and isotopic distributions in the assemblies.
- The fuel assembly tie plates, fuel rod end plugs, fuel nose piece, fuel channel and bypass flow regions are appropriately represented above and below the active fuel elevations. These components and regions are modeled using the same geometry elements as the reactor core.
- A combination of rectangular and cylindrical elements is used to describe the transition parts between the rectangular boundary of the core region and the cylindrical boundary of the core shroud.
- Cylindrical, conical, and wedge elements are used to model the components and regions that extend outward from the core region (core shroud, downcomer, RPV, etc.).
- Each jet pump assembly in the downcomer region includes appropriate representations for the riser pipe, mixer pipes, diffuser pipes, nozzles, couplers, rams head, hold down bracket, riser brace and yoke assembly, riser brace pads, etc. and are modeled using combinations of cylindrical, box, conical and wedge elements.
- The reactor vessel surveillance capsules are modeled with arc elements at their nominal radial, azimuthal, and elevational positions behind the jet pumps in the downcomer region. Using azimuthal symmetry conditions, all surveillance capsules are represented in the quadrant-symmetric fluence model.
- The above-core region includes accurate representations of the top guide, upper fuel assembly parts, core spray spargers and piping, and upper core shroud. Combinations of rectangular parallelepiped, cylindrical, and toroidal elements are used to describe the above-core components and coolant regions.
- The below-core region includes appropriate representations for the lower fuel assembly parts, fuel support pieces, core support plate, core support plate rim bolts, core coolant inlet regions, cruciform control rods, and control rod guide tubes. Combinations of rectangular parallelepiped, cylindrical, spherical, toroidal, and wedge elements are used to describe the below-core components and coolant regions.
- The biological shield is appropriately represented as a cylinder with cladding on the inside and outside surfaces of the biological shield wall. The biological shield is described with cylindrical elements.

3.2.3 Particle Transport Calculation Parameters

The accuracy of the transport method is based on a numerical integration technique that employs ray-tracing to characterize the geometry, anisotropy treatments to determine the density and directional flow (i.e., angular flux) of particles, and convergence parameters to determine the overall accuracy of the converged flux. Plant-specific values are determined for each significant integration and ray-tracing parameter.

Two key parameters for the calculation of accurate angular flux are the angular quadrature set and Legendre order of scattering used in the transport calculation. The importance of the angular quadrature set is specifically addressed in Regulatory Position 1.3.5 of Regulatory Guide 1.190, where it is cited that an S^8 angular quadrature (which is used in traditional transport models) may not be adequate when used in cavity transport calculations. The fluence model used in this analysis employs a higher-order S^{10} angular quadrature for all transport calculations to improve computational accuracy over the extended RPV beltline region.

The transport calculations also use the highest order of Legendre expansion of the scattering cross sections that is available on the nuclear data library for the anisotropy treatment. For the actinide and zirconium nuclides, this corresponds to a P^5 expansion of the scattering cross sections, while for all other nuclides, a P^7 expansion of the scattering cross sections is used.

Additional parameters of the calculation control the saturation of rays throughout the geometry by means of the parallel and axial ray densities as well as ray depths. The overall accuracy of the neutron flux calculation is determined using an iterative technique that converges the particle fluxes in all regions of the transport model.

3.2.4 Fission Spectrum and Neutron Source

Modern core simulator software is capable of providing three-dimensional core power distributions and fuel isotopic in high-definition detail, viz., on a pin-by-pin basis. This allows fluence models to be constructed with a high-level of modeling detail for representing unique fission spectrum and neutron source terms for the transport calculation. This detail is incorporated into the fluence model.

The fission spectrum is determined for each transport calculation based on the relative weights of the ^{235}U, ^{238}U, ^{239}Pu, ^{240}Pu, ^{241}Pu and ^{242}Pu isotopes in the fuel materials. The fission spectra for the uranium and plutonium isotopes are derived from information that is provided in the BUGLE-96 nuclear data library [20] and the VITAMIN-B6 data library [21].

The spatial neutron source distribution is determined for each transport calculation using the pin-wise power density factors obtained from the core simulator software and data from the nuclear data library.

For fluence evaluations, the peripheral fuel assemblies are specifically modeled to preserve the pin-wise power gradient at the core edge, as these bundles have the greatest effect on the determination of fluence in the reactor pressure vessel.

3.2.5 Parametric Sensitivity Analyses

Several plant-specific sensitivity analyses are performed to evaluate the accuracy and predictability of the neutral particle transport methodology for determining RPV fluence.

Geometric meshing and numerical integration parameters are among the items pre-evaluated to ensure that the transport solution provides consistent results in all azimuthal, radial and axial dimensions of the reactor fluence model. The ultimate validation of the model is the demonstration that predicted activations for reactor surveillance dosimetry and boat samples, if available, meet the requirements of Regulatory Guide 1.190.

3.3 Surveillance Capsule Activation and Fluence Results

This section documents the activation analysis and fast neutron fluence that was performed for the DAEC 288º-R surveillance capsule. The activation results form the basis for validating the RAMA fluence methodology as applied to the DAEC reactor in accordance with Regulatory Guide 1.190. Regulatory Guide 1.190 requires fluence calculational methods to be validated by comparisons with measurements from operating reactor dosimetry for the specific reactor being evaluated, or from reactors with similar design. In accordance with Regulatory Guide 1.190, the acceptance criteria for determining best-estimate fluence with no discernable bias is that the comparison to-measurement (C/M) ratio be less than or equal to 20%. The DAEC 288°-R reactor capsule measurement comparisons meet the Regulatory Guide 1.190 criteria and, as such, no bias adjustment is required to be applied to the computed RPV fluence.

3.3.1 Summary of the DAEC 288°-R Surveillance Capsule Activation and Fluence

The DAEC 288º-R surveillance capsule is a reconstituted capsule that was reinserted into the DAEC reactor at the beginning of Cycle 9 and was removed at the end of Cycle 27. Activation measurements were performed for the flux wires extracted from the capsule. A comparison of the calculated activities to measurements is presented in Table 3-5. It is shown that the average calculated-to-measured (C/M) ratio and standard deviation for the flux wires is 1.04 ± 0.06. Table 3-5 also shows that the fast neutron fluence accumulated in the Charpy specimens during their overall periods of irradiation is 32.7E+17 n/cm^2.

Table 3-5
Summary of Activity Comparisons and Fast Neutron Fluence Determined for the Duane Arnold 288°-R Reconstituted Capsule

Dosimeter	Time of Removal	Accumulated Exposure (EFPY)	Fast Neutron Fluence (>1.0 MeV, n/cm^2)	Number of Measurements	Calculated vs. Measured (C/M)	Standard Deviation (σ)
288°-R Capsule	EOC 27	34.3	32.7E+17	9	1.04	0.06

3.3.2 Comparison of DAEC 288°-R Flux Wire Activations to Measurements

The comparison of predicted activations to measurements for the DAEC Cycle 27 flux wires are presented in this subsection. Copper, iron, and nickel flux wires were irradiated in the DAEC 288°-R surveillance capsule from the start of Cycle 9 to the end of Cycle 27. The wires were removed after being irradiated for a total of 28.4 EFPY. Activation measurements were performed for the following reactions: ^{63}Cu (n,α) ^{60}Co, ^{58}Ni (n,p) ^{58}Co, and ^{54}Fe (n,p) ^{54}Mn.

Table 3-6 provides a comparison of the calculated specific activities and the measured specific activities for each flux wire specimen. The average calculated-to-measured (C/M) ratio and standard deviation for the flux wires irradiated in the 288°-R capsule is determined to be 1.04 ± 0.06.

Table 3-6
Comparison of Calculated Flux Wire Activities to Measurements for the 288°-R Surveillance Capsule Removed from DAEC at EOC 27

Flux Wire	Measured Activity (dps/mg)	Calculated Activity (dps/mg)	Calculated vs. Measured (C/M)	Standard Deviation (σ)
Iron				
G41	252.87	261.06	1.03	-
G42	249.09	261.06	1.05	-
G43	248.19	261.06	1.05	-
Iron Average	-	-	**1.04**	**0.01**
Copper				
G41	42.61	41.06	0.96	-
G42	42.30	41.06	0.97	-
G43	41.61	41.06	0.99	-
Copper Average	-	-	**0.97**	**0.01**
Nickel				
G41	3057.54	3428.25	1.12	-
G42	3191.50	3428.25	1.07	-
G43	3135.90	3428.25	1.09	-
Nickel Average	-	-	**1.10**	**0.02**
Flux Wire Average	-	-	**1.04**	**0.06**

It is noted in the surveillance capsule test report that the dosimetry wires that were loaded in the Charpy packets were free-standing at various axial and radial distances within the surveillance capsule basket. It was further observed in photographs of the packets that the dosimetry wires appeared to reside closer to the back of each packet between the end of the Charpy specimens

and the packet side wall. Therefore, the activation calculations for the dosimetry flux wires were performed at the center elevation on the back face of the basket.

3.3.3 Capsule Fluence Calculations

Table 3-7 lists the best-estimate fast neutron fluence that was determined for the Charpy specimens that were removed from the DAEC 288°-R surveillance capsule at the end of Cycle 27. The Charpy specimens that were irradiated in the 288°-R capsule were reconstituted specimens that were originally irradiated in the reactor from the beginning of Cycle 1 to the end of Cycle 7. Selected original specimens were reconstituted and reinserted into the reactor at the beginning of Cycle 9 and irradiated until the end of Cycle 27. The accumulated irradiation for the specimens at EOC 27 was determined to be 34.3 EFPY, accounting for the absence of the capsule from the reactor during Cycle 8. The precise positioning of the individual Charpy specimens in the capsule is not known at the time of analysis; therefore, the fast neutron fluence calculated for the specimens was performed at the center of the capsule container.

Table 3-7
Best-Estimate Fluence for the Reconstituted 288°-R Duane Arnold Charpy Specimens

Capsule Location	Irradiation Period	Accumulated Exposure for the Charpy Specimens (EFPY)	Accumulated Fast Neutron Fluence (n/cm^2)
288°	BOC 1 to EOC 7 and BOC 9 to EOC 27	34.3	3.27E+18

The calculated-to-measured activation comparisons for the surveillance capsule presented in the previous sections show no discernable bias in the computational fluence method. Therefore, the best-estimate fluence reported in Table 3-7 is the unbiased fast neutron fluence computed by the RAMA fluence methodology. This is discussed further in the next section.

3.4 Capsule Fluence Uncertainty Analysis

This section presents the combined uncertainty analysis and the determination of bias for the DAEC capsule fluence evaluation. The combined uncertainty is comprised of two components. One component is the uncertainty factors developed from plant-specific measurements and the other is an analytic uncertainty factor. When combined, these components provide a basis for determining the combined uncertainty (1σ) and bias in the computed fluence.

The requirements for determining the combined uncertainty and bias for light water reactor pressure vessel fluence evaluations are provided in Regulatory Guide 1.190 [17]. The approach for determining combined uncertainty and bias for reactor component fluence is demonstrated in BWRVIP-189 [22].

For capsule fluence evaluations, two uncertainty factors are considered: comparison factors and uncertainty introduced by the measurement process. After analysis of these factors, it was determined that the combined uncertainty for the DAEC 288°-R capsule fluence was 12.29%, and that no adjustment for bias was required for the calculated capsule fast neutron fluence presented in Section 3.3.

3.4.1 Comparison Uncertainty

Comparison uncertainty factors are determined by comparing calculated activities with activity measurements. For capsule fluence evaluations, two comparison uncertainty factors are considered: plant-specific comparison factors and benchmark comparison factors. Comparison uncertainty factors based upon measurements also involve the combination of two components: the calculated-to-measured (C/M) activity ratio and a measurement uncertainty.

3.4.1.1 Operating Reactor Comparison Uncertainty

TransWare has evaluated activation measurements for several BWR plants ranging from BWR/2-class plants to BWR/6-class plants. Each class of BWRs can have one or several variations of reactor core configurations, each having different radial diameters for the core shroud, reactor pressure vessel, and biological shield components. In addition, each can have different placements of the jet pumps and surveillance capsules in the reactor vessels.

The Duane Arnold reactor is a BWR/4 class design. A total of 242 plant-specific dosimetry measurements have been evaluated for BWR/4-class plants using the RAMA Fluence Methodology. The overall C/M and standard deviation for the BWR/4-class plant measurements is determined to be an unbiased 1.03 ± 0.11. Of the 242 measurements, thirty-six samples were taken from Duane Arnold. A total of 721 credible activation measurement comparisons have been previously performed for a broad spectrum of BWR configurations and designs using the RAMA Fluence Methodology. The overall comparison ratio for all BWR class plants evaluated as of the date of this report is 1.01 ± 0.10. Note that only the BWR/4-class plant measurement data is utilized in this analysis to determine the operating reactor uncertainty factor.

3.4.1.2 Benchmark Comparison Uncertainty

The benchmark comparison uncertainty is based on a set of industry standard simulation benchmark comparisons. In accordance with the guidelines provided in Regulatory Guide 1.190, it is appropriate to include comparisons of vessel simulation benchmark measurements in the overall fluence uncertainty evaluation. Two vessel simulation benchmarks are evaluated: the Pool Critical Assembly (PCA) and VENUS-3 experimental benchmarks.

The PCA experimental benchmark includes 27 activation measurements at the mid-plane elevation in various simulated reactor components. The VENUS-3 experimental benchmark includes 386 activation measurements at a range of elevations in various simulated reactor components. Table 3-8 summarizes the calculated-to-measurement (C/M) results determined for these vessel simulation benchmarks.

Table 3-8
Summary of Comparisons to Vessel Simulation Benchmark Measurements

Benchmark	Number of Measurements	Average Calculated-to-Measured (C/M)	St. Dev. (1σ)
Pool Critical Assembly	27	0.99	±0.05
VENUS-3	386	1.03	±0.05
Total Simulated Vessel Comparisons	**413**	**1.03**	**±0.05**

3.4.2 Analytic Uncertainty

The calculational models used for fluence analyses are comprised of numerous analytical parameters that have associated uncertainties in their values. The uncertainty in these parameters needs to be tested for its contribution to the overall fluence uncertainty.

The uncertainty values for the geometry parameters are based upon uncertainties in the dimensional data used to construct the plant geometry model. The uncertainty values for the material parameters are based upon uncertainties in the material densities for the water and nuclear fuel materials and the compositional makeup of typical steel materials.

The uncertainty values for the fission source parameters are based upon uncertainties in the fuel exposure and power factors for the fuel assemblies loaded on the core periphery. The transport method used in the fluence analysis employs a fission source calculation that accounts for the relative contributions of the uranium and plutonium fissile isotopes in the fuel and the relative power density of the fuel in the reactor. Both fission source parameters are derived directly from information calculated by three-dimensional core simulator codes. The uncertainty values for the nuclear cross-section parameters are based upon uncertainties in the number densities for the predominant nuclides that make up the reactor materials.

The uncertainty parameters for the fluence model inputs are based upon geometry meshing and numerical integration parameters used in the neutron flux transport calculation. Several mesh size and numerical integration parameter sensitivity cases are run to determine the optimum values for the transport calculation and to determine their corresponding impact on the analytic uncertainty.

3.4.3 Combined Uncertainty

The combined uncertainty for the DAEC 288°-R surveillance capsule fluence evaluation is determined with a weighting function that combines the analytic, plant-specific comparison, and benchmark comparison uncertainty factors. Table 3-9 shows that the combined uncertainty (1σ) determined for the DAEC capsules is 12.29% for neutron energy exceeding 1.0 MeV.

It is shown in Table 3-9 that the combined uncertainty is well below the 20% uncertainty limit specified in Regulatory Guide 1.190. In accordance with Regulatory Guide 1.190, there is no discernable bias in the computed capsule fluence. Therefore, no adjustment to the calculated capsule fast neutron fluence, presented in Section 3.3, is required.

Table 3-9
Duane Arnold Surveillance Capsule Combined Uncertainty for Energy >1.0 MeV

Uncertainty Term	Value
Combined Uncertainty (1σ)	12.29%
Bias[1]	None

1. The bias term is less than its constituent uncertainty values, concluding that no discernable bias exists in the computed fluence.

4
CHARPY TEST DATA

4.1 Charpy Test Procedure

Charpy impact tests were conducted in accordance with ASTM Standards E 185-82 and E 23-02. The 1982 version of E 185 has been reviewed and approved by NRC for surveillance capsule testing applications. This standard references ASTM E 23. The tests were conducted using a Tinius Olsen Testing Machine Company, Inc. Model 84 impact test machine with a 300 ft-lb (406.75 J) energy capacity. The Model 84 is equipped with a dial gage as well as the MPM optical encoder system for accurate absorbed energy measurement. The machine is also equipped with an instrumented striker, so a total of three independent measurements of the absorbed energy were made for all tests. The optical encoder measured energy was reported as the impact energy. The optical encoder energy is much more accurate than the analog dial. The optical encoder can resolve the energy to within 0.04 ft-lbs. (0.054 J), whereas, for the dial, the resolution is around 0.25 ft-lbs. (0.34 J). The impact energy was corrected for windage and friction for each test performed. The velocity of the striker at impact was nominally 18 ft/s (5.49 m/s). The MPM encoder system measures the exact impact velocity for every test. Calibration of the machine was verified as specified in ASTM E 23, and verification specimens were obtained from the National Institute for Standards and Technology (NIST) and tested in accordance with the standard.

The ASTM E 23 procedure for specimen temperature control using an in-situ heating and cooling system was followed. The advantage of using the MPM in-situ heating/cooling technology is that each specimen is thermally conditioned right up to the instant of impact. Thermal losses associated with liquid bath systems, such as those resulting from transfer of a specimen from a liquid bath to the test machine, are completely eliminated. Each specimen was held at the desired test temperature for at least 5 minutes prior to testing, and the fracture process zone temperature was held to within ± 1.8 °F (± 1°C) up to the instant of strike. Precision calibrated tongs were used for specimen centering on the test machine.

The percentage of shear fracture area was determined by integrating the ductile and brittle fracture areas using the MPM Digital Optical Comparator (DOC) image analysis system which is calibrated for distance measurements from reticles which are traceable to NIST. As shown in Figure 4-1, each fracture surface image is captured, outlined to delineate the brittle area, and outlined to define the outer ductile fracture region. The DOC software then performs a pixel area integration and automatically calculates the shear fracture area. This method for shear area determination is the most accurate method given in ASTM E 23 and is far superior to the commonly used photograph comparison method. The lateral expansion (LE) was determined from measurements made using the MPM Digital Optical Comparator (DOC) image analysis system. A line is placed on the image of the fracture surface along the bottom edge of the notch. From there perpendicular lines are placed on either side of the notch. The largest distance each shear lip extends beyond the perpendicular line on that side of the specimen is measured for the

lateral expansion calculation in ASTM E 23. An example of the DOC method is shown in Figure 4-2.

The number of Charpy specimens for measurement of the transition region and upper shelf was limited. Therefore, the choice of test temperatures was very important. Prior to testing, the Charpy energy-temperature curve was predicted using embrittlement models and previous data. The first test was then conducted near the middle of the transition region, and test temperature decisions were then made based on the test results. Overall, the goal was to perform two or three tests on the upper shelf, and to use the remaining specimens to characterize the 30 ft-lb (41 J) index. This approach was successful and the transition region and upper shelf energy are well defined.

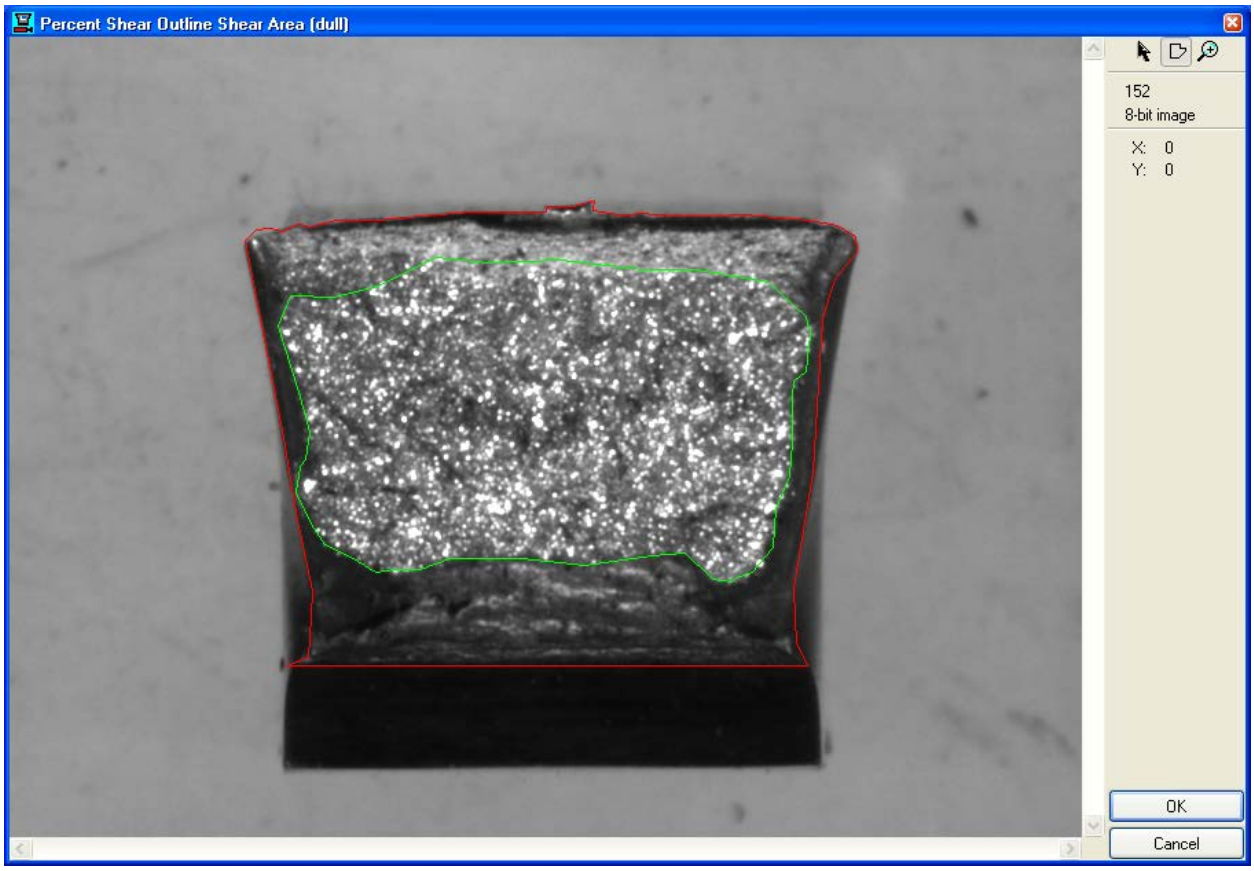

Figure 4-1
Illustration of Digital Optical Comparator Measurement of Shear Fracture Area

First, the Brittle Fracture Area is Outlined (within green line). Next, the Outer Ductile Fracture Area is Outlined (within red line). Finally, the Software Integrates the Areas and Calculates the Percent Shear Fracture Area.

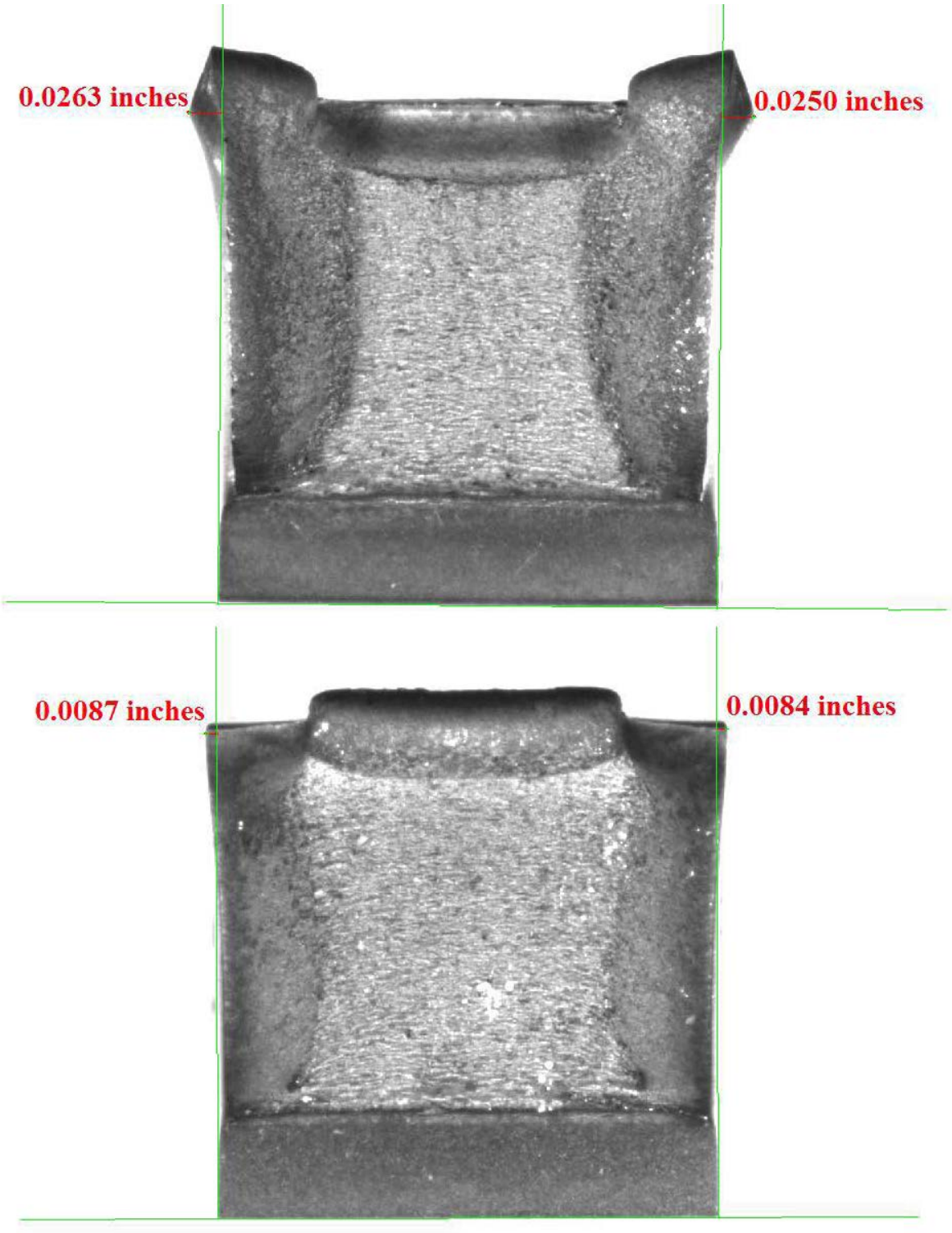

Figure 4-2
Illustration of Digital Optical Comparator Measurement of Lateral Expansion

The DOC Software Automatically Finds the Notch Edge and Draws Two Perpendicular Lines to Define the Reference for LE. The Line Perpendicular to this Line is then Drawn to the Furthest Extent of the Deformed Material to Determine the Lateral Expansion Result.

4.2 Charpy Test Data for the DAEC 288°-R Capsule

A total of fifteen irradiated base material and twelve irradiated weld material specimens were tested over the transition region temperature range and on the upper shelf. The data are summarized in Tables 4-1 and 4-2. In addition to the energy absorbed by the specimen during impact, the measured lateral expansion values and the percentage shear fracture area for each test specimen are listed in the tables. The Charpy energy was acquired from the optical encoder signal and has been corrected for windage and friction in accordance with ASTM E 23. The impact energy is the energy required to initiate and propagate a crack in the Charpy specimen. The optical encoder and the dial cannot correct for tossing energy or losses in the test machine, and therefore this small amount of additional energy, if present, may be included in the data for some tests. The instrumented striker energy does not include tossing energy or machine vibration energy since the energy, in this case, is measured only during a few milliseconds of contact between the striker and specimen. Based on comparison between the instrumented striker energy and the optical encoder energy, it has been shown that the tossing energy, and other losses, are small for most tests.

The lateral expansion is a measure of the transverse plastic deformation produced by the contact edge of the striker during the impact event. Lateral expansion is determined by measuring the maximum change of specimen thickness along the sides of the specimen. Lateral expansion is a measure of the ductility of the specimen. The nuclear industry tracks the embrittlement shift using the 35 mil (0.89 mm) lateral expansion index. In accordance with ASTM E 23, the lateral expansion for some specimens, which could not be broken by hand after the impact test, should not be reported as broken since the lateral expansion of the unbroken specimen is less than that for the broken specimen. Therefore, when these conditions exist, the value listed is the unbroken measurement and a footnote is included to identify these specimens. All of the 288°-R capsule specimens that did not separate during the test could be broken by hand under the ASTM E 23 requirements.

The percentage of shear fracture area is a direct quantification of the transition in the fracture modes as the temperature increases. All metals with a body centered cubic lattice structure, such as ferritic pressure vessel materials, undergo a transition in fracture modes. At low test temperatures, a crack propagates in a brittle manner and cleaves across the grains. As the temperature increases, the percentage of shear (or ductile) fracture increases. This temperature range is referred to as the transition region and the fracture process is mixed mode. As the temperature increases further, the fracture process is eventually completely ductile (i.e., no brittle component) and this temperature range is referred to as the upper shelf region.

Table 4-1
Irradiated Charpy V-Notch Impact Test Results for Surveillance Base Metal Specimens (Heat B0673-1) from the Duane Arnold 288°-R Surveillance Capsule

Base Irradiated: Heat B0673-1 (LT) 288°-R Capsule							
Specimen ID	Test Temperature °F	(°C)	Impact Energy ft-lb	(J)	Lateral Expansion mils	(mm)	Percent Shear (%)
EBJB	-100.8	(-73.8)	2.50	(3.39)	2.0	(0.05)	1.2
EC1A	-50.6	(-45.9)	5.00	(6.78)	2.3	(0.06)	1.9
EBLB	12.6	(-10.8)	13.14	(17.82)	11.1	(0.28)	7.6
EBYB	29.5	(-1.4)	6.64	(9.00)	3.4	(0.09)	12.1
EBYA	47.1	(8.4)	16.47	(22.33)	12.4	(0.31)	12.1
EBPA	57.2	(14.0)	27.10	(36.74)	19.0	(0.48)	16.5
EC1B	68.9	(20.5)	37.38	(50.68)	28.8	(0.73)	22.8
EBLA	98.6	(37.0)	53.64	(72.73)	38.7	(0.98)	26.1
EBKB	122.0	(50.0)	69.85	(94.70)	52.4	(1.33)	41.4
EBPB	145.0	(62.8)	82.90	(112.40)	55.6	(1.41)	48.4
EBUA	169.3	(76.3)	96.99	(131.50)	66.9	(1.70)	65.1
EBTA	210.4	(99.1)	126.44	(171.43)	83.8	(2.13)	99.7
EBKA	251.4	(121.9)	128.15	(173.75)	79.9	(2.03)	100.0
EBTB	302.4	(150.2)	130.24	(176.58)	90.7	(2.30)	100.0
EBUB	377.8	(192.1)	133.71	(181.28)	81.9	(2.08)	100.0

Table 4-2
Irradiated Charpy V-Notch Impact Test Results for Surveillance Weld Metal Specimens (Heat DA1 SMAW) from the Duane Arnold 288°-R Surveillance Capsule

Weld Irradiated: Heat DA1 SMAW, 288°-R Capsule							
Specimen ID	Test Temperature °F	(°C)	Impact Energy ft-lb	(J)	Lateral Expansion mils	(mm)	Percent Shear (%)
EJ3B	-99.8	(-73.2)	4.24	(5.75)	1.8	(0.05)	12.9
EE3A	-50.4	(-45.8)	21.75	(29.49)	13.9	(0.35)	14.2
EE4A	-40.4	(-40.2)	38.78	(52.58)	37.0	(0.94)	21.8
EE5A	-26.7	(-32.6)	91.04	(123.43)	82.1	(2.09)	56.1
EJ1A	-1.8	(-18.8)	3.32	(4.50)	1.8	(0.05)	6.7
EJ3A	-0.8	(-18.2)	53.78	(72.91)	55.8	(1.42)	38.6
EE4B	35.8	(2.1)	69.94	(94.82)	53.8	(1.37)	68.8
EE2A	69.4	(20.8)	95.06	(128.88)	80.7	(2.05)	82.5
EJ2A	126.6	(53.1)	89.72	(121.64)	71.1	(1.81)	93.8
EE5B	197.1	(91.7)	118.42	(160.55)	101.3	(2.57)	99.9
EJ4A	303.1	(150.6)	97.05	(131.58)	87.2	(2.21)	100.0
EJ1B	396.5	(202.5)	141.82	(192.28)	97.3	(2.47)	100.0

5
CHARPY TEST RESULTS

5.1 Analysis of Impact Test Results

For analysis of the Charpy test data, the BWRVIP ISP has selected the hyperbolic tangent (tanh) function as the statistical curve-fit tool to model the transition temperature toughness data. A hyperbolic tangent curve-fitting program named CVGRAPH [12] was used to fit the Charpy V-notch (CVN) energy and lateral expansion data. Analysis methodology (e.g., definition of upper fixed shelf and lower shelf) followed the BWRVIP conventions established for analysis of all ISP data [11]. The impact energy curve-fit from CVGRAPH are provided in Figure 5-1 (plate heat B0673-1) and Figure 5-2 (weld heat DA1 SMAW). The lateral expansion curve fits are provided in Figure 5-3 (plate heat B0673-1) and Figure 5-4 (weld heat DA1 SMAW). HAZ results are not used in the BWRVIP ISP; thus, the HAZ data were not fit.

For the analysis of Charpy energy test data, lower shelf energy was fixed at 2.5 ft-lb (3.4 J). Upper shelf energy was fixed at the average of all test energies exhibiting shear greater than or equal to 95%, consistent with ASTM Standard E185-82 [3]. For analysis of the lateral expansion test data, the lower shelf was fixed at 1.0 mils; the fixed upper shelf was defined as the average of the lateral expansion test data points exhibiting shear greater than or equal to 95%, consistent with the approach used for upper shelf energy.

5.2 Irradiated Versus Unirradiated CVN Properties

Table 5-1 summarizes the T_{30} [30 ft-lb (41 J) Transition Temperature], T_{35mil} [35 mil (0.89 mm) Lateral Expansion Temperature], T_{50} [50 ft-lb (68 J) Transition Temperature], and Upper Shelf Energy for the unirradiated and irradiated materials and shows the change (shift) from baseline values. The unirradiated values of T_{30} and T_{50} were taken from the CVGRAPH fits provided in Figures 2-5 and 2-6; the unirradiated values of T_{35mil} were taken from the CVGRAPH fits provided in Figures 2-7 and 2-8. The irradiated values are from the index temperatures determined in Figures 5-1 and 5-2 for impact energy and Figures 5-3 and 5-4 for lateral expansion.

Table 5-2 provides a comparison of the measured T_{30} shift to the predicted shift for plate heat B0673-1 and weld heat DA1 SMAW. Predicted shift is based on the formula provided in Regulatory Position 1.1 of Reg. Guide 1.99, Rev. 2 [6] as shown in Note 3 to Table 5-2. The fluence was input as 32.7×10^{17} n/cm^2, as reported in Table 3-7 for the DAEC 288°-R surveillance capsule. The measured shift values for the surveillance plate and weld are less than the value expected (e.g., the measured shift is less than predicted shift + margin).

Measured percent decrease in USE is presented in Table 5-3 and compared to the percent decrease predicted by Regulatory Position 1.2 and Figure 2 of Reg. Guide 1.99, Rev. 2. The measured percent decrease in USE for the surveillance plate and weld are less than the predicted percent decrease.

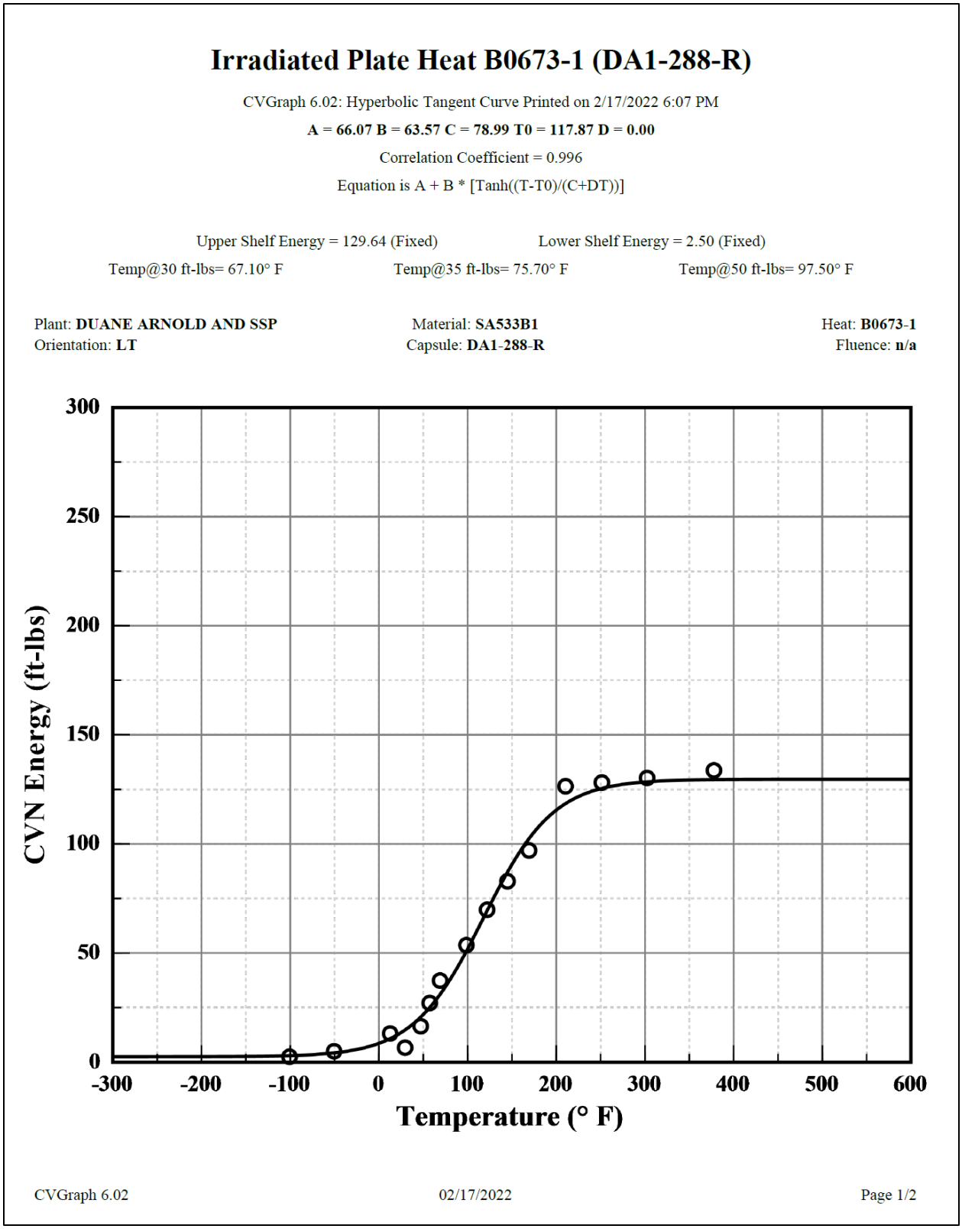

Figure 5-1
Irradiated Plate Heat B0673-1 Charpy Energy Plot (DAEC 288°-R Capsule) (LT)

Plant: **DUANE ARNOLD AND SSP** Material: **SA533B1** Heat: **B0673-1**
Orientation: **LT** Capsule: **DA1-288-R** Fluence: **n/a**

Irradiated Plate Heat B0673-1 (DA1-288-R)

Charpy V-Notch Data

Temperature (° F)	Input CVN	Computed CVN	Differential
-101	2.5	3.0	-0.50
-51	5.0	4.3	0.74
13	13.1	10.8	2.37
30	6.6	14.8	-8.12
47	16.5	20.7	-4.19
57	27.1	25.0	2.08
69	37.4	31.0	6.34
99	53.6	50.9	2.78
122	69.9	69.4	0.46
145	82.9	87.1	-4.18
169	97.0	102.5	-5.47
210	126.4	118.5	7.94
251	128.2	125.5	2.69
302	130.2	128.5	1.78
378	133.7	129.5	4.25

CVGraph 6.02 02/17/2022 Page 2/2

Figure 5-1 (Continued)
Irradiated Plate Heat B0673-1 Charpy Energy Plot (DAEC 288°-R Capsule) (LT)

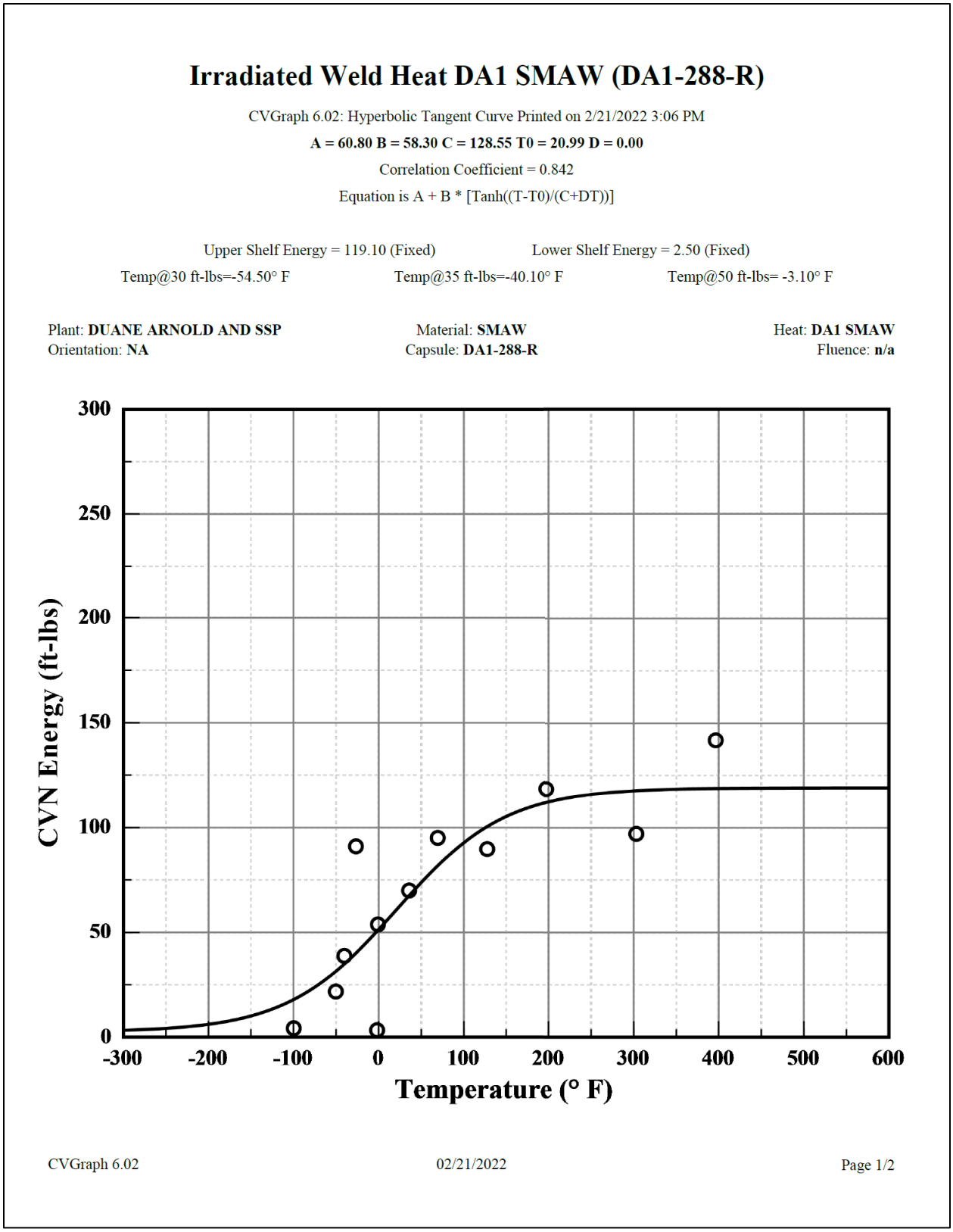

Figure 5-2
Irradiated Weld Heat DA1 SMAW Charpy Energy Plot (DAEC 288°-R Capsule)

Plant: **DUANE ARNOLD AND SSP** Material: **SMAW** Heat: **DA1 SMAW**
Orientation: **NA** Capsule: **DA1-288-R** Fluence: **n/a**

Irradiated Weld Heat DA1 SMAW (DA1-288-R)

Charpy V-Notch Data

Temperature (° F)	Input CVN	Computed CVN	Differential
-100	4.2	17.9	-13.71
-50	21.8	31.4	-9.64
-40	38.8	34.9	3.88
-27	91.0	40.1	50.93
-2	3.3	50.6	-47.25
-1	53.8	51.0	2.77
36	69.9	67.5	2.45
69	95.1	81.8	13.29
128	89.7	100.5	-10.73
197	118.4	112.0	6.39
303	97.1	117.7	-20.62
397	141.8	118.8	23.06

CVGraph 6.02 02/21/2022 Page 2/2

Figure 5-2 (Continued)
Irradiated Plate Heat DA1 SMAW Charpy Energy Plot (DAEC 288°-R Capsule)

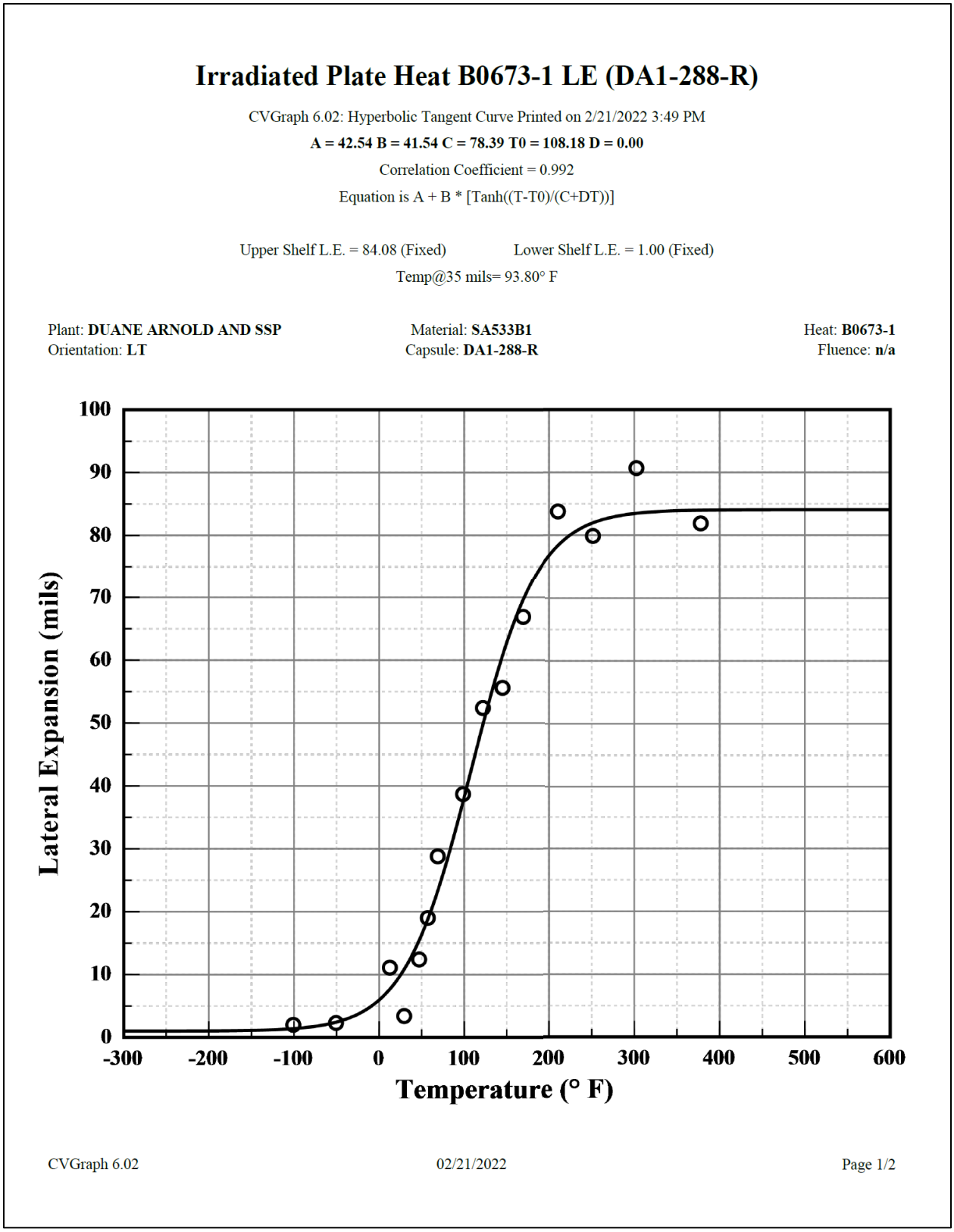

Figure 5-3
Irradiated Plate Heat B0673-1 Lateral Expansion Plot (DAEC 288°-R Capsule) (LT)

Plant: **DUANE ARNOLD AND SSP** Material: **SA533B1** Heat: **B0673-1**
Orientation: **LT** Capsule: **DA1-288-R** Fluence: **n/a**

Irradiated Plate Heat B0673-1 LE (DA1-288-R)

Charpy V-Notch Data

Temperature (° F)	Input L. E.	Computed L. E.	Differential
-101	2.0	1.4	0.60
-51	2.3	2.4	-0.12
13	11.1	7.7	3.43
30	3.4	10.8	-7.44
47	12.4	15.4	-3.05
57	19.0	18.8	0.22
69	28.8	23.3	5.49
99	38.7	37.5	1.21
122	52.4	49.8	2.61
145	55.6	60.7	-5.13
169	66.9	69.6	-2.74
210	83.8	78.4	5.42
251	79.9	82.0	-2.08
302	90.7	83.5	7.20
378	81.9	84.0	-2.09

CVGraph 6.02 02/21/2022 Page 2/2

Figure 5-3 (Continued)
Irradiated Plate Heat B0673-1 Lateral Expansion Plot (DAEC 288°-R Capsule) (LT)

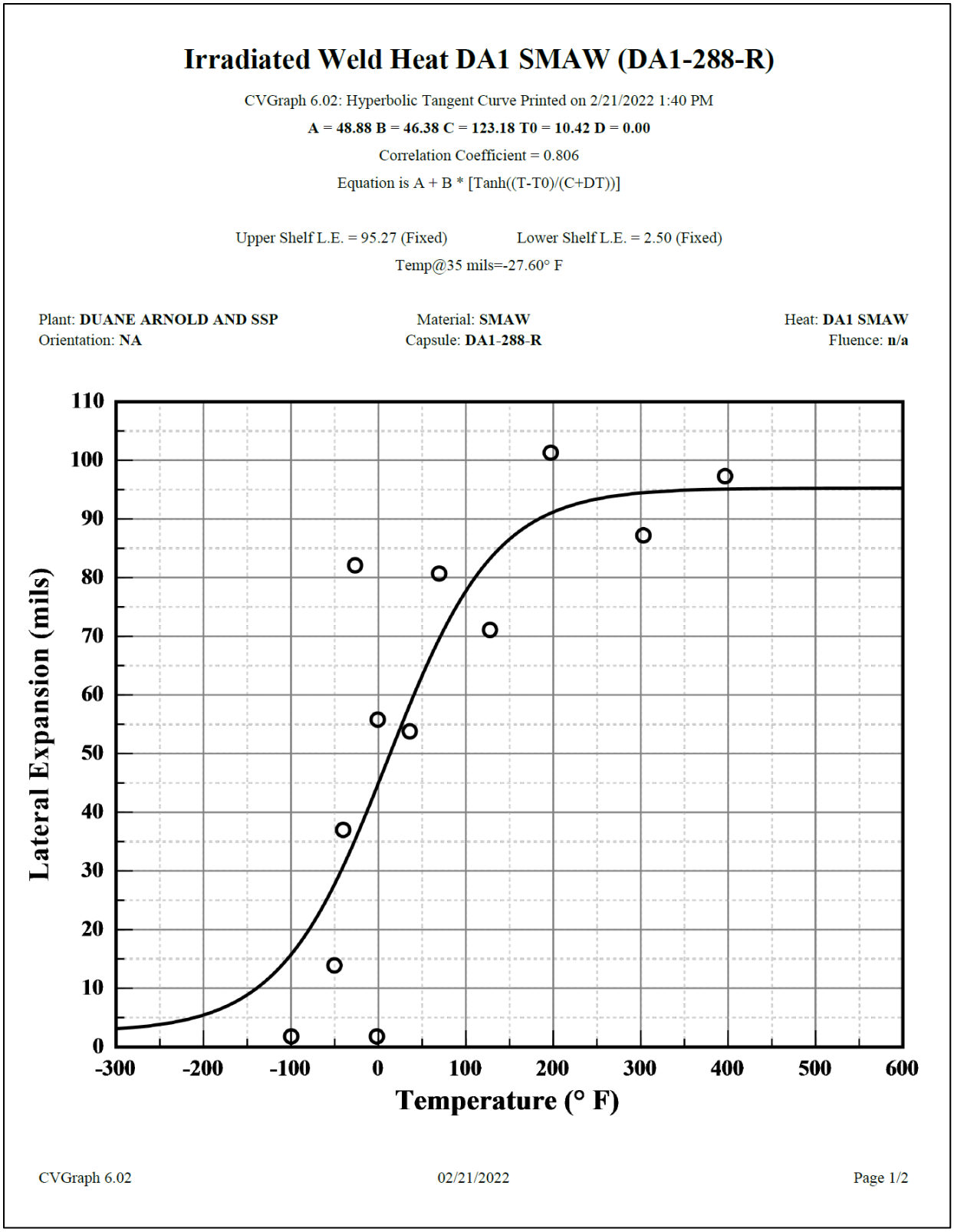

Figure 5-4
Irradiated Weld Heat DA1 SMAW Lateral Expansion Plot (DAEC 288°-R Capsule)

Plant: **DUANE ARNOLD AND SSP** Material: **SMAW** Heat: **DA1 SMAW**
Orientation: **NA** Capsule: **DA1-288-R** Fluence: **n/a**

Irradiated Weld Heat DA1 SMAW (DA1-288-R)

Charpy V-Notch Data

Temperature (° F)	Input L. E.	Computed L. E.	Differential
-100	1.8	15.8	-13.98
-50	13.9	27.7	-13.78
-40	37.0	30.8	6.24
-27	82.1	35.3	46.79
-2	1.8	44.3	-42.50
-1	55.8	44.7	11.13
36	53.8	58.3	-4.51
69	80.7	69.5	11.16
128	71.1	83.2	-12.13
197	101.3	91.0	10.30
303	87.2	94.5	-7.28
397	97.3	95.1	2.21

CVGraph 6.02 02/21/2022 Page 2/2

Figure 5-4 (Continued)
Irradiated Weld Heat DA1 SMAW Lateral Expansion Plot (DAEC 288°-R Capsule)

Table 5-1
Effect of Irradiation (E>1.0 MeV) on the Notch Toughness Properties of the DAEC 288°-R Capsule Surveillance Materials

Material Identity	T_{30}, 30 ft-lb (40.7 J) Transition Temperature			T_{50}, 50 ft-lb (67.8 J) Transition Temperature			T_{35mil}, 35 mil (0.89 mm) Lateral Expansion Temperature			CVN Upper Shelf Energy (USE)		
	Unirrad °F (°C)	Irradiated °F (°C)	ΔT_{30} °F (°C)	Unirrad °F (°C)	Irradiated °F (°C)	ΔT_{50} °F (°C)	Unirrad °F (°C)	Irradiated °F (°C)	ΔT_{35mil} °F (°C)	Unirrad ft-lb (J)	Irradiated ft-lb (J)	Change ft-lb (J)
B0673-1 (LT Orientation)	-35.5 (-37.5)	67.1 (19.5)	102.6 (57.0)	-7.3 (-21.8)	97.5 (36.4)	104.8 (58.2)	-23.6 (-30.9)	93.8 (34.3)	117.4 (65.2)	158.1 (214.4)	129.6 (175.8)	-28.5 (-38.6)
DA1 SMAW	-45.4 (-43.0)	-54.5 (-48.1)	-9.1 (-5.1)	-10.2 (-23.4)	-3.1 (-19.5)	7.1 (3.9)	-37.3 (-38.5)	-27.6 (-33.1)	9.7 (5.4)	99.0 (134.2)	119.1 (161.5)	20.1 (27.3)

Table 5-2
Comparison of Actual Versus Predicted Embrittlement of the DAEC 288°-R Capsule Surveillance Materials

Identity	Material	Fluence[1] (E>1.0 MeV, x10^{17} n/cm^2)	Measured Shift[2] °F (°C)	RG 1.99 Rev. 2 Predicted Shift[3] °F (°C)	RG 1.99 Rev. 2 Predicted Shift+Margin[3,4] °F (°C)
B0673-1 (LT orientation)	Duane Arnold surveillance plate	32.7	102.6 (57.0)	77.1 (42.8)	111.1 (61.7)
DA1 SMAW	Duane Arnold surveillance weld	32.7	-9.1 (-5.1)	18.7 (10.4)	37.4 (20.8)

1. Fluence value is reported in Table 3-7.
2. The measured shift is taken from Table 5-1.
3. Predicted shift = CF × FF, where CF is a Chemistry Factor taken from the base metal table in USNRC RG 1.99, Rev. 2 [6], based on each material's Cu/Ni content, and FF is Fluence Factor, $f^{0.28-0.10 \log f}$, where f = fluence in units of 10^{19} n/cm^2 (E > 1.0 MeV) specified.
4. Margin = $2\sqrt{(\sigma_i^2 + \sigma_\Delta^2)}$, where σ_i = the standard deviation on initial RT_{NDT} (σ_i is taken to be 0°F), and σ_Δ is the standard deviation on ΔRT_{NDT} (28°F for welds and 17°F for base materials, except that σ_Δ need not exceed 0.50 times the mean value of ΔRT_{NDT}). Thus, margin is defined as 34°F for plate materials and 56°F for weld materials, or margin equals shift (whichever is less), per Reg. Guide 1.99, Rev. 2.

Table 5-3
Percent Decrease in Upper Shelf Energy of the DAEC 288°-R Capsule Surveillance Materials

Identity	Material	Fluence[1] (E>1.0 MeV, x10^{17} n/cm^2)	Measured Decrease in USE (%)	Predicted Decrease in USE[2] (%)
B0673-1 (LT orientation)	Duane Arnold surveillance plate	32.7	18.0	18.4
DA1 SMAW	Duane Arnold surveillance weld	32.7	--[3]	12.3

1. Fluence value is reported in Table 3-7.
2. Based on the equations for Figure 2 of Reg. Guide 1.99, Rev. 2 [6] as provided in Reg. Guide 1.162 [23].
3. Value less than zero.

6
REFERENCES

1. 10 CFR 50, Appendices G (*Fracture Toughness Requirements*) and H (*Reactor Vessel Material Surveillance Program Requirements*), Federal Register, Volume 60, No. 243, dated December 19, 1995.
2. American Society of Mechanical Engineers (ASME) Boiler and Pressure Vessel Code (Code), Section XI, "*Rules for In service Inspection of Nuclear Power Plant Components,*" Nonmandatory Appendix G, Fracture Toughness Criteria for Protection Against Failure.
3. ASTM E185-82, *Standard Practice for Conducting Surveillance Tests for Light-Water Cooled Nuclear Power Reactor Vessels*, E706 (IF), American Society for Testing and Materials, Philadelphia, PA, 1982.
4. *BWRVIP-86, Revision 1-A: BWR Vessel and Internals Project, Updated BWR Integrated Surveillance Program (ISP) Implementation Plan.* EPRI, Palo Alto, CA: 2012. 1025144.
5. 10 CFR 50, Appendix B, "*Quality Assurance Criteria for Nuclear Power Plants and Fuel Reprocessing Plants,*" August 28, 2007.
6. U.S. NRC Regulatory Guide 1.99, Revision 2, "*Radiation Embrittlement of Reactor Vessel Materials,*" Revision 2, May 1988.
7. "*Guideline for the Management of Materials Issues*," NEI 03-08, Nuclear Energy Institute, Washington, DC, Latest Edition.
8. "*Duane Arnold Energy Center Reactor Pressure Vessel Surveillance Materials Testing,*" T. A. Caine, GE Nuclear, NEDC-31166, Rev.1, July 1986.
9. "*Duane Arnold RPV Surveillance Materials Testing and Analysis*," L. J. Tilly, GE Nuclear Energy, GE-NE-B1100716-01, July 1997.
10. *BWRVIP-279NP: BWR Vessel and Internals Project, Testing and Evaluation of the Duane Arnold 108° Surveillance Capsule*. EPRI, Palo Alto, CA: 2014. 3002002134.
11. *BWRVIP-135, Revision 4: BWR Vessel and Internals Project, Integrated Surveillance Program (ISP) Data Source Book and Plant Evaluations*. EPRI, Palo Alto, CA: 2021. 30020020996.
12. CVGRAPH, "*Hyperbolic Tangent Curve Fitting Program,*" Developed by ATI Consulting, Version 6.02, April 2014.
13. "*Laser Weld Reconstitution of Conventional and Miniaturized Notch Test (MNT) Specimens,*" M.P. Manahan Sr., J. Williams, and R.P. Martukanitz, ASTM STP1204, 1993, pp. 62-76.
14. *BWRVIP-126, Revision 2: BWR Vessel Internals Project, RAMA Fluence Methodology Software*, *Version 1.20*. EPRI, Palo Alto, CA: 2010. 1020240.

15. *BWRVIP-121-A: BWR Vessel and Internals Project, RAMA Fluence Methodology Procedures Manual*, EPRI, Palo Alto, CA: 2009. 1019052.

16. *BWRVIP-114-A: BWR Vessel and Internals Project, RAMA Fluence Methodology Theory Manual*, EPRI, Palo Alto, CA: 2009. 1019049.

17. U.S. NRC Regulatory Guide 1.190, "*Calculational and Dosimetry Methods for Determining Pressure Vessel Neutron Fluence,*" March 2001.

18. U.S. Nuclear Regulatory Commission. Office of Nuclear Reactor Regulation. "*Safety Evaluation Report with Open Items Related to the License Renewal of Seabrook Station,*" Docket Number 50-443. Washington, D.C.: Office of Nuclear Reactor Regulation, 2012.

19. J. R. Askew, "*A Characteristics Formulation of the Neutron Transport Equation in Complicated Geometries,*" United Kingdom Atomic Energy Authority, AEEW-M 1108, 1972.

20. "*BUGLE-96: Coupled 47 Neutron, 20 Gamma-Ray Group Cross Section Library Derived from ENDF/B-VI for LWR Shielding and Pressure Vessel Dosimetry Applications,*" RSICC Data Library Collection, DL2C-185, March 1996.

21. "*VITAMIN-B6: A Fine-Group Cross Section Library Based on ENDF/B-VI Release 3 for Radiation Transport Applications,*" RSICC Data Library Collection, DLC-184, December 1996.

22. *BWRVIP-189: BWR Vessel and Internals Project, Evaluation of RAMA Fluence Methodology Calculation Uncertainty*. EPRI, Palo Alto, CA: 2008. 1016938.

23. U.S. NRC Regulatory Guide 1.162, "*Format and Content of Report for Thermal Annealing of Reactor Pressure Vessels,*" February 1996.

A
DOSIMETER ANALYSIS

A.1 Dosimeter Material Description

The DAEC 288°-R surveillance capsule primary dosimeter materials are pure metal wires which were located within the surveillance capsule packets. The high purity wire types provided for the DAEC surveillance program are iron, copper, and nickel. Each wire is typically about 3 inches (7.62 cm) long. The G42 packet leaked during plant operation and the dosimeter wires were damaged. MPM carefully cleaned the damaged wires and was able to extract short wire segments which could be counted and weighed.

A.2 Dosimeter Cleaning and Mass Measurement

At the time the Charpy packets were opened, the dosimeter wires were wiped to remove the loose contamination. Upon receipt at the radiometric lab, the wires were visually inspected under a low magnification optical microscope. There was evidence of oxidation indicating the need for chemical etching and further cleaning. This was accomplished by soaking the Fe wire segments in a 4N solution of hydrochloric acid until the oxidation was etched from the surface. Similarly, the Cu and Ni wires were immersed in a 2N solution of nitric acid. The wires were then rinsed with distilled water, wiped, final rinsed with alcohol, and dried in air at room temperature. The wires then exhibited a clean, shiny appearance. In general, the iron, nickel, and copper wires experience significant oxidation that must be removed before counting and weighing. Figures A-1 through A-9 show low-power magnifications of the dosimetry wires as they were found prior to cleaning, and after cleaning and coiling.

The total mass of each wire was measured using a Mettler Toledo XS105DU analytical digital balance. Table A-1 lists the results of these measurements, as well as the identification assigned to each dosimeter. The dosimeter identifications were assigned as the Charpy packet numbers followed by the type of dosimeter material.

The wires were tightly coiled for subsequent counting and weighing. Each wire was wrapped around a thin metal rod to form a coil of approximately 0.5 inch (12.7 mm) diameter or less, which yields a reasonable approximation to a point source geometry at the distance the dosimeter wires are placed from the gamma detector. The coiled wire segments were pressed firmly against a hard surface to flatten the coil to yield the best counting geometry.

A.3 Radiometric Analysis

Radiometric analysis was performed using high resolution gamma emission spectroscopy. In this method, gamma emissions from the dosimeter materials are detected and quantified using solid state gamma ray detectors and computer-based signal processing and spectrum analysis. The specifications of the gamma ray spectrometer system (GRSS) are listed in Table A-2. The GRSS

features a hyper pure germanium (HPGe) detector that is housed in a lead-copper shield to reduce background count rates. Standard background subtraction procedures were used.

GRSS calibration was performed using a National Institute for Standards and Technology (NIST) traceable mixed gamma quasi-point source. The Canberra analysis software provides the capability for energy resolution and efficiency calibration using specified standard source information. Calibration information is stored on magnetic disk for use by the spectrographic analysis software package.

Since detector efficiency depends on the source-detector geometry, a fixed-reproducible geometry must be selected for the gamma spectrographic analysis of the dosimeter materials. For the dosimeter wires, the counting geometry was that of a quasi-point source (coiled wire) placed five inches (12.7 cm) vertically from the top surface of the detector shell. In this way, extended sources up to 0.5 inch (1.27 cm) can be analyzed with a good approximation to a point source. The coiled wires were well within the area needed to approximate a point source geometry. The HPGe detector was calibrated for efficiency using the NIST traceable source. The accuracy of the efficiency calibration was checked using a gamma spectrographic analysis of the NIST traceable mixed gamma source. The isotopes contained in the source emit gamma rays which span the energy response of the detector for the dosimeter materials. These measurements show that the efficiency calibration is providing a valid measurement of source activity. The acceptance criteria for these measurements are that the software must yield a valid isotopic identification, and that the quantified activity of each correctly identified isotope must be comparable to the uncertainty specified in the source certification. Validation of system performance was made prior to starting the counting tasks, and upon completion of all counting work for DAEC. The counting system performance was acceptable in each case, indicating that the counting system properties did not change during the course of the counting procedure.

Table A-3 shows the counting schedule established for this work. There was no requirement for order of counting since the dosimeter materials still contained sufficient quantities of activation products to allow accurate radio assay. Counting times were more than sufficient to achieve the desired statistical accuracy for gamma emissions of interest in all cases.

Neutrons interact with the constituent nuclei of the dosimeter materials producing radionuclides in varying amounts depending on total neutron fluence, its energy spectrum, and the nuclear properties of the dosimeter materials. Table A-4 lists the reactions of interest and their resultant radionuclide products for each element contained in the dosimeters. These are threshold reactions involving an n-p or n-α interaction.

Finally, Table A-5 presents the primary results of interest for flux and fluence determination. The specific activity units are in dps/mg, which normalizes the activity to dosimeter mass. The activities are specified for a useful reference date/time, which is the DAEC plant shutdown date and time within $\pm$ 1 hour of the shutdown date/time of August 10, 2020, at 11:49:00 AM eastern standard time.

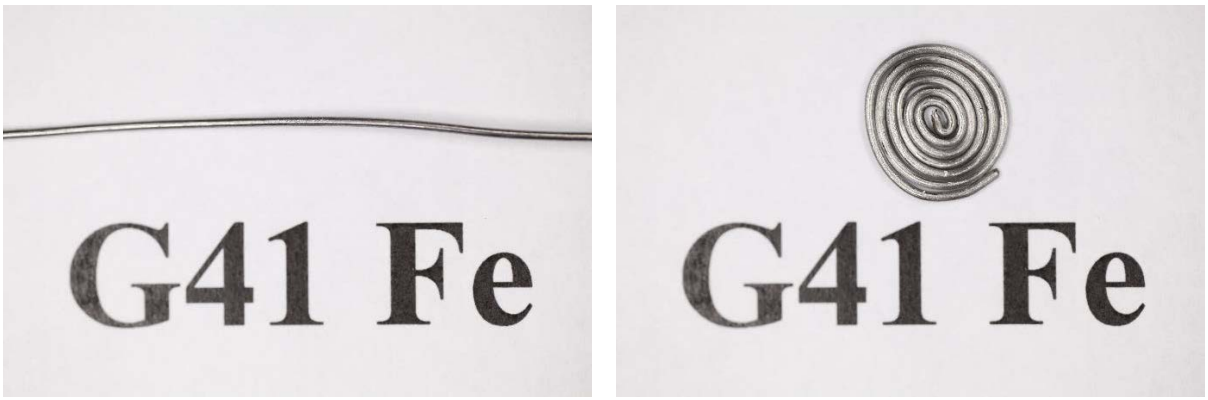

Figure A-1
DAEC 288°-R Capsule Packet G41 Fe Dosimeter Wire G41 Fe: Prior to Cleaning (left); and After Cleaning/Coiling (right)

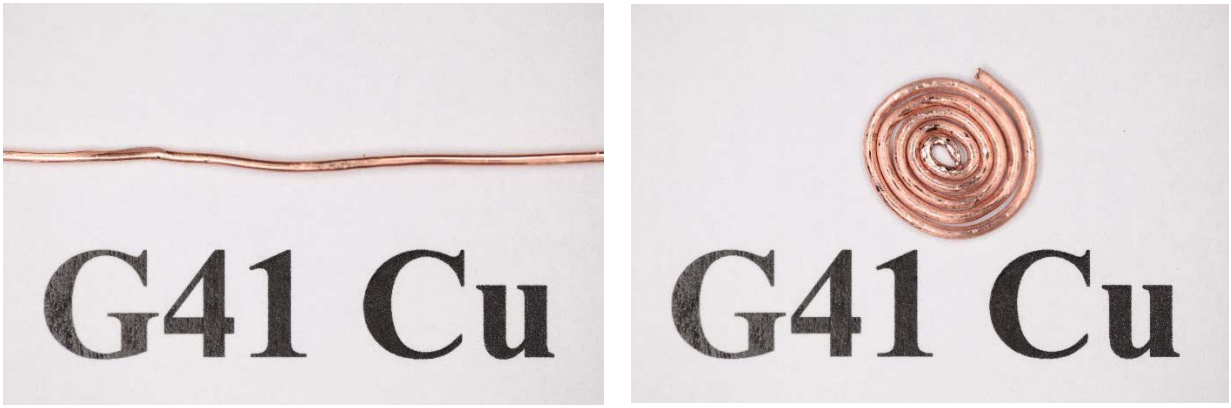

Figure A-2
DAEC 288°-R Capsule Packet G41 Cu Dosimeter Wire G41 Cu: Prior to Cleaning (left); and After Cleaning/Coiling (right)

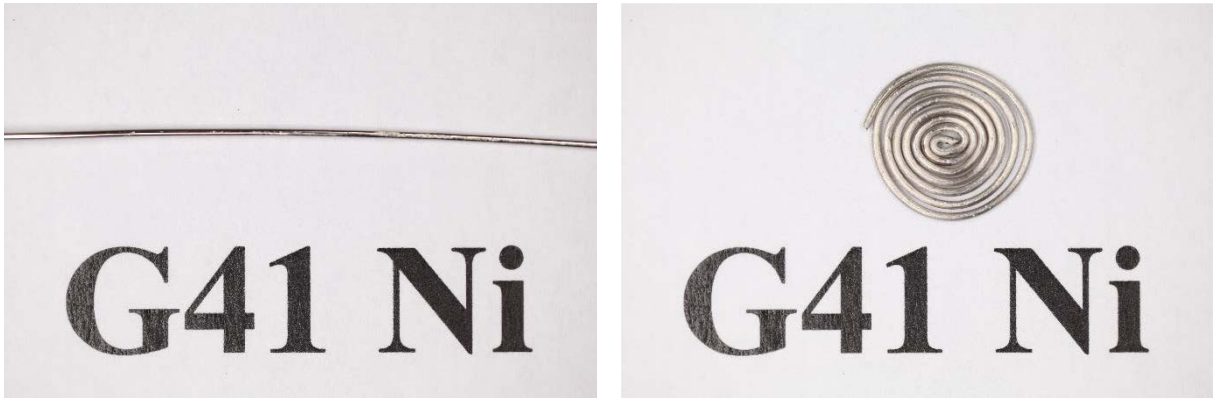

Figure A-3
DAEC 288°-R Capsule Packet G41 Ni Dosimeter Wire G41 Ni: Prior to Cleaning (left); and After Cleaning/Coiling (right)

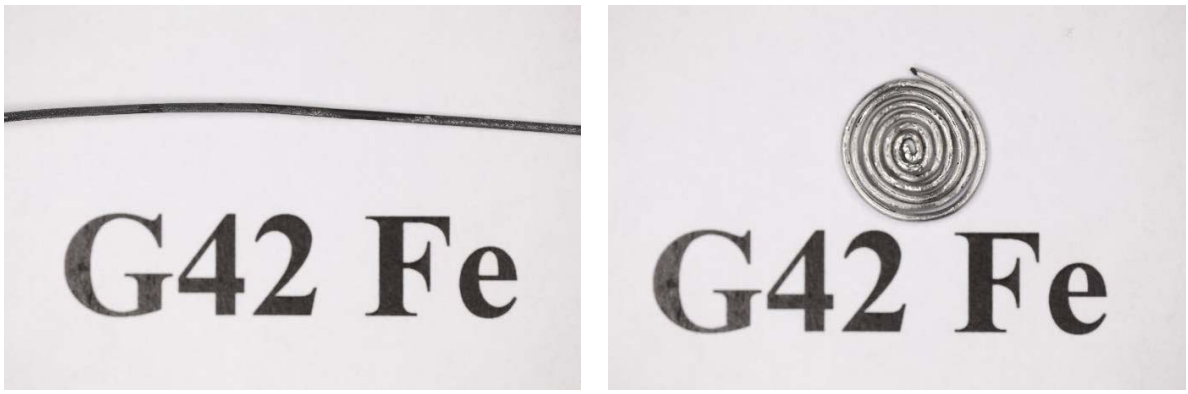

Figure A-4
DAEC 288°-R Capsule Packet G42 Fe Dosimeter Wire G42 Fe: Prior to Cleaning (left); and After Cleaning/Coiling (right)

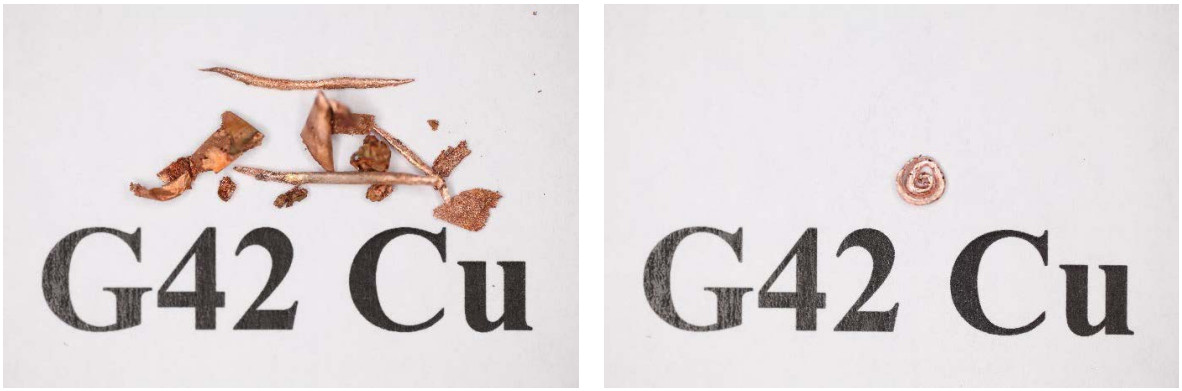

Figure A-5
DAEC 288°-R Capsule Packet G42 Cu Dosimeter Wire G42 Cu: Prior to Cleaning (left); and After Cleaning/Coiling (right)

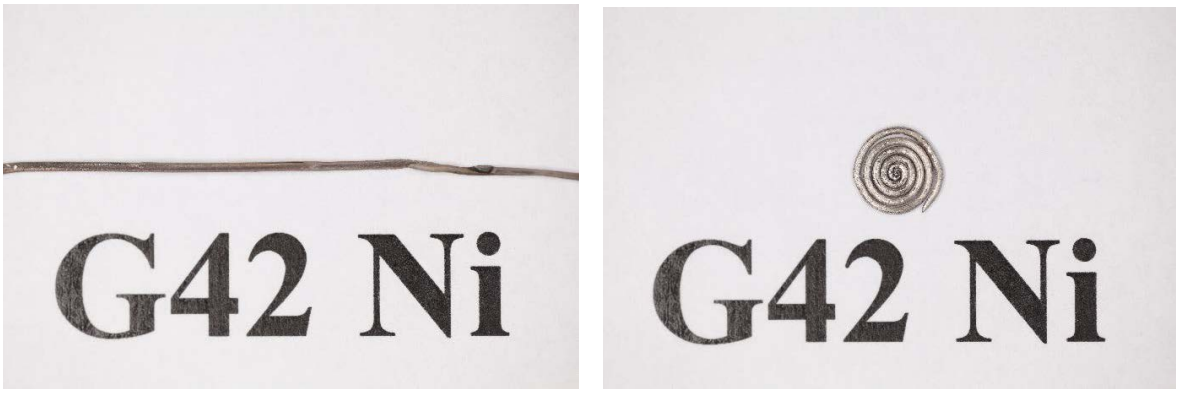

Figure A-6
DAEC 288°-R Capsule Packet G42 Ni Dosimeter Wire G42 Ni: Prior to Cleaning (left); and After Cleaning/Coiling (right)

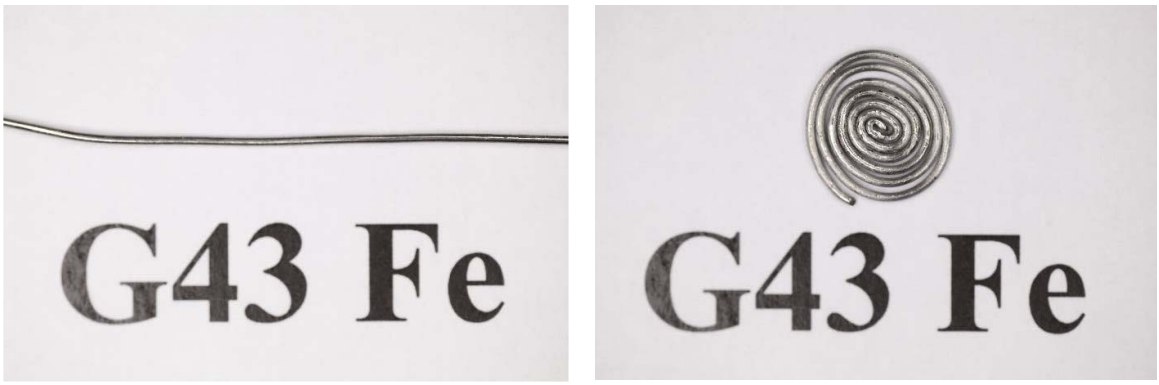

Figure A-7
DAEC 288°-R Capsule Packet G43 Fe Dosimeter Wire G43 Fe: Prior to Cleaning (left); and After Cleaning/Coiling (right)

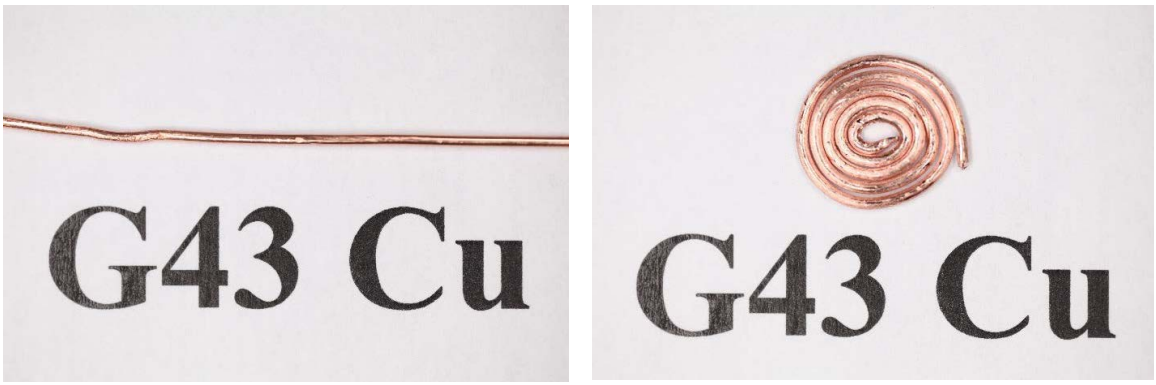

Figure A-8
DAEC 288°-R Capsule Packet G43 Cu Dosimeter Wire G43 Cu: Prior to Cleaning (left); and After Cleaning/Coiling (right)

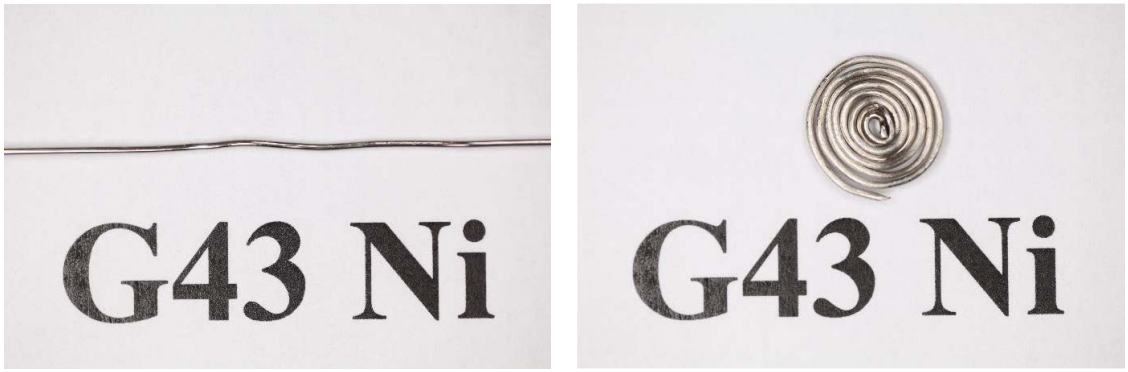

Figure A-9
DAEC 288°-R Capsule Packet G43 Ni Dosimeter Wire G43 Ni: Prior to Cleaning (left); and After Cleaning/Coiling (right)

Table A-1
DAEC 288-R° Capsule Charpy Packet Dosimeter Wire Masses

Wire Dosimeter ID	Mass (mg)
G41 Fe	222.41
G41 Cu	362.96
G41 Ni	199.67
G42 Fe	191.62
G42 Cu	20.12
G42 Ni	62.14
G43 Fe	220.64
G43 Cu	365.43
G43 Ni	201.76

Table A-2
Gamma Ray Spectrometer System (GRSS) Specifications

System Component	Description and/or Specifications
Detector	Canberra Model BE3830
Energy Resolution	<1.9 keV FWHM @ 1.33 MeV
Detector Efficiency Relative to a 3 inch x 3 inch NaI Crystal	33.3% at 1.3 MeV
Amplifier/Multichannel Analyzer	Canberra DAS-1000
Computer System	Intel i5-4460 CPU at 3.20 GHz, 16 GB Main Memory, 931 GB Hard Disk, 23-inch Monitor, HP LaserJet Printer
Software	Canberra Apex v 1.4

Table A-3
Counting Schedule for the DAEC 288°-R Capsule Dosimeter Materials

Dosimeter ID	Count Start Date	Count Start Time (EST)	Count Duration (Live Time Seconds)
G41 Fe	3/1/2021	12:40:35 PM	86,400
G41 Cu	3/11/2021	7:18:24 AM	86,400
G41 Ni	3/5/2021	3:34:00 PM	86,400
G42 Fe	3/2/2021	3:52:40 PM	86,400
G42 Cu	3/12/2021	2:22:52 PM	259,200
G42 Ni	3/8/2021	7:39:41 AM	86,400
G43 Fe	3/4/2021	7:11:25 AM	86,400
G43 Cu	3/15/2021	4:17:33 PM	86,400
G43 Ni	3/9/2021	9:58:02 AM	86,400

Table A-4
Neutron-Induced Reactions of Interest

Dosimeter Material	Neutron-Induced Reaction	Reaction Product Radionuclide
Iron	$Fe^{54}(n,p)Mn^{54}$	Mn^{54}
Copper	$Cu^{63}(n,\alpha)Co^{60}$	Co^{60}
Nickel	$Ni^{58}(n,p)Co^{58}$	Co^{58}

Table A-5
Results of DAEC 288°-R Capsule Radiometric Analysis

Dosimeter ID	Isotope ID	Activity at Reference Date/Time[1] (µCi)	Specific Activity at Reference Date/Time[1] (dps/mg)	Activity Uncertainty (%)
G41 Fe	^{54}Mn	1.52E+00	252.87	2.14
G41 Cu	^{60}Co	4.18E-01	42.61	1.61
G41 Ni	^{58}Co	1.65E+01	3,057.54	2.17
G42 Fe	^{54}Mn	1.29E+00	249.09	2.14
G42 Cu	^{60}Co	2.30E-02	42.30	1.62
G42 Ni	^{58}Co	5.36E+00	3,191.50	2.16
G43 Fe	^{54}Mn	1.48E+00	248.19	2.13
G43 Cu	^{60}Co	4.11E-01	41.61	1.62
G43 Ni	^{58}Co	1.71E+01	3,135.90	2.18

[1] August 10, 2020 at 11:49:00 AM EST is the reference date and time.

About EPRI

Founded in 1972, EPRI is the world's preeminent independent, non-profit energy research and development organization, with offices around the world. EPRI's trusted experts collaborate with more than 450 companies in 45 countries, driving innovation to ensure the public has clean, safe, reliable, affordable, and equitable access to electricity across the globe. Together, we are shaping the future of energy.

Program:

Nuclear Power

Boiling Water Reactor Vessel and Internals Program (BWRVIP)

3002023520

EPRI
3420 Hillview Avenue, Palo Alto, California 94304-1338 • PO Box 10412, Palo Alto, California 94303-0813 USA
800.313.3774 • 650.855.2121 • askepri@epri.com • www.epri.com